NTNU

Norwegian University of
Science and Technology

Reservoir Sedimentation Study for the Bunakha Hydro-electric Project

Choten Duba

Hydropower Development
Submission date: June 2016
Supervisor: Jochen Aberle, IVM

Norwegian University of Science and Technology
Department of Hydraulic and Environmental Engineering

Choten Duba

Reservoir Sedimentation Study for the Bunakha Hydro-electric Project

Master's Thesis: TVM4915 HYDROPOWER DEVELOPMENT Vår 2016

Trondheim, 10 June 2016

Supervisor: Prof. Jochen Aberle, IVM

Norwegian University of Science & Technology

Faculty of Engineering Science and Technology

Department of Hydraulic and Environmental Engineering

NTNU

Norwegian University of Science and Technology

ABSTRACT

This thesis presents a study on the sedimentation of the reservoir of the Bunakha Hydro-electric Project in Bhutan. Although the Detailed Project Report for this peaking reservoir scheme has already been completed, it has been used for further and additional investigations related to reservoir sedimentation. The sediment inflow into the reservoir was determined through two independent studies: i) Application of Pacific Southwest Interagency Committee (PSIAC) and Revised Universal Soil Loss Equation (RUSLE) approach integrated with Geographic Information System (GIS), ii) Data analysis of available suspended sediment data of Tamchu gauging station.

The application of the PSIAC approach taking into account three different boundary conditions related to catchment properties resulted in estimates of the average annual sedimentation rate for the Bunakha catchment/watershed at the location of gauging station as 0.4 mm/year, 0.18 mm/year, and 0.63 mm/year, respectively.

The determination of sedimentation rates based on the RUSLE approach was implemented in a GIS and estimated in two stages. First, the annual soil loss was determined using the RUSLE Model and in the second stage, the Sediment Delivery Ratio (SDR) was applied to estimate sediment yield. Using three different empirical SDR-equations, the estimated average annual sedimentation rate at the gauging station location using this approach was 0.303 mm/year, 0.203 mm/year, and 0.226 mm/year, respectively.

The sediment load to the reservoir was also estimated from available data for the period 2009-2015 employing two approaches. In the first approach, the measured suspended sediment load was combined with bed load transport rates estimated from various computational approaches. In the second approach, both the suspended and bed load were computed. The average annual sedimentation rate resulted from these approaches ranged from 0.13-1.22 mm/year and that of bed load calculated ranged from 10-25% of the suspended sediment load.

The comparison of the results from the different approaches showed that the estimated sedimentation rate ranged from 0.13-0.63 mm/year. For the subsequent prediction of the reservoir sedimentation, a mean value of 0.50 mm/year was used taking into consideration a safety factor of 1.3 to account for potential extreme events resulting from landslides due to glacier lake outbursts. New Zero-capacity Elevation (NZE) determined with the application of Empirical Area Reduction method for 30, 50 and 70 years are 1908 m, 1926 m and 1944 m respectively indicating that even after 70 years of reservoir operation, the sediment deposit level will be well below the Minimum Draw Down Level (MDDL) if there is no flushing of the

sediments. However, the sediment will be flushed during monsoon season with low level spillway sluice that will be installed at 1915 m, whereby sediment will never rise beyond this level (DHPS, 2013). The perspective downstream impact due to reservoir sedimentation were studied through literature reviews.

DECLARATION

The thesis work titled "Reservoir Sedimentation Study for Bunakha Hydro-electric Project" has been undertaken from January 2016 to June 2016 at the Department of Hydraulic and Environmental Engineering, Faculty of Engineering Science and Technology, Norwegian University of Science and Technology (NTNU) as the partial fulfillment for the Msc. Hydropower Development.

The author hereby declares that the presented work is my own and significant outside input has been duly acknowledged.

Choten Duba

June 2016

NTNU, Trondheim, Norway

ACKNOWLEDGEMENT

I would like to express my sincere gratitude to my supervisor, Professor Jochen Aberle, Department of Hydraulic and Environmental Engineering, Norwegian University of Science and technology (NTNU), for his constant supervision and immense support rendered throughout the Thesis period without which this development of this Thesis would not have been possible.

My gratitude also goes to Professor Knut Alfredson and Msc. Hydropower Developed graduate student Abebe Girmay Adera for their helping hand in using GIS application for my thesis.

My sincere thanks goes to officials of Department of Hydro-met Service under Ministry of Economic Affairs (MoEA), Bhutan, namely Mr. Pushupati Sharma, Mr. Tshencho Dorji, Mr. Pema Wangdi and Mr. Ajay Pradhan, and officials of Department of Hydropower and System, MoEA, Bhutan namely Ms. Dechen Wangmo and Ms. Kinzang Wangmo for supplying all the necessary data required for the Thesis amidst their busy schedule. I would also like to express my thanks to Mr. Minjur of Department of Renewable Energy, MoEA, Bhutan for facilitating the data collection which I believe had expedited the process.

I would also like to express my gratitude to Ms. David Alan Wright and Mr. Morten Berthelsen Johnsen of Norwegian Water Resources and Energy Directorate (NVE) for facilitating my stay in Norway without which it would not have been possible to come to Norway to study Mrs. Hydropower Development at NTNU.

I would like convey to my thanks to my wife Tshering Choden and daughter Tenzing Tshering Yangden for their continued encouragement, inspiration and support during my pursuit of Master program and moreover bearing with me for having gone from their life for two long years.

Last but not the least, I would like to take this opportunity to dedicate this Thesis work to my dearest parents, near or far, who have always been there by my side with all the love and care in this world.

Table of Contents

LIST OF FIGURES

LIST OF TABLES

ABBREVIATIONS

BHEP – Bunakha Hydro-electric Project

DEM – Digital Elevation Model

DHMS – Department of Hydro-meteorology Services

DHPS – Department of Hydropower and Power Systems

DSMW – Digital Soil Map of World

GIS – Global Information System

HWSD – Harmonized World Soil Data

IDW – Inverse Distance Method

MCM – Million Cubic Meter

MoEA – Ministry of Economic Affairs

PSIAC – Pacific Southwest Inter-Agency Committee

RUSLE – Revised Universal Soil Loss Equation

SDR – Sediment Delivery Ratio

SSL - Suspended Sediment Load

USLE – Universal Soil Loss Equation

CHAPTER 1: INTRODUCTION

1.1 General Background

The kingdom of Bhutan is a landlocked country at the eastern end of the Himalayas which is characterized by many snow and glacial fed rivers with steep slopes and large discharges. Consequently, Bhutan has a rather large hydropower potential of around 30,000 MW of which about 23,760 MW are found to be technically feasible and around 6.8 % being exploited until today (DHPS, 2013).

99% of the electricity generation in Bhutan is from Hydropower and it is the main source of revenue for the country beside Tourism Industry. Most of the hydropower plants developed until today are of the type "run-of-the-river" with only a small peaking storage. These plants produce electricity which is mostly exported and the energy supply for domestic consumption is met from the royalty energy provided constituting about 12-18 % percent of the installed capacity of large and mega plants and from micro/mini hydropower plants. During the low flow period in the winter season the energy generated from the existing plants are at the lowest level thereby directly influencing the revenue generation of the country. The volume of water available, which is considerably dependent on monsoon precipitation and partly from snow melt is expected to worsen due to the effect of climate change. In this regard, hydropower with reservoir scheme may offer a possible solution to address future challenges and it is of the view that it is the right time for Bhutan to plan for the same.

A novel hydropower project in Bhutan which is yet to be cleared is the 180 MW Bunakha reservoir scheme. The project, which is one of the first reservoir schemes planned in Bhutan, is expected to be implemented after June 2016. With an estimated cost of 29.5 billion Bhutanese Ngultrum (equivalent to 3.6 billion NOK or US$ 442 million), the project is presently planned to be undertaken as a joint venture between the two public sector companies – Druk Green Power corporation (DGPC) and Tehri Hydro Development corporation limited (THDC), India, with an equity shareholding of 50 percent each.

The planned reservoir will collect the discharge from a catchment area of 3558 km^2 and will have a gross storage of 329.16×10^6 m^3 (live storage 250.62×10^6 m^3) and an area under submergence at full reservoir level (corresponding to 2006 m.a.s.l.) of 6.82 km^2. The mean annual discharge at the site corresponds to $2{,}619 \times 10^6$ m^3 and the probable maximum flood to 10,028 m^3/s. An uncertain issue with regard to the planned reservoir scheme is related to the sedimentation rate in the reservoir which has been assumed to correspond to 1 mm/year (DHPS, 2013). One reason for this uncertainty is related to the limited available data comprising only

the period from 2008 until today. The present thesis will therefore investigate sediment inflow in the reservoir and hence reservoir sedimentation in more detail.

1.2 Objective of the study

A literature review showed that sediment yield studies at the catchment scale in Bhutan are basically absent but the studies exist that were carried out at the country scale. However, the use of generalized sediment yield values from such large scale studies can result in either overestimation/underestimation for the design of the sediment facilities of the hydropower project. It has been a general trend in Bhutan to establish sediment gauging stations only when these are required for the planning of hydropower plants, i.e. that it is rare to find such gauging stations installed when there are no prospective plans for hydropower project development. Due to this reason, most of the sediment gauging stations have been established only recently and hence the available data spans only a very short time period.

Bearing this background information in mind, the following objectives can be formulated for the thesis:

1. Literature review on methods to determine reservoir sedimentation rates at sites with limited available data including a critical review on corresponding uncertainties.
2. Description of the Bunakha reservoir scheme, catchment characteristics, and the available hydraulic and sediment data.
3. Determination of the sediment yield/budget for the reservoir using appropriate methods identified in the literature review.
4. Estimation of the annual sedimentation rate based on the determined sediment yield
5. Comparison of the obtained results with the results presented in the detailed design report.
6. Predicting Bunakha reservoir sedimentation based on the sedimentation rate obtained.

1.3 Methodology of the study

For the reservoir sedimentation study of Bunakha Hydro-electric Project, the present study attempts to study the sedimentation yield of the Bunakha Catchment through two independent approaches viz. i) Application of Pacific Southwest Interagency Committee (PSIAC) and Revised Universal Soil Loss Equation (RUSLE) approach integrated with Geographic Information System (GIS) which are found to be well applicable in scarce data situation like in the case of study area, and ii) Data analysis of available suspended sediment data of a gauging station located close to the planned Bunakha reservoir.

The trapping efficiency of the reservoir were estimated using Brune's curve (Brune, 1953) and for the prediction of sediment deposit in the reservoir, the Empirical Area Reduction Method was used which was developed to distribute sediment deposits within a reservoir as a function of depth. It projects the shift in the stage-storage curve as a result of sediment deposit (Morris and Fan, 1998) and from the New Zero-capacity Elevation (NZE) computed for different time horizons, the revised storage capacity and area of the reservoir were also determined. The perspective downstream impact due to reservoir sedimentation were studied through literature reviews. The flow chart illustrating the methodology used is presented in Figure 1.1 below:

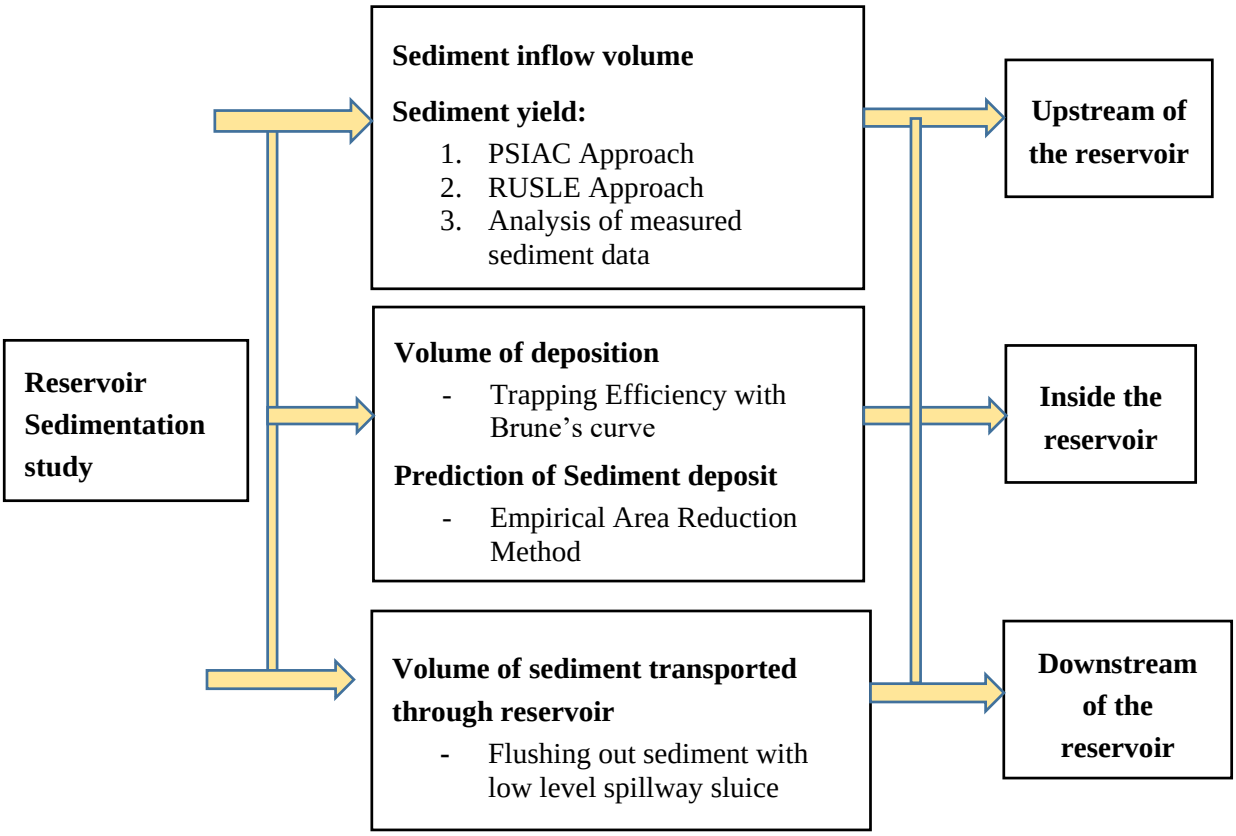

Figure 1.1: Flow chart for methodology of Reservoir sedimentation study for the Bunakha Hydro-electric Project.

It is to be noted that the detail literature review of methods adopted for estimating sediment yield for the current study such as PSIAC and RUSLE approaches in integration with GIS and computation methods used for sediment data analysis are detailed out in their respective chapters for convenient where they are applied.

1.4 Organization of the Thesis

The present study is based on two different approaches identified in a literature review related to reservoir sedimentation rate as well as the analysis of observed suspended sediment data obtained from gauging station for reservoir scheme Bunakha Hydro-Electric Project. Each chapter of the thesis is described in brief below.

Chapter 1 describes a general background about hydropower, sediment data situation and planned Bunakha Hydro-electric Project in Bhutan. It also briefly describes the importance of reservoir scheme hydropower projects amidst numerous run-off-river hydropower projects and hence establishes the objective to determine sedimentation yield with chosen methods.

Chapter 2 points out the reservoir sedimentation study in global context, sediment studies done in other Himalaya regions followed by past sedimentation studies carried out in Bhutan in particular. It also provides the sediment rates estimated in various Detail Project Report (DPR) of hydropower projects in Bhutan.

Chapter 3 provides the salient features of Bunakha Hydro-electric Project which are relevant for sedimentation study along with current status of the project. The catchment characteristics of Bunakha is also briefly described in this Chapter.

Chapter 4 gives brief information about gauging station, suspended data collection method, assessment of data quality, and predicting and filling in the missing suspended sediment data.

Chapter 5 provides sediment yield determination by PSIAC approach with GIS integration. The reasons for choosing such a method are also described. This chapter explains in detail the preparation of each parameter in GIS and how it leads to estimates of sediment yield using the rating guidelines for each parameter/factor provided by PSIAC (1968). The results are discussed at the end of this chapter.

Chapter 6 provides sediment yield estimation with RUSLE approach with GIS integration. This chapter explains in detail the preparation of each factor involved using GIS and discusses the results obtained at the end.

Chapter 7 provides the sediment yield estimation from the observed suspended sediment data and computation of bed loads using various empirical bed load equations. It also attempts to compute suspended sediment load and compares with the observed one. At the end, it also summarizes the sediment yield obtained from PSIAC, RUSLE and data analysis and determines the sedimentation rate to be used for predicting reservoir sedimentation.

Chapter 8 provides the predicting of reservoir sedimentation using Empirical Area Reduction method and also estimates the exhaustion period of reservoir. Long terms perspective of the

sediment yields due to disturbances upstream and impact of Bunakha reservoir to the downstream plants are also described in brief.

Chapter 9 discusses the results obtained from different methods adopted and summarizes the conclusions, points out limitation of the present study and recommendations.

The detail calculations and other necessary enclosures for the thesis are presented in Appendices.

CHAPTER 2: SEDIMENTATION STUDIES

2.1 Reservoir Sedimentation

Continual storage loss due to sedimentation is one of the problems faced by reservoirs apart from numerous other sediment related issues. Even a slightest percentage of the reservoir volume sedimented were found to affect the operation of the reservoir. In due course of time, as the sediments continue to accumulate, so will be the severity of its affect (Morris and Fan, 1998). However, the rate at which reservoirs loss its capacity depends on the sediment inflow rate into the reservoir, its operational plan, shape, etc. and therefore, varies from region to region. Globally, the overall annual rate of reservoir storage capacity loss is estimated at 1-2 % of the total storage capacity (Xiaoqing and Yang, 2003, Mahmood, 1987). The cost of restoring the loss and rebuilding the dams was estimated at US$ 13 billion (Palmieri et al., 2003). Due to this fact, restoration of loss or rebuilding large reservoir in most cases become irreversible process. Therefore, if future generation has to benefit from the reservoir operations, that should be through constant preservation and utilization of existing reservoir, not through continued exploitation of already rapidly shrinking resources for reservoir (Morris and Fan, 1998)

2.2 Sediment studies in Himalaya regions

In the Himalaya region, rivers mostly originate from glaciers from high reaches of mountains as step pool streams on bed rock. As they further torrent downstream, there is drastic change of river beds from boulder to gravel before they flow gently on a bed of sand and silt. Owing to such characteristics, Himalayan watersheds have very complex nature of sediment transport. It has been reported that sediment transportation pattern in Himalaya varies from one region to another as well as from river to river, and sediment studies become even more difficult when data are limited, especially at the area of interest (Støle, 1993).

Numerous sediment studies have been carried out in the Himalaya region and a few selected ones are briefly discussed here.

Gabet et al. (2008) computed erosion rates for 10 watersheds in Nepal to establish that in tectonically active areas, which is one of the main characteristics of Himalaya region, the annual erosion rates increase with increase in precipitation and runoff. They hypothesized that spatial distribution of increased precipitation and erosion are connected to tectonic process. The estimated rates showed that the values range from negligible (zero) to as high as 3.0 mm/year. The higher rates were found in places having high runoff value. It was also found that higher

elevation has relatively lower erosion rate compared to lower elevation of the wet southern Himalaya region.

Collins and Hasnain (1995) studied runoff and sediment transport from glacierized basins at the Himalayan scale. At upper Indus basin, Karakoram mountains which encompass the Batura glacier region, the discharge along with the sediment content of the meltwater were measured at desired time travels. It was found that Batura glacier contributed 6068 ton/km^2/year of sediment load where the sedimentation rate is considered higher than other glacier of the same region namely Choota-Shigri and Dokriani, contributing 60% of the sediment loads of the rivers in the Karakoram. On the other hand, although the upper Indus basin constitutes 17% of the area, it contributes 35% of discharge to the region and that might be the reason for immense sediment rate.

Hasnain (1996) observed a relationship between suspended sediment transport and discharge. It was found that sediment transport rate reacts variably and slowly to discharge on the seasonal scale. The study concludes that the sediment transportation rates are affected by glacier area, glacier advancing/retreating and change of glacier drainage systems.

The study of bedload to suspended load ratio by Pratt-Sitaula et al. (2007) identified that ~35% of the sediment transportation rate constitutes bed load which is within the range (5 - 35%) of bed load portion suggest by Lane and Borland (1951), depending upon the constituents of bed materials of stream channels. However, they proposed that for more accurateness of the sediment load computation, bed load should be considered 50% of the total suspended load in the region of rapidly eroding mountain catchments.

Cornwell et al. (2003) made use of field measurement data and computer models to estimate sediment transport and denudation rate for the Raikot and Buldar drainage basins and upper reach of the Rupal drainage basin situated in Nanga Parbat Himalaya, Pakistan. The modern denudation rates calculated on Nanga Parbat ranged from less than 1 mm in upper Rupal drainage to 6 mm/year in Raikot, and Buldar drainage networks which is characterized by high flow energy compared to the upper Rupal drainage.

2.3 Past studies of Sedimentation in River Basins of Bhutan

Past studies with regard to sedimentation in rivers basins of Bhutan are rare to find. Over the past years, there have been only few studies carried out on sedimentation study as listed below:

1. Thesis work carried out by Mr.Tashi Dorji at NTNU, Norway on “Headworks Design and Sediment Handling at Punatsangchu Hydropower Plant” in 2003 in which the

headworks design and sediment handling of the 870 MW Punatsangchhu-I Hydropower Project were reviewed and assessed.

2. Thesis work carried out by Ms. Sonam Choden at Lund University on "Sediment Transport Studies in Punatsangchu River, Bhutan" where the sedimentation rate for the basin was computed to 0.28 mm/year based on the data period of 1992-2008. The thesis also comprises a detailed literature review about the Himalaya sedimentation situations.

In addition, there exist numerous Detail Project Reports (DPR) which were prepared for various upcoming and already constructed hydropower projects in Bhutan. As per their findings, most of the sediment rates were found to be lower than what can be expected in the Himalaya region. There could be several reasons for such findings, one being the quality of the collected sediment data. Thus, in order to assess the quality of available sediment data, a separate study should be carried addressing the adopted sediment data collection methods and laboratory set ups of Bhutan. The sediment rates reported in DPR of Wangchu Hydro-Electric Project (4x142.5 MW) obtained from Department of Hydropower and Power System, MoEA, Bhutan are shown in Table 2.1. The DPR had also reported that sediment rate computed for the existing Tala Hydro-electric Plant (1020 MW) located in the same river but downstream of the planned Wangchu Hydro-electric Project was 0.2 mm/year (DHPS, 2014).

Table 2.1: Sediment rates as reported in DPR of Wangchu Hydro-Electric Project

SN	Sediment measuring station	Period of availability	Average Sediment Rate (mm/yr)	Remarks
1	Wanggkha Chukha D/S	1994-2002	0.0851	Complete data not available for 1996 & 2000
2	Chukha TRT	2005-2009	0.0709	Complete data not available for 2006, 2008 & 2009
3	Chukha	2005-2009	0.0017	Complete data available for 2006
4	Downstream of Chukha confluence with Lobichu	2005-2009	0.0678	Complete data not available for 2009
5	Lobichu	1994-2007	0.0763	Complete data not available for 2005
6	Piping	1994-1995	0.5601	

Most of the rates illustrated in the table are rather low and the reason could be that these sediment rates were recorded downstream of the existing Chukha Hydro-electric Plant (CHEP) developed along Wangchu river, where suspended sediment loads might have been intercepted by the Chukha dam. However, Piping, a river which joints the Wangchu river as the tributary further downstream has a computed average annual sediment rate as 0.56 mm/year. This rate is much higher than what was observed downstream of the existing CHEP and this can be explained by the river damming.

In the DPR of Kholongchu Hydro-electric Project (4x150 MW), the sediment data from gauging stations of Bjizam in Mangdechu River and Kurjey in Kurichu River were used for the computation of sediment transportation load. The computed average annual sediment rates were 0.15 mm/year for Bjizam and 0.56 mm/year for Kurjey sediment gauging stations. The assumed bed load was reported as 20% of the suspended load in the computations and was hence not based on any bed load measurements.

As far as the available information from the DPRs are concerned and despite the fact that most of the DPR studies for hydropower projects have their computed sediment rates ranging up to 0.56 mm/year, a sediment rate of 1mm/year was often adopted for the design of headworks and assessment of sediment inflow into the reservoir. It was reported that the reason for adopting sedimentation rate as 1mm/year is related to sediment yield studies of tributary rivers of Brahmaputra river which descends from other Himalaya regions. However, the assumption that this value can be used generally for the rivers of Bhutan has not been validated so far. Nevertheless, the rate of 1 mm/year has been used as the design input for almost all the hydropower projects and hence, this might have caused over/under design of the headword components and dam structures associated with sediments.

CHAPTER 3: BRIEF DESCRIPTION OF BUNAKHA HYDRO-ELECTRIC PROJECT

3.1 Salient feature of the project

It is to be noted that only those features of the project which are relevant for the current study has been described below.

Location and reservoir

The project is located in Bunakha village at 27°08'00''N and 89°32'33''E within Wangchu Basin. The planned reservoir will collect the discharge from a catchment area of 3558 km^2 and will have a gross storage of 329.16x10^6 m^3 (live storage 250.62x10^6 m^3). An area under submergence at full reservoir level (corresponding to 2006 m.a.s.l.) of 6.82 km^2 and estimated to stretch about 17.25 km upstream. The mean annual discharge at the site corresponds to 2,619x10^6 m^3 and the probable maximum flood to 10,028 m^3/s. The elevation which corresponds to Minimum Draw Down Level (MDDL) or also referred to as Lowest Regulated Water Level (LRWL) is 1950 m.a.s.l. The capacity inflow ratio of the reservoir was computed as 0.13 or 13% and the sedimentation rate adopted for the design of headwork was 1 mm/year. (DHPS, 2013). Location of Bunakha Hydro-electric Project is illustrated in Figure 3.1 below.

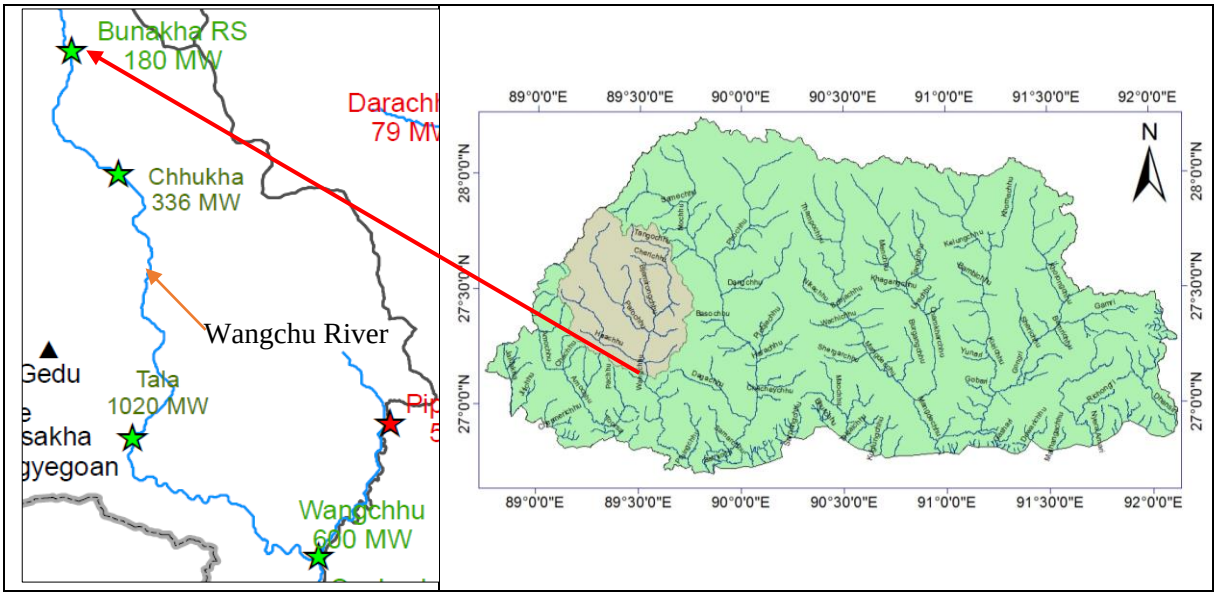

Figure 3.1: Location of Bunakha Hydro-electric Project. Source DHPS, MoEA, Bhutan.

Installation

The nominal capacity of the Bunakha Hydro-electric Project will be 180 MW in total with 3 units of 60 MW each and it will be developed as a reservoir storage scheme for peaking purpose. The power house will be located at the Dam toe in the left bank of Wangchu River (DHPS, 2013)

Sluice Bay Radial Gates (Low level Spillway sluice)

The low level spillway sluice which is of Sluice Bay Radial Gates types of 6 numbers are proposed to be installed for flushing sediment load at an elevation 1915 m.a.s.l where its level of center of trunnion will be at 1926 m.a.s.l. It will be operated by lowering or raising under unbalanced head conditions with double cylinder hydraulic hoist of 175 Metric Tons lifting capacity (DHPS, 2013).

Detail about intake gates and Trash racks are illustrated below:

Table 3.1: Intake gate features (DHPS, 2013)

Intake Gates	
Type of gate:	Fixed wheel with downstream skin plate & downstream seals
No. of bays:	3
Size of opening:	3.50 m (wide) x 4.25 m (high)
Sill level:	EL. 1940 m.a.s.l
Design head:	66.0 m
Operation gate:	By Hydraulic Hoist

Table 3.2: Trash Racks features (DHPS, 2013).

Trash Racks	
Type of trash racks:	Inclined
No. of bays:	6 (3 tunnels having two bays each)
Clear width:	5.75 m
Total vertical height of trash rack	9.15 m
Sill level:	EL. 1939 m.a.s.l
Operation:	By auxiliary hoist attached with trash racks; 7.5 MT capacity

Project Status:

With an estimated cost of Nu 29.5 as of 2013 rate billion (equivalent to 3.6 billion NOK or US$ 442 million), the project would be undertaken as a joint venture between the two public sector companies – Druk Green Power corporation (DGPC) and Tehri Hydro Development corporation limited (THDC), India – with an equity shareholding of 50 percent each. Currently, it is being followed up with the Government of India and implementation of selected projects will be taken up in subsequent years after obtaining Government of India's investment clearances.

3.2 Catchment Characteristic of Bunakha

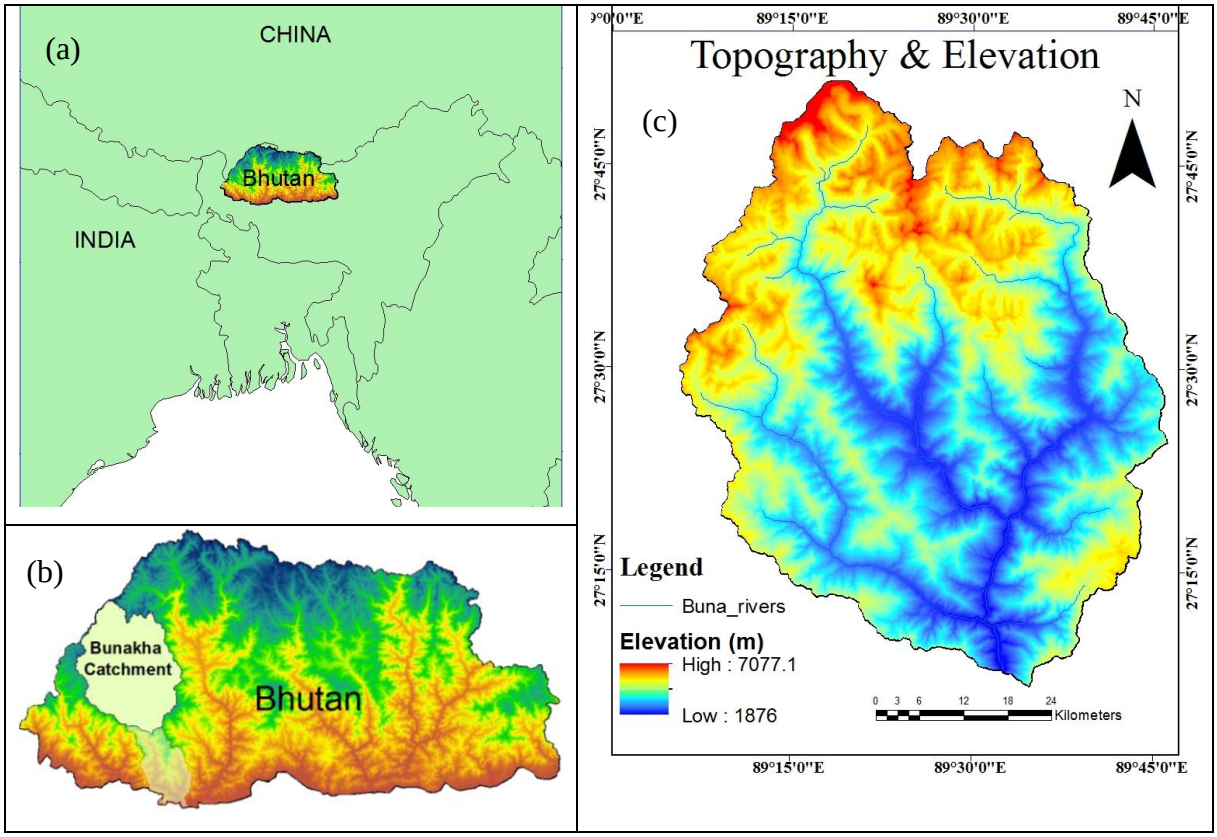

Figure 3.2: (a) Location of Bhutan relative to surrounding countries; (b) Location of Bunakha Catchment within Wangchu Basin in Bhutan map and (c) Digital elevation map of Bunakha catchment. Source: DHPS, MoEA, Bhutan

As shown in the Figure 3.2, Bunakha catchment is located within Wangchu Basin towards western part of Bhutan within 89°6'-89°46'E and 27°6'-27°51' with a total drainage area of approximately 3558 km^2. It is characterized by steep terrain with altitude ranging from 1876 m.a.s.l to as high as 7077 m.a.s.l with majority of the terrain slope exceeding 30% as per the extraction of Digital Elevation (DEM) Map. Some part of the catchment area lies into the glacier zone attributed to its high altitude. The annual average rainfall ranges from 555-2373 mm/year based on the five rainfall gauging station data period from 2008-2015 (refer Table 5.6). The mean annual runoff as reported in DPR is 2619 mil. m^3 (DHPS, 2013) at the point of reservoir location. It was reported that majority of the runoff is driven by the summer monsoon rains. It is possible that snow melt would also be contributing to the flow, however, further study is still required to be done in order to quantify its contribution (Xue et al., 2013).

Geologically, the Bunakha catchment lies in the Western Bhutan spread over three physiographic zones namely Greater Himalaya, Tethyan Himalaya and Lesser Himalaya (refer

Table 5.4). Upper reaches of the catchment fall in the Kula Gangri-Chomolhari mountain range with sharp-crested ridges and deep-set glacial valleys, margined in the east by Chumbi and Natu valleys as also discussed in section 5.2.2 of Chapter 5.

The analysis of the land cover/use map shows that the most dominant land cover in the Bunakha Catchment is forest with 84.18% followed by water bodies of 9.64% which includes snow, glaciers, reservoir, rivers and lakes. Agricultural land constitutes of 3.13 % of the total catchment area. The remaining 3.05% encompasses settlements, non-built-up areas, screes and moraines land covers (refer section 5.2.6 of Chapter 5)

The soil type in the catchment is dominated by sandy clay loam soil with 75.41% followed by loam soil with 24.56% of the total catchment area.

More detail about the catchment characteristics covering topography, surface geology, runoff, precipitation, land cover/use and soil are discussed in detail while estimating sediment yield using PSIAC and RUSLE approach in Chapter 5: and Chapter 6: respectively.

3.3 Sediment Management Plan

As per DPR of Bunakha Hydro-electric Project, provision for flushing out sediment through the dam structure by incorporating low level spillway sluice for the sediment management has been proposed. The low level gated spillways are to be set below power intake level (i.e. at 1940 m.a.s.l) with invert at an elevation of 1915 m.a.s.l. There will be six spillways of 6m width and 9m height. It has also been reported that the capacity of the low level gated spillway will comfortably exceed the minimum flows required for sediment flushing, emergency drawdown and other control requirements. The intake level is proposed to be located 25m above the level of the spillway crest which will keep the intake well clear of sediment deposits in the reservoir (DHPS, 2013).

CHAPTER 4: SEDIMENT DATA

4.1 Available Data and its Quality Control

The gauging station from which the suspended sediment data used in this present study is located at 89.5245 E and 27.2503 N about 3 km upstream of the planned Bunakha Hydro-electric Project. The data measurement was started in mid of 2008 only. For the present study the data series for the period 2008-2015 was acquired from DHMS, MoEA, Bhutan. However, it was observed that the data for the year 2008 was incomplete, therefore, it was not used for the computation of suspended loads.

The suspended sediment data is measured on a daily basis consisting of fines (d <0.062mm) and sand (d>0.062 mm) concentration in Parts per Million (ppm) with a depth integrating sediment sampler operated from the cableway facilities while the daily discharge which is required for suspended load computation is measured from stage-discharge record. The gauging station has bank operated cable way facilities installed as shown in the picture below.

Picture 4.1: Cableway facilities installed at Tamchu sediment gauging station at Tamchu (Source: DHMS, MoEA, 2015)

Visual inspection of sediment concentration data of both fines and sand, was carried out to assess its completeness. It was found that there were few missing data in every month except for the year 2010. Therefore, in order to predict the missing suspended concentration, a method with Sediment Rating Curve reported by Julien (2002) was used for this study and the missing data were filled accordingly. The curve is usually presented in one of the basic forms, either as a suspended sediment concentration to streamflow or suspended discharge to streamflow relationship (Walling, 1977) and for this study the former approach is used.

The SRC is expressed as:

$$SSC_{(t)} = aQ_{(t)}^{b} \qquad \text{Eq. 4.1}$$

Where:

$SSC_{(t)}$ = Daily Suspended sediment concentration (ppm);

a and b are contanst which depends upon river flow characteristics ;

$Q_{(t)}$ = Daily river discharge (m^3/sec).

For determining the SRC, log transformation of suspended sediment concentrations and flow data were carried out.

Though, predicting suspended sediment concentration by using SRC has limitations (Walling, 1977), it was nevertheless decided to use it as the missing data are few in numbers and its effect of limitations will not be significant for the larger picture.

The SRC equations developed were as follows:

$$SSC_{(t)} = 0.0052Q_{(t)}^{1.7527} \qquad \text{For fine suspended sediment data}$$

$$SSC_{(t)} = 0.0495Q_{(t)}^{1.3878} \qquad \text{For sand suspended sediment data}$$

The discharge data measured at the gauging station were found to be 100% complete. In order to check if the discharge values were consistent with other gauging stations, their consistency and homogeneity were checked with discharge records of both upstream and downstream gauging stations. Hence, double mass curves were plotted against cumulative discharge series of Tamchu with Lungtenphu station located (27.440 N, 89.660 E) upstream (refer Figure 4.1) and Chukha Dam stations located (27.10 N,89.53 E) downstream stream of Tamchu (refer Figure 4.2).

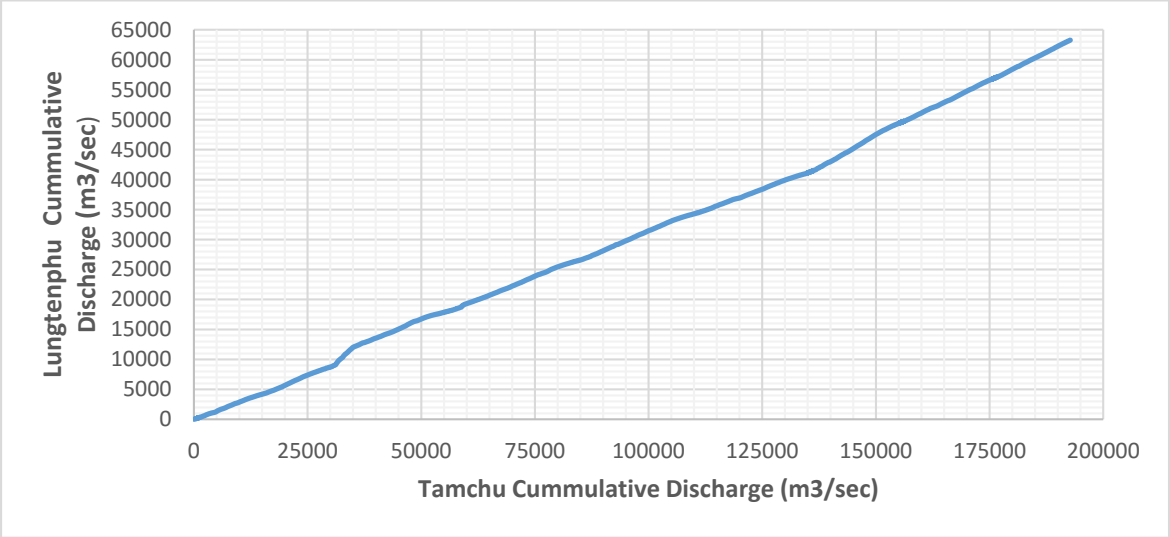

Figure 4.1: Double mass curve-Tahmchu station vs Lungtenphu station (located upstream)

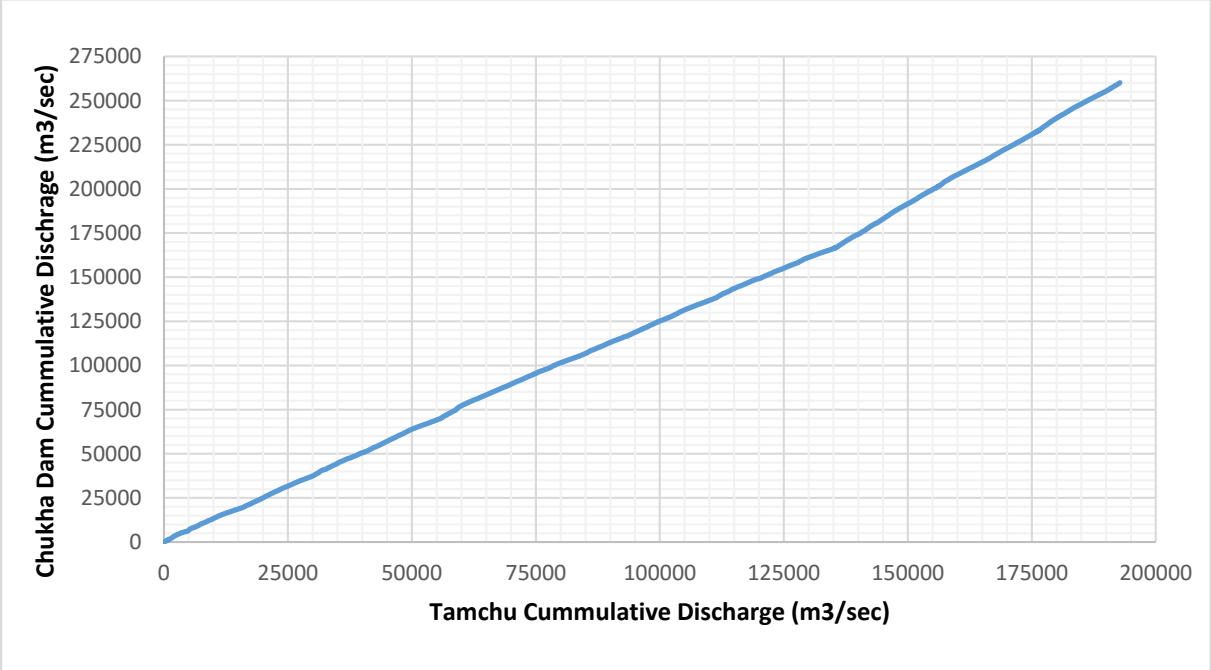

Figure 4.2: Double mass curve-Tahmchu station vs Chukha Dam station (located downstream)

Since there is no significant change in the slope of plot line for cumulative discharges of Tamchu plotted against cumulative discharges of its both upstream and downstream rivers as illustrated Figure 4.1 and Figure 4.2 respectively, Tamchu's discharge data series can be considered as having good consistency with respect to both upstream and downstream gauging stations.

CHAPTER 5: SEDIMENT YIELD DETERMINATION BY PSIAC APPROACH

5.1 Concept & methodology for PSIAC Approach

There are numerous models available for estimating soil loss and sediment yield such as Soil and Water Assessment Tool (SWAT), Water Erosion Prediction Project (WEPP), etc., however, they are considered to be data extensive and partly too complex to be used as a planning tool. Therefore, for the present study, a simple and more generic approach known as PSIAC (Pacific Southwest Inter Agency) model was applied to estimate the sediment yield. Unlike other models, it requires less data and computational resources (Ndomba, 2013) and it is easy to use as well.

The PSIAC approach for estimating sediment from a watershed was introduced by Pacific Southwest Inter Agency in 1968 for the planning purposes in the United States for watershed larger than 26 km^2. It involves taking into consideration of 9 factors of the watershed of the study area viz. i) Topography; ii) Surface Geology; iii) Soil; iv) Climate; v) Runoff; vi) Ground/Land Cover; vii) Land use; viii) Upland erosion; and ix) Channel Erosion (PSIAC, 1968).

The PSIAC approach for estimating sediment yield falls in category of semi-quantitative model which is based on the combination descriptive and quantitative approaches to characterize a drainage basin. The results obtained are quantitative or sometimes qualitative at basin level. Though the development of PSIAC model was primarily for arid and semi-arid areas in the southern USA, its application was also proven to be effective in Himalaya region as well using GIS environment (Garg and Jothiprakash, 2011).

The accuracy of the prediction of sediment yield using the PSIAC approach largely depends on ratings adopted for a given watershed and their representability to the watershed's variability. This calls for the use of a Geographic Information System (GIS) which in the past has shown its effectiveness in analyzing large numbers of spatially diverse watershed (Woida et al., 2001). Woida et al. (2001) have tested the GIS adaptation of PSIAC for predicting the sediment yield and their study showed that it is not only possible to build GIS that replicates the PSIAC procedure in more detail, but that the approach can also be applied to a much larger catchment area and that GIS is able to produce detailed view of each factor as a spatial visual map. One of the identified major advantages was that the PSIAC approach linked with GIS is time saving provided that maps and data for preparing factors of the basin are readily available, especially compared to a manual assessment of the catchment characteristics that restricts its application to smaller catchment areas due to the requirement of laboursome measurement in the field.

The effectiveness of PSIAC approach was also proven by researchers (De Vente et al., 2005, Tangestani, 2006) and was also validated by Ndomba (2013) in ungauged catchments in Tanzania where the results obtained were found to be fairly close to the measured data.

5.1.1 Rating guidelines suggested by (PSIAC, 1968)

The nine factors defining the characteristics of the basin were assigned a numerical rating value representing the relative importance of each factor involved in the sediment yield estimation. The summation of the individual factor rating gives the total PSIAC index which can be translated into an estimated sediment yield in tons/ha/year as summarized in the Table 5.1. The rating guidelines for each of the nine factors for developing the PSIAC model are enclosed as Appendix A, Table A1.

Table 5.1: PSIAC total rating ranges and its sediment yield classification

PSIAC Index (Total Rating)	Estimated Sediment yield ranges (tons/ha/year); For the Pacific Southwest USA	Class
>100	>18.3	Very high
75 – 100	6.1 – 18.3	High
50 – 75	3.0 – 6.1	Moderately high
25 – 50	1.2 – 3.0	Moderate
0 - 25	<1.2	Low

5.2 Data & material preparation for PSIAC Approach

Using a DEM raster map with 25m resolution obtained from Department of Hydropower and Power Systems under Ministry of Economic Affairs (MoEA), Bhutan, the first and foremost task was the catchment delineation, also referred to as creating watershed boundary for Bunakha catchment. Therefore, as the initial process, the DEM raster map was filled using “Fill” tool available within Spatial Analyst tool of ArcMap in order to eliminate artefact depressions and flat areas. Then the next step was to create flow direction followed by flow accumulation. With pour point inserted on the streamline coinciding with the location of Bunakha Hydro-electric Project location and using watershed tool, the Bunakha catchment boundary was thus delineated.

In the present study, in order to carry out PSIAC approach with GIS integration, Bunakha Catchment was divided into 1km by 1km grid cell sizes. PSIAC rating were assigned to each grid cell and subsequently, sediment yield was estimated after summing up PSIAC index in each cell and then after translating it to yield in tons/ha/year. It was also possible to produce

thematic maps for various rating indexes related to each factor which were later spatially joint to provide a map of sediment yield to represent its spatial distribution. The conceptual framework of sediment yield estimation by PSIAC approach is enclosed as Appendix A, Figure A1.

The procedure adopted for determining each factor of PSIAC with use of ArcMap tool is illustrated in the following sections.

5.2.1 Topography

The DEM raster map was processed in ArcMap to generate the slope percent map of the study area. The topographic parameter for PSIAC which is further translated to slope percent map were generated using the ArcMap tool. The topography of Bunakha catchment is characterized by steep terrain with altitude ranging from 1876 m.a.s.l to as high as 7077 m.a.s.l as per the extraction of Digital Elevation Map (DEM) as shown in the Figure 5.1 below.

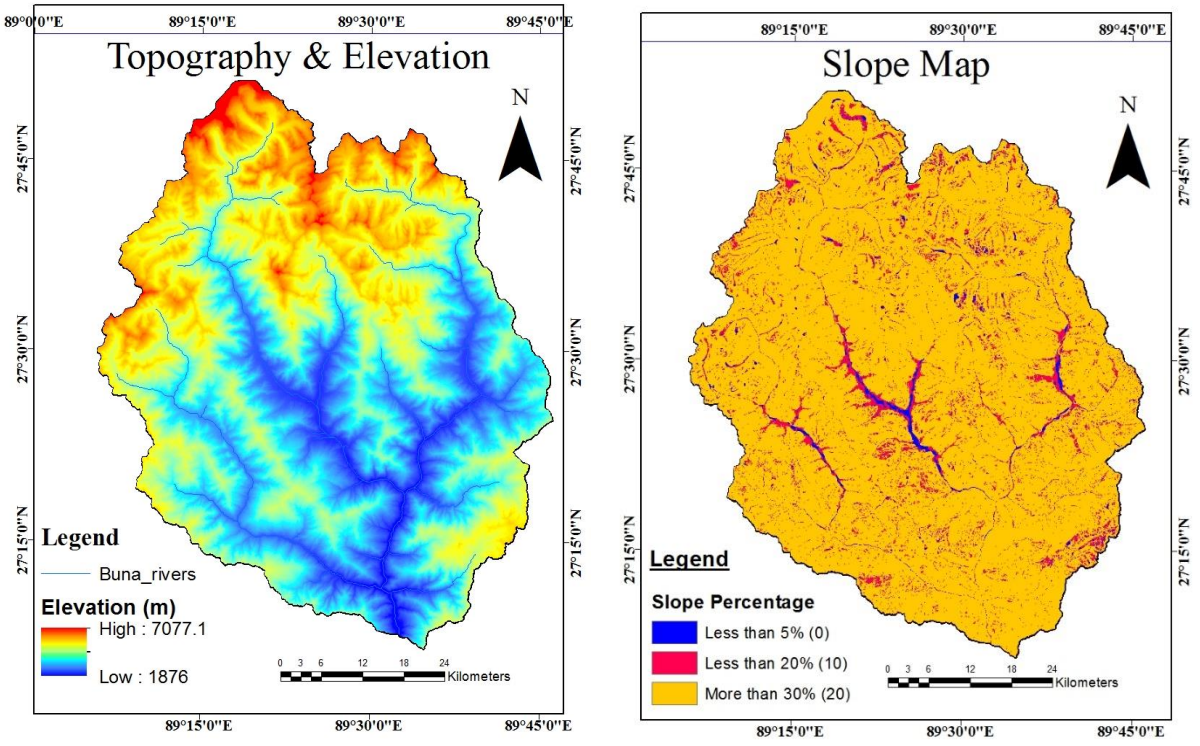

Figure 5.1: DEM Map (*Left*) and slope percentage map with ratings for each class for Bunakha Catchment (*Right*).

Some part of the catchment area has high altitude and lies in the glacier zone. The map is classified into three slope classes viz. i) less than 5%, ii) Less than 20% and ii) in excess of 30% with ratings 0, 10 and 20 respectively as suggested in PSIAC approach. The slope percent map showing the rating for each class is presented in Figure 5.1 and visualizes that the majority

of the area falls within slope class in excess of 30% indicating that the catchment has high potential for sediment yield as steep slopes result in rapid runoff. However, the steep slope mountains are seen to produce varying sediment yield depending on parent materials, soil types and land cover (PSIAC, 1968). Table 5.2 below shows the slope percentage and area that each class occupies in the catchment along with their assigned ratings.

Table 5.2: Slope class and its area coverage in the catchment

SN	Slope Class	Area (sq.km)	PSIAC rating	Area %
1	< 5%	57	0	1.60
2	< 20%	285	10	8.01
3	20% to 30%	348		9.78
4	> 30 %	2868	20	80.61

The slope percent map was converted into vector format and spatially joint with the gridded map of the study area. The attribute table which contains the slope percent in each cells were exported in Excel file format. Using Excel, the PSIAC ratings were assigned to each grid point according to the slope it contains and thereafter joint with gridded attribute table with ArcMap for combination with other factors of the PSIAC approach.

5.2.2 Surface Geology

The geological map (scale-1:500,000) obtained from Journal of Maps developed by Long et al. (2011) were in the PDF format. In order to process and classify the map for rating using the GIS tool in a convenient way, the map was manually digitized after geo-referencing into an appropriate coordinate system (see Figure 5.2)

Geologically, Bhutan Himalaya consists of four physiographic zones viz. Sub-Himalayan Zone, Lesser Himalayan zone, Greater Himalaya Zone and Tethyan Himalayan Zone separated by East-West trending major tectonic boundaries which show overlapping relationship with thrusted/faulted contacts. The Higher Himalaya in the north pass into north-south trending ranges and valleys of the Lesser Himalaya those contain both antecedent and consequent rivers flowing towards the plains of Assam and Bengal (India) with the Brahmaputra River as the base level. The sub-Himalaya zone consists of Siwalik Group; Lesser Himalaya consists of Buxa/ Gondwana, Daling and Shumar Groups and Higher Himalaya consists of Thimphu and Paro Groups. Main Boundary Thrust (MBT) separating sedimentary rocks of Siwalik Group from Buxa/ Gondwana Groups while the Main Central Thrust (MCT) forms the contact between

Lesser Himalayan metasedimentary rocks and the crystalline metamorphic rocks of Higher Himalaya.

The Bunakha catchment lies in Western Bhutan and spreads over the aforementioned three physiographic zones (refer Table 5.4). Upper reaches of the catchment fall in the Kula Kangri-Chomolhari mountain range with sharp-crested ridges and deep-set glacial valleys, margined in the east by Chumbi and Natu valleys.

The dam and reservoir area of BHEP is located in the Higher Himalayan physiographic zone where crystalline metamorphic of Proterozoic age are represented by the Thimphu Gneissic Complex and Paro Group (Shanker et al., 1989); whereas the upstream of the catchment extends into the Tethyan Himalayan zone.

Similar to the study of Garg and Jothiprakash (2011) for the Himalaya region in India, the catchment was divided into five classes viz. slight stoniness, slight-moderate stoniness, moderate stoniness, moderate-strong stoniness and strong stoniness. The classification was based on Mohs Hardness value and also taking into consideration the degree of weathering of the dominant rock of the surface geology as presented in brief in Table 5.4 and its details are enclosed as Appendix A, Table A5 . It was considered that harder rock types are more resistant to erosion while softer and weaker rocks are prone to erosion thereby yielding more sediment to the catchment (PSIAC, 1968). Therefore, the PSIAC rating was adopted similar to the one by Garg and Jothiprakash (2011). The classified geological map for this parameter is shown in Figure 5.2.

Table 5.3: Adopted rating for geological surface class based on Mohs Hardness Scale

Class	Hardness Mohs Scale	Allotted PSIAC Rating
Strong	7 & above	0
Moderate-Strong	5 to 6	2
Moderate	3 to 4/weathered rocks	5
Slight-Moderate	2 to 3/massive weathered rocks	7
Slight	2 & below	10

Table 5.4: Classification of surface geology and their allotted PSIAC rating

Zone	Map Units	Class	Allotted PSIAC Rating
Greater Himalaya	Ghlml	Moderate-Strong	2
	Ghlmu	Moderate-Strong	2
	Ghlo	Slight-Moderate	7
	Tgr	Strong	0
Tethyan Himalaya	Thu	Slight	10
	Tr-Jru	Slight-Moderate	7
	Pzu	Moderate	5
	Pzc	Slight	10
Lesser Himalaya	Pzpu/m3	Slight-Moderate	7
	Pzpm/m2/m1	Slight-Moderate	7
	Pzo	Strong	0
	Pzpl	Slight-Moderate	7

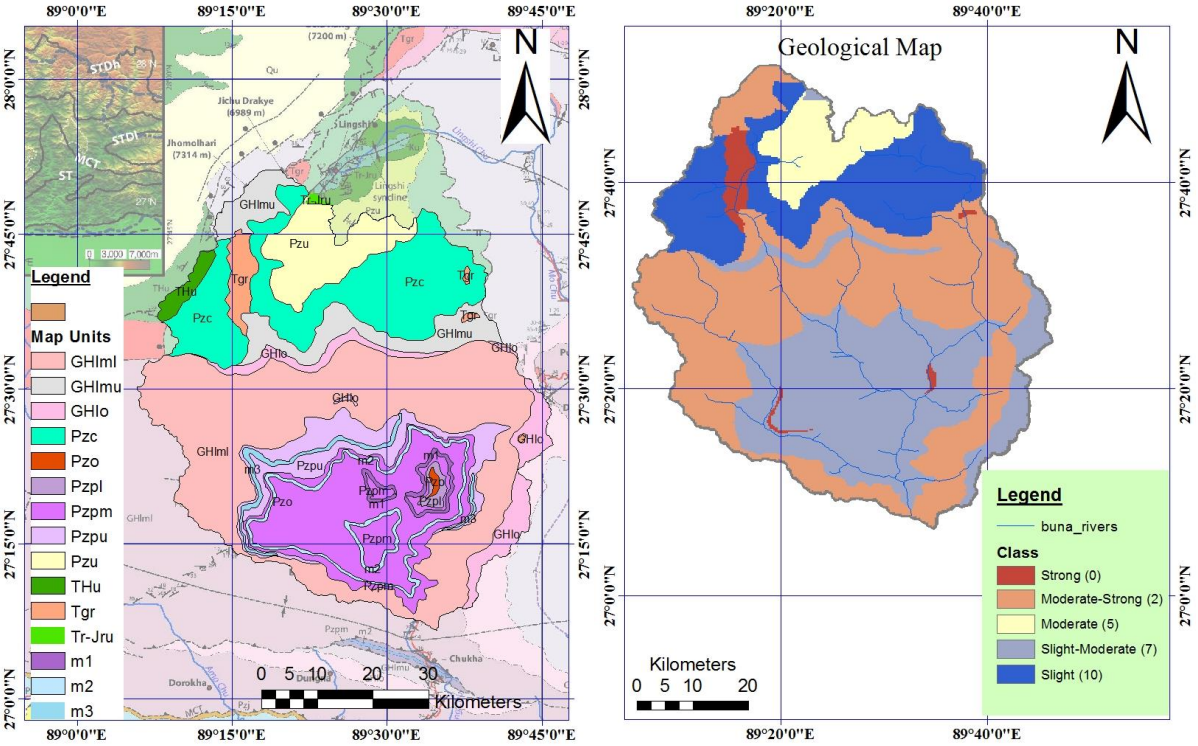

Figure 5.2: Geological map of Bunakha catchment, digitized (Left) and Classified geology map of the Bunakha Catchment based on surface stoniness

The classified geologic raster map of Bunakha catchment was linked with the corresponding PSIAC rating. The raster map was converted to vector file format, spatially joint with the gridded map (so that each grid cell gets assigned with their respective PSIAC rating depending

upon the geological class it has attained) in order to estimate the sediment yield in combination with other factors of PSIAC in each grid cell.

5.2.3 Climate and Runoff

The climate factor is considered as one of the important parameters for vegetation growth which also determines the amount of precipitation and runoff. Climate also determines the distribution of precipitation across the region. It is understood that regions with high intensity of rainfall generate high intensity of runoff volume. High precipitation and runoff results in eroding top soil due to detachment of soil particles by their energy and resulting sediment yield out of it. However, erosion of top soil is depended on the density of vegetation cover. Regions with less vegetation are eroded more than those of high vegetation density (PSIAC, 1968).

5.2.4 Runoff

For the purpose of assessing the runoff characteristic, the runoff map was needed to be generated. One possible way to generate such a map was the use of an interpolation method from the available gauged runoff data series of the study area. However, as seen from Figure 5.4, the density of gauged stations is low and, moreover, the stations are concentrated in the southern region of the catchment. If the runoff map were to be interpolated, there would be huge uncertainty in the far reach end of the catchment due to lack of data coverage.

One of the alternative options to generate the runoff map is to make use of Satellite precipitation data with high temporal and spatial resolution. Such data have the additional advantage that they represent areal precipitation. However, it is to be noted that the data obtained must be carefully analyzed and evaluated before utilization. This involves numerous processes such as conversion of data into required format, rotation, filling of missing data, clipping and arrangement of data into desired temporal format (Tamrakar and Alfredsen, 2013) requiring considerable amount of time.

Therefore, the best strategy in hand in view of the limited time available for the preparation of the thesis was to resort to an already prepared raster runoff map (see Figure 5.3) which was available from the Department of Hydropower and Power Systems, MoEA, prepared by (Beldring and Voksø, 2011). The runoff map was the result of Hydrological modelling for the period 1981-2010. The sediment data available is from the period 2008-2015 and runoff map should also be of the same period for sediment yield estimation. However, as mentioned above, due to limited availability of runoff data, the spatial and temporal variability of the runoff, which was associated with a different period (1981-2010), was considered for the study period

with the assumption that runoff characteristic of the past period would have remained same as the study period. The runoff map for the Bunakha Catchment was extracted using the GIS tool and it is presented in shown in Figure 5.4.

The runoff map was subsequently classified into 6 different classes based on the varying magnitude of the mean annual runoff values. In PSIAC approach, the rating range from 0 to 10 was allocated to the runoff factor depending on its magnitude. The rating was allotted in a similar way as by Garg and Jothiprakash (2011) for the Himalaya region in India although these runoff values were much higher owing to the huge catchment size. Therefore, in order to create a reasonable rating for the Bunakha Catchment, the runoff values were scaled down and accordingly rated for each class as shown in Table 5.5. The rating allocation show in Table 5.5 clearly depicts that the higher the runoff volume, the higher is the assigned rating value since there will be more sediment yield due to its capability to detach the soil particles with its energy as it flows.

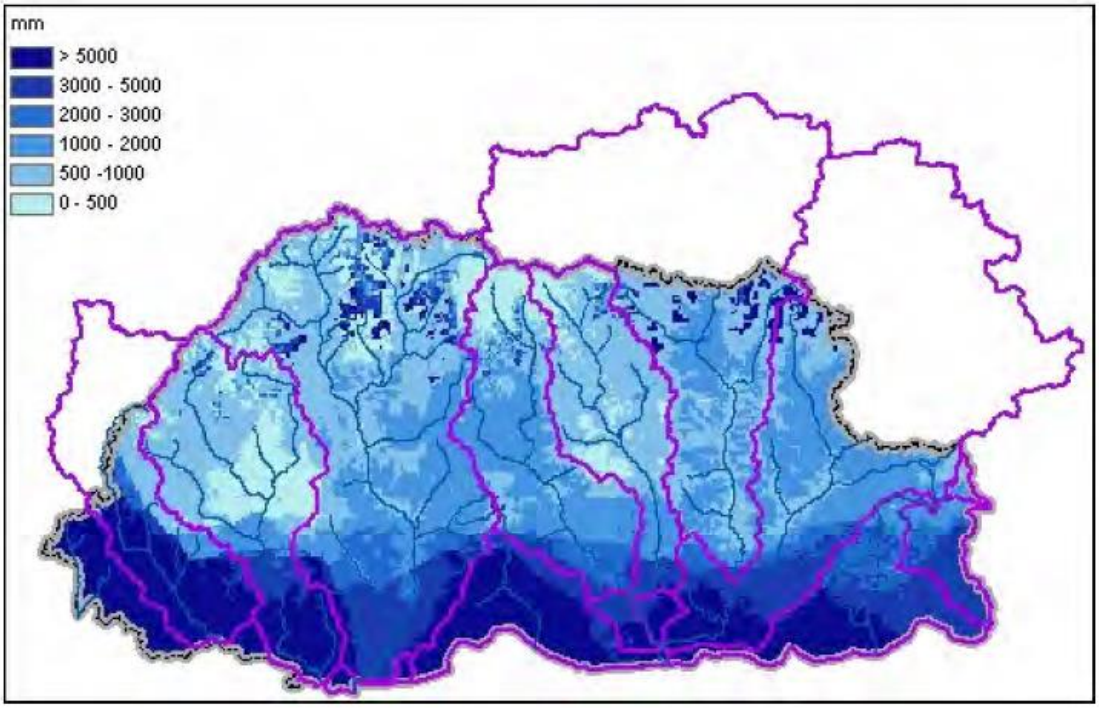

Figure 5.3: Mean annual runoff (mm) for the period 1981-2010 (Source: DHPS,MoEA, 2015)

Table 5.5: Runoff class and PSIAC Rating

SN	Runoff (mm) class	Allotted PSIAC Rating
1	<2500	5
2	2500 to 3000	6
3	3000 to 3500	7
4	3500 to 4000	8
5	4000 to 4500	9
6	>4500	10

Using ArcMap tool, the mean annual runoff raster map was converted to vector file format and spatially joint with the gridded map of Bunakha catchment followed by exporting its attribute table into Excel file. Using Excel functions, the PSIAC ratings were assigned according to their ranges so that they can be combined with the attributes of other factors of PSIAC for estimation of sediment yield at the end.

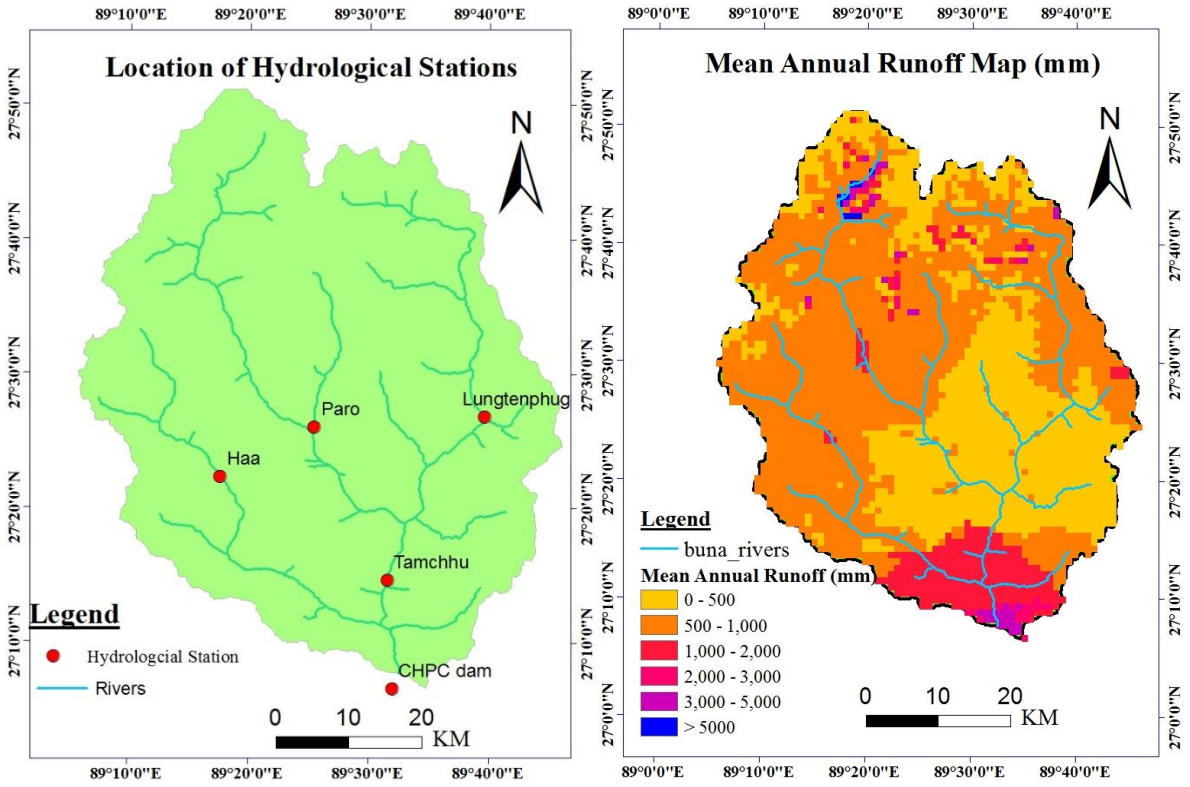

Figure 5.4: Location of hydrological stations (*left*) and extracted raster map (*Right*)of Mean Annual Runoff (mm) for Bunakha Catchment

5.2.5 Precipitation

Similar to the runoff factor, an annual mean precipitation map was required for this factor as well. Unlike gauging stations for the discharge, the existing precipitation gauging stations are

much denser and few extend to the northern part of the catchment as well. Relative location of the 11 gauging stations available within and vicinity to the study area are shown map presented as Figure 5.5 (*Left*) and their respective annual average precipitation value is shown in Table 5.6.

Table 5.6: Precipitation gauging stations with their annual mean precipitation (mm)

S #	Station Name	Latitude (Degree Decimal)	Longitude (Degree Decimal)	Elevation (m)	Data Period Considered	Annual Average Rainfall (mm)
1	Chukha	27.4415	89.6628	1600	2008-2015	1519.96
2	Betikha	27.3872	89.4196	2660	2008-2015	2372.56
3	Chapcha	27.3864	89.2785	2450	2008-2015	841.38
4	Begana	27.4423	89.6628	2490	2008-2015	1016.96
5	MoEA	27.3847	89.5753	2380	2008-2015	660.40
6	Namjayling	27.5733	89.6425	2751	2008-2015	875.01
7	Paro DCS	27.5000	89.3331	2406	2008-2015	622.08
8	Simtokha	27.2523	89.4229	2310	2008-2015	599.04
9	Gidakom	27.6111	89.2869	2210	2008-2015	554.70
10	Drugyel	27.0664	89.5664	2547	2008-2015	983.84
11	Gunitsawa	27.2000	89.5500	2800	2008-2015	880.50

With the available precipitation gauged data, the precipitation map can be generated by employing interpolation methods. There are numerous methods for carrying out spatial interpolation of precipitation data using ArcMap, but their effectiveness depends upon the purpose of the study and territorial context. Inverse Distance Method (IDW) has been found to give more accurate estimate (Keblouti et al., 2012) and same has also been reported by Noori et al. (2014). However, in these studies their findings were evaluated by comparing the interpolated precipitation with the observed values. For the Bunakha catchment's case it was assumed that such a method will yield the same accuracy and a validation of the results was not carried out. The mean annual precipitation map prepared with the chosen method is presented in Figure 5.5 (*Right*).

For the PSIAC rating purpose, which ranges from 0 to 10 for this factor, Daneshvar and Bagherzadeh (2012) assigned comparatively higher rating compared to what was adopted by Garg and Jothiprakash (2011). This might be attributed to different topographical and climatic zones. Since the rating characteristic adopted by the latter study was applied to the Himalayan region of India, it was assumed to be more applicable and therefore, the same rating pattern was chosen for the Bunakha Catchment (shown in the table below):

Table 5.7: Precipitation class and its allotted rating

SN	Precipitation (mm) class	Allotted PSIAC Rating
1	<500	4
2	500 to 600	5
3	600 to 700	6
4	700 to 800	7
5	800 to 900	8
6	900 to 1000	9
	>1000	10

Using ArcMap tool, the mean annual precipitation raster map was converted to vector file format, then it was spatially joint with the gridded map of Bunakha catchment followed by exporting its attribute table into Excel. Using excel functions, PSIAC ratings were assigned according to their values ranges so that it can be combined with the attributes of other factors of PSIAC for estimation of sediment yield at the end.

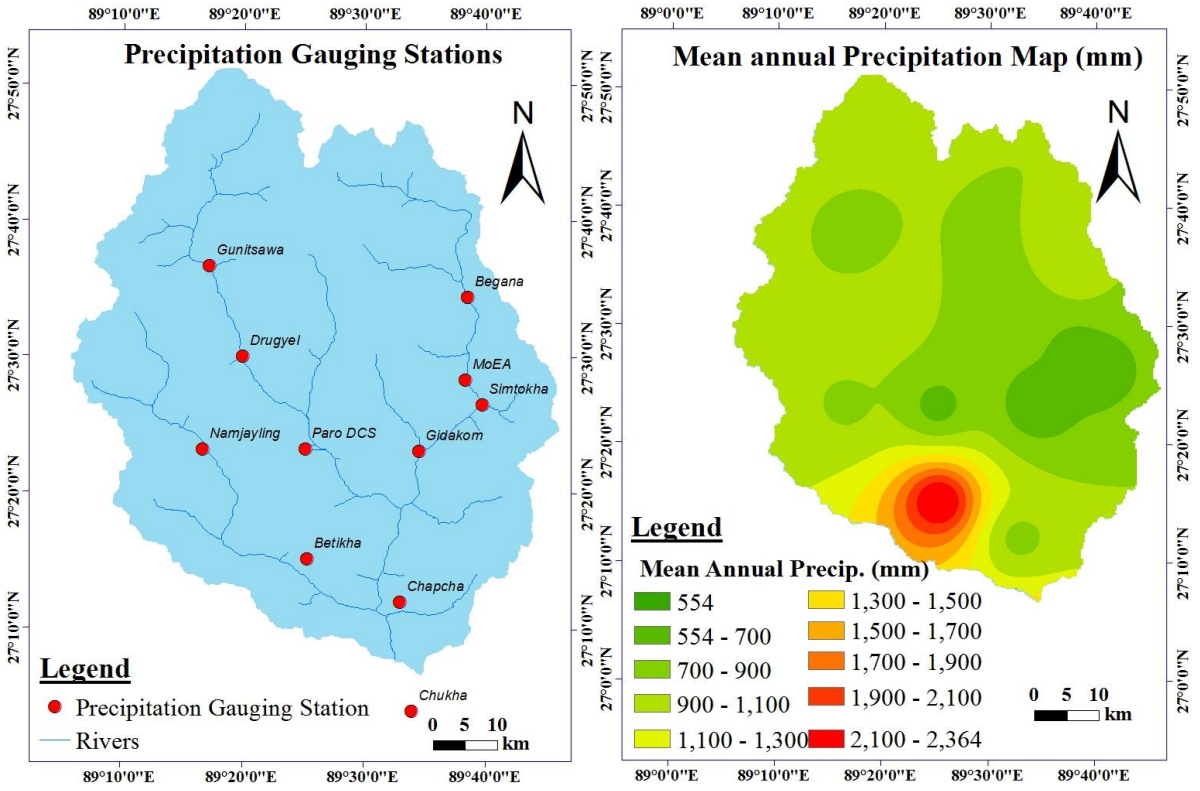

Figure 5.5: Location of precipitation gauging stations (*left*) and mean annual runoff map (*right*) of Bunakha catchment

5.2.6 Land Cover & Land Use

The land cover map was obtained from National Soil Service Centre, Department Agriculture under Ministry of Agriculture and Forest, Bhutan. It classifies the Bunakha catchment into 20 classes of land cover/use. With the usage of ArcMap tool, the land cover map for Bunakha catchment was extracted as shown in Figure 5.6 (*left*). It was found that the most dominant land cover in the Bunakha Catchment is forest with 84.18% followed by water bodies of 9.64% which includes snow, glaciers, reservoir, rivers and lakes. Agricultural land constitutes of 3.13 % of the total catechumen area. The remaining 3.05% encompasses settlements, non-built-up areas, screes and moraines land covers. Details are presented in Table 5.8 below.

Table 5.8**:** Landcover, area coverage and allotted PSIAC Rating

SN	Landcover	Landover Equivalent to USGS class	Area (sq.km)	Area %	Allotted PSIAC Rating
1	Chuzhing	Irrigated Cropland & Pasture (CRIR)	22.89	0.64	20
2	Kamshing	Dryland Cropland & Pasture (CRDY)	68.03	1.91	20
3	Built-up Areas	Urban & built up Land (BUILT)	21.26	0.60	-20
4	Landslides	-	0.17	0.00	-20
5	Broadleaf Forests	Evergreen Broad leaf Forest (FOEB)	110.69	3.11	-20
6	Broadleaf +Conifer	Mixed Forest (FOMI)	9.65	0.27	-12
7	Fir	Evergreen needle leaf Forest (FOEB)	334.89	9.41	-16
8	Mixed Conifer	Evergreen needle leaf Forest (FOEB)	1102.45	30.98	-16
9	Meadows	Grassland (GRASS)	275.45	7.74	-10
10	Non-Built-up Areas	Barren or Sparsely Vegetated (BSVG)	0.51	0.01	0
11	Snow and Glaciers	Snow or Ice (SNOW)	331.18	9.31	0
12	Rock Outcrops	-	51.60	1.45	-20
13	Shrubs	Shrub land (SHRUB)	711.23	19.99	-8
14	Lakes	Water Bodies (WATB)	4.42	0.12	0
15	Rivers	Water Bodies (WATB)	7.40	0.21	0
16	Reservoirs	Water Bodies (WATB)	0.01	0.00	0
17	Blue pine	Evergreen needle leaf Forest (FOEB)	450.85	12.67	-16
18	Apple Orchards	Deciduous Broadleaf Forest (FODB)	20.30	0.57	-20
19	Screes	Barren or Sparsely Vegetated (BSVG)	28.06	0.79	0
20	Moraines	Barren or Sparsely Vegetated (BSVG)	7.09	0.20	0

Table 5.9: USGS land cover and their adopted rating

Land use/land cover description as per USGS	***PSIAC Rating*** *(Garg and Jothiprakash, 2011)*
Urban and Built-Up Land (BUILT)	-10
Dryland Cropland and Pasture (CRDY)	10
Irrigated Cropland and Pasture (CRIR)	10
Mixed Dryland/Irrigated Cropland and Pasture (MIXC)	8
Cropland/Grassland Mosaic (CRGR)	6
Cropland/Woodland Mosaic (CRWO)	8
Grassland (GRAS)	-5
Shrubland (SHRB)	-4
Mixed Grassland/Shrubland (MIGS)	-4
Savannah (SAVA)	-5
Deciduous Broadleaf Forest (FODB)	-10
Deciduous Needle leaf Forest (FODN)	-8
Evergreen Broadleaf Forest (FOEB)	-10
Evergreen Needleleaf Forest (FOEN)	-8
Mixed Forest (FOMI)	-6
Water Bodies (WATB)	0
Herbaceous Wetland (WEHB)	-2
Wooded Wetland (WEWO)	-5
Barren or Sparsely Vegetated (BSVG)	0
Herbaceous Tundra (TUHB)	-5
Wooded Tundra (TUWO)	-5
Mixed Tundra (TUMI)	-5
Bare Ground Tundra (TUBG)	0
Snow or Ice (SNOW)	0

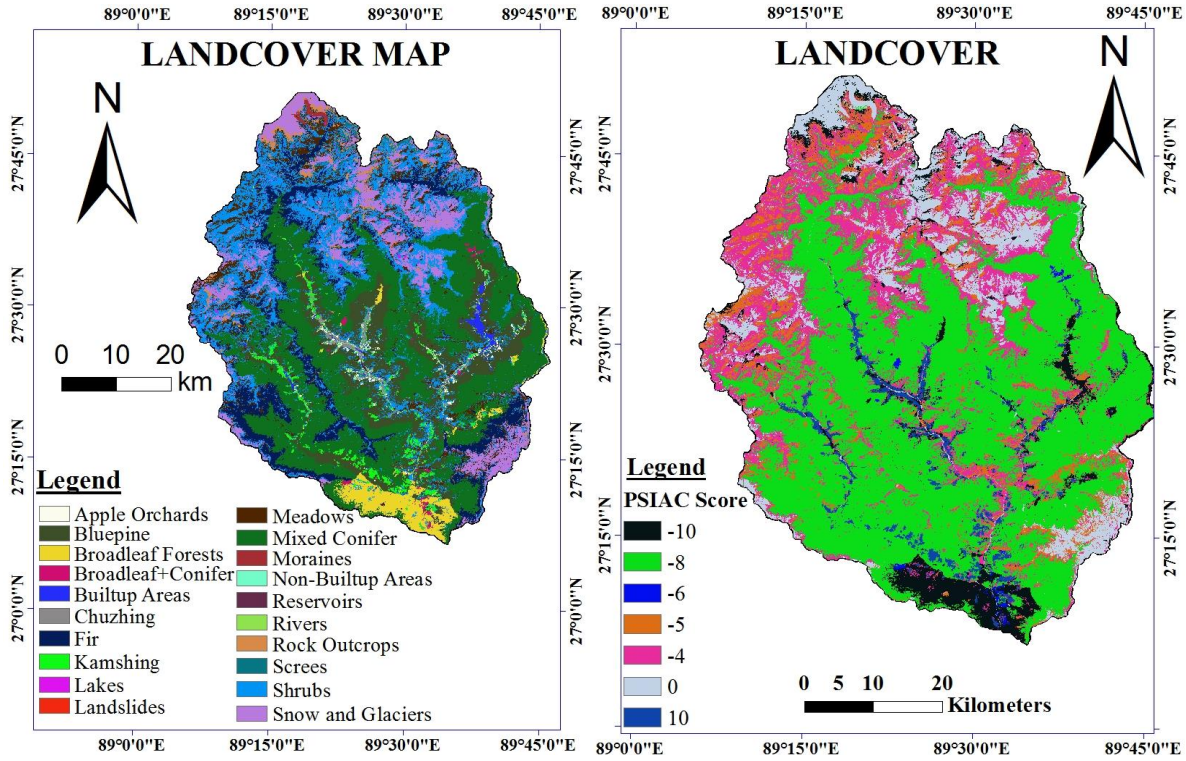

Figure 5.6: Landcover map showing 20 classes (*Left*) and classified landcover map according to the assigned PSIAC Rating (*Right*) of Bunakha Catchment.

In the PSIAC approach, a range from -10 to 10 was assigned to the landuse factor. The basis of PSIAC rating for the different land cover was taken similar to what was adopted by Garg and Jothiprakash (2011). Therefore, landcover classes for the catchment were converted to USGS class equivalents to enable rating. These classes are presented in Table 5.9. A negative rating of -10 was assigned to the landcover with dense vegetation since such areas are well protected and tend to reduce soil erosion from the surface. In case of sparsely vegetated areas, which are considered to have insufficient protection against erosion when coupled with other factors such as rain and other erosion agents, a rating of 0 was assigned. The landcover class for agricultural land (both wet and dry) and landslide areas are known to accelerate the effect of erosion process (Daneshvar and Bagherzadeh, 2012) and therefore such areas were characterized by the highest rating of 10. The landcover map classified according to the assigned PSIAC rating is presented in Figure 5.6. Considering the landcover parameter, the southernmost part of the catchment, close to reservoir area, is less prone to erosion owing to its dense vegetation particularly broadleaf forest while landcover which would be prone to erosions are located along the valley attributed to agricultural land in the vicinity of settlement areas.

When it comes to the PSIAC parameter of landuse, its classification for rating purpose was found to be overlapping with the landcover attributes. In order to take the landuse factor into consideration as well, the score assigned for the landcover factor was doubled (refer Table 5.8).

The classified land cover and land use map were converted to vector maps and then spatially joined with the gridded map so that each grid has a rating assigned depending upon the landcover/use class in it. These maps were later combined with other factor attributes of the PSIAC for estimation of sediment yield in each grid cell at the end.

5.2.7 Soil

The ESRI shape file format of the soil map, referred to as Digital Soil Map of the World (DSMW) version 3.6 at 1:5,000,000 scale, was obtained from FAO-UNESCO and it was extracted (see Figure 5.7) and analyzed in ArcMap for the study area. The most dominant soil category in the Bunakha Catchment is Orthic Acricols which stretches across 75.41 % of the total area, followed by Lithosols of 23.52% situated at the extreme north, and the least soil category consisted of Dystric Cambisols located at the extreme south. Based on the characteristics of the soil textures, properties and extend of weathering as reported in FAO-UNESCO (1977), PSIAC rating was accordingly assigned to these soil types.

In the PSIAC approach, a range from 0 to 10 was assigned to soil factor. As it can be observed from Table 5.10 below, the highest rating of 6 was assigned to Lithosols which are mostly found at steep slopes and are characterized by shallow depths. Dystric Cambisol soils are found at the southern extreme of the catchment and were assigned the lowest rating of 4 as they are located in dense vegetation and contains high organic matter content which is found to protect soil from erosion agents thereby being less prone to erosion.

With ArcMap tool, after having assigned their respective rating, the soil map was converted to vector map followed by spatially joining with the gridded map so that it can be combined with other factors' attributes of PSIAC for estimation of sediment yield of Bunakha catchment in each grid cell.

Table 5.10: Soil Description, its allotted rating and their area coverage in the Bunakha catchment.

Soil Type	Description	Remark	Allotted PSIAC Rating	Area %
Orthic Acrisols)	• Occurs in humid tropical areas • Occupies well-drained hill sites and form good land for plantation • Have attained advanced stage of weathering and have low natural fertility	Hill type, Acrisols	5	75.41
Lithosols	• Occurs in areas with climates ranging from arid to humid and most at steep slopes • Characterized by shallowness, and therefore suffers widely from erosion including wind erosion. It is barren in high altitude • Such areas are mainly used for grazing by animals in arid regions	Mountain type, Lithosols	6	23.52
Dystric Cambisols	• Occurs in high rainfall area of the Himalaya region, most common in medium-altitude zone • Occupy moderate to steep slopes and are mainly under forest or are used for grazing • Soil type present: Sandy clay loam and loamy soils • Contains high organic matter	Hill type, Cambisols	4	1.07

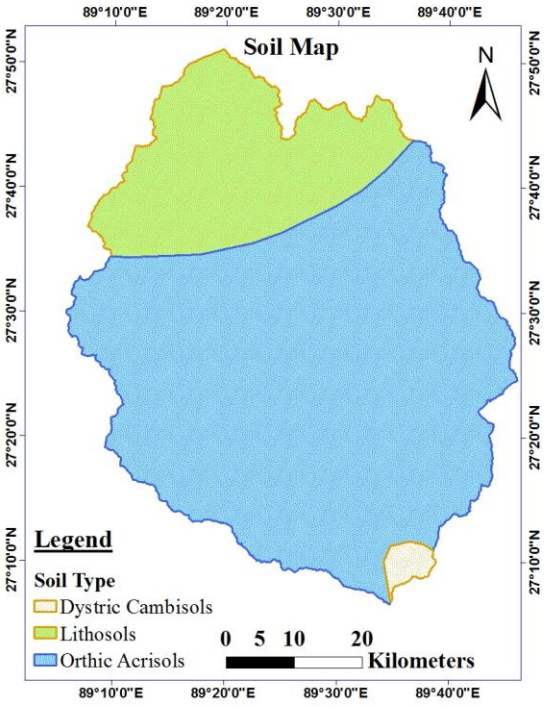

Figure 5.7: Soil Map of Bunakha Catchment

5.2.8 Channel Erosion

Both river bank erosion and transportation of sediments by flood events are considered important in this factor. The erosion in the channel takes place due to eroding of main stream river banks during flood periods and in the rainy season (Daneshvar and Bagherzadeh, 2012). In addition to the erosion of the channel banks, the sediment which may be deposited in the river bed and side bank during the series of low flow period are washed away by subsequent large flows (PSIAC, 1968). In the PSIAC approach, a rating range of 0 to 25 was assigned to this factor.

For rating purposes, since there is no detailed study available on the characteristics of river channel banks and their bed materials to assess their erodibility, the sensitivity of three scenarios were tested to investigate the magnitude of their contribution to sediment yield in the catchment. These scenarios are described in the following:

Scenario 1: The map was classified into two main categories viz. (i) the main rivers denoted as main stream and (ii) minor branches which remain without water most of the period as presented in Figure 5.8. For these categories, ratings of 15 and 2 were assigned respectively. The rating pattern was taken from Daneshvar and Bagherzadeh (2012).

Scenario 2: Assuming river channels of moderate flow depths and medium flow duration with occasionally eroding banks or bed, a rating value of 10 was assigned to the river channels as per the PSIAC rating guidelines.

Scenario 3: (a) Assuming the worst case where river channels are considered to have continuously eroding banks or that they erode in frequent intervals with large depths and long flow duration, and (b) active head cuts and degradations in tributary channels, the highest value of 25 was assigned to the river channels as per the PSIAC rating guidelines.

In the PSIAC rating guideline there is a category assigning the rating 0 when the channel characteristics consist of wide shallow with flat gradients. This scenario was not considered for evaluation as the topography of the catchment is characterized by very steep terrain with most of its area falling above 30 % slope gradient with narrow gorge river valley.

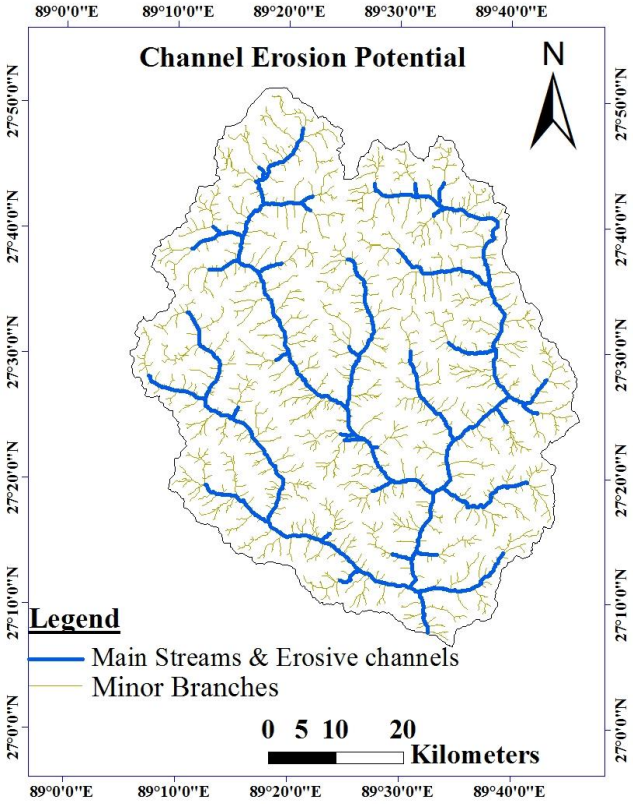

Figure 5.8: Channel Erosion potential map of Bunakha Catchment

5.2.9 Upland Erosion

In PSIAC approach, the rating for this factor ranges from 0 to 25.

The Himalaya ranges, where Bhutan is located, are considered geologically fragile. The most common landslide events are rainfall induced during the monsoon season and hence their incidence is directly correlated to the amount of rainfall. The areas that are highly susceptible to rainfall induced landslide are heavily fractured and weathered rocks. Currently, Bhutan does not have estimate of the scale, spatial or temporal occurrence of land sliding published except for the mapping of hazardous areas along the highways (Kuenza et al., 2004).

The data available to assess the upland erosion was found to be very limited with few landslide zones mapped close to prospective reservoir areas which was carried out during the Detail Project study for the development of BHEP and during the hazardous mapping as mentioned above.

Therefore, the catchment's sediment yield was tested for three scenarios along with their respective ratings:

Scenario 1: With the limited available data of mapped landslide zones. The area which falls in the landslides were all assigned the rating 25 since it is considered as the most prone zone for sediment yielding.

Scenario 2: Assuming that more than 25% of the area characterized by rill and gully or land slide erosion, a rating of 10 was assigned.

Scenario 3: Assuming that more than 50% of the area are characterized by rill and gully or land slide erosion and a rating of 25 (maximum rating) was uniformly assigned throughout the catchment area.

The rating 0 could be assigned when there is no sign of erosion. However, it was not considered for evaluation since the situation is too unrealistic for the steep mountainous region of the Bunakha catchment.

5.2.10 Sediment Yield from PSIAC Approach

The spatially distributed data of each parameter prepared as a thematic layer in ArcMap describing the Bunakha viz. topography, land-use and land-cover, climate & runoff, soil, upland erosion, channel erosion and geology were spatially overlaid and summed up one to one grid to estimate PSIAC index in each grid/cell (1km by 1km) based on the assigned rating/weights. The sediment yield map was also prepared classifying it into five different classes as categorized in PSIAC (1968) viz low, moderate, moderately high, high and very high based on the PSIAC Index value as presented in Figure 5.9.

Table 5.11: Sediment Yield summary of the Bunakha Catchment with PSIAC approach

Category	PSIAC Index		
	(S1)[1] & (S1)[2]	(S2)[3] & (S2)[4]	(S3)[5] & (S3)[6]
min	-2.00	8.00	23.00
Max	107.00	90.00	120.00
Average	33.61	41.60	58.69
Average Sediment Yield of the catchment (ton/km^2/year)	**181.97**	**279.17**	**362.58**
Sediment Yield estimation at Gauging station (ton/km^2/year)	**805.20**	**364.80**	**1293.20**

[1] Considering Scenario 1 of the channel erosion parameter
[2] Considering Scenario 1 of the upland erosion parameter
[3] Considering Scenario 2 of the channel erosion parameter
[4] Considering Scenario 2 of the upland erosion parameter
[5] Considering Scenario 3 of the channel erosion parameter
[6] Considering Scenario 3 of the upland erosion parameter

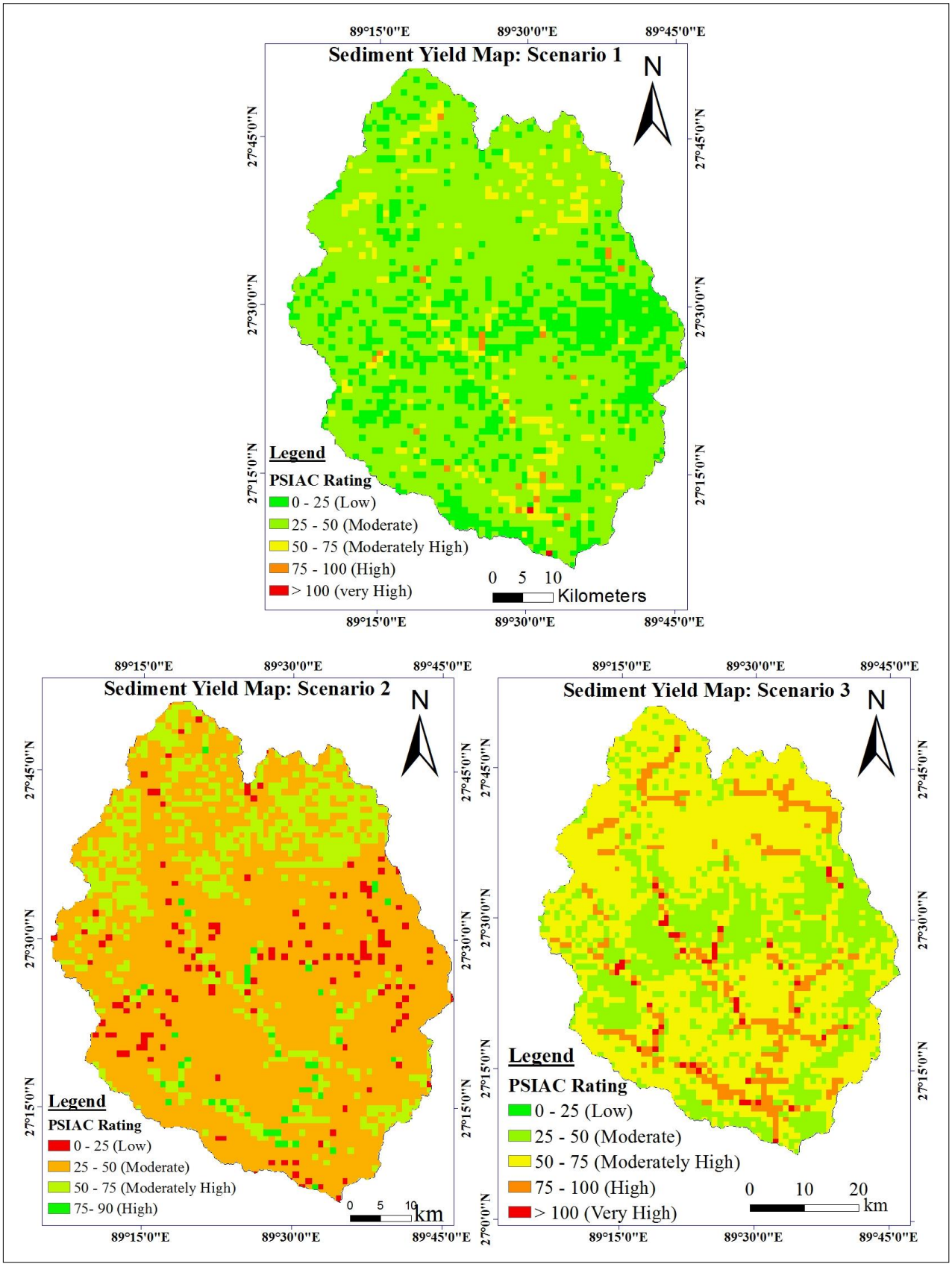

Figure 5.9: Sediment Yield Map: Scenario 1 (top), Scenario 2 (bottom left) and Scenario 3 for Bunakha Catchment

In order to estimate and detect the potential sediment yielding zones of Bunakha catchment, the spatially distributed data of overall average annual runoff and precipitation data along with other factors discussed and prepared above using GIS viz. topography, surface geology, upland and channel erosion were considered. The thematic maps of each of these factors were prepared and assigned ratings depending upon their susceptibility to soil erosion. These thematic layers were spatially overlaid (grid cell to grid cell) using ArcMap to estimate sediment yield in each grid cells. The summation of ratings of all the factors in each grid cell varied from -2 to as high as 120 depending upon the scenario in consideration (refer Table 5.11).

PSIAC ratings in each grid cell extracted from ArcMap are enclosed as Appendix A, Table A3 and A4.

5.3 Discussion

The results of sediment yield estimated with the use of PSIAC approach for Bunakha Catchment indicate that yield values lie between 181.97 to 362.98 tons/year/km^2 for the catchment. For the location of the gauging station, the yield estimation ranges from 365 to 1293 tons/year/km^2 which differs from the average value of the whole catchment. The grid cell which coincides with the location of the sediment gauging station was considered as the yield of the gauging station. The yield values obtained were 805.20, 364.80 and 1293.20 tons/year/km^2 which translate to sedimentation rate as 0.4 mm/year, 0.18 mm/year and 0.63 mm/year for scenario 1, scenario 2 and scenario 3 respectively assuming porosity as 30%. As it can be seen from the Table 5.11, for estimation of sediment yield in each grid cell (1km x 1km), Scenario 1 of channel erosion factor was considered in combination with scenario 1 of the upland erosion and so forth while values of other factors were taken as it is.

It is interesting to see high sediment yield concentrated along the river channel, almost replicating the path of the river channel, when considering scenario 2 and 3 of channel erosion and upland erosion factor of PSIAC, and such pattern is more prominent for sediment yield map produced for scenario 3. The reason for such an outcome is associated with the higher ratings assigned to river channels. From Figure 5.9, it can be seen that there is considerable erosion from the river channel and such an outcome would have to be validated by further studies since it may be the case in actual scenario in the rivers in Himalayan region which torrent down with high energy. Similarly considering scenario 1, where limited available landslide data in combination with the assumption that no erosion takes place in the catchment area were considered, it is obvious from the map presented as Figure 5.9 (top) that the majority of the catchment area falls under moderate annual sediment yield class (120-300 ton/km^2/year)

followed by few sparely distributed patches of moderately high annual sediment yield class (300-610 tons/km^2/year). The same is the case for the scenario 2 sediment yield but with lesser area falling into moderate class and increased area falling into moderately high class of annual sediment yield. The sediment yield map produced for scenario 3 indicates that most of the catchment area fall under moderately high annual sediment yielding class while high sediment yield class (610-1830 tons/km^2/year) are concentrated along the river.

CHAPTER 6: SEDIMENT YIELD ESTIMATION WITH RUSLE APPROACH

6.1 Concept & Methodology for USLE approach

Numerous models have been developed to determine the soil erosion such as European Soil Erosion Model (EUROSEM) (Morgan et al., 1998) Soil & Water Assessment Tool (SWAT) (Arnold et al., 1998) and Universal Soil Loss Equation (Wischmeier and Smith, 1978).

Among these models, the Universal Soil Loss Equation (USLE) approach for determining sediment yield is the least data demanding model that has been developed so far and it has been widely applied at different catchment scales and regions throughout the world due to its simplicity in application. This model was developed based on regression analysis of soil erosion rates on plot of 22.13 m of length in the USA in 1978 (Arekhi et al., 2012) and has been modified and revised by several researchers thereafter to make it applicable to their area of interest. One of these revised versions is called RUSLE (Revised USLE) by Renard et al. (1997) as the original USLE was developed only for the gentle sloping condition in a cropland of USA.

Soil erosion by RUSLE is estimated using an empirical equation below:

$$A = R * K * LS * C * P \qquad \text{Eq. 6.1}$$

Where:

A = the mean annual soil loss (metric tons $ha^{-1}year^{-1}$)

R = Rainfall Erosivity Factor (MJ mm h^{-1} ha^{-1} $year^{-1}$)

K = Soil Erodibility Factor (metric tons ha^{-1} MJ^{-1} mm^{-1})

LS = Slope length-steepness factor (dimensionless)

C = Cover & management factor (dimensionless: 0-1)

P = Support Practice Factor (Dimensionless: 0-1)

The RUSLE approach does not consider the sediment delivery ratio to estimate the sediment delivered to the downstream point of interest (Arekhi et al., 2012) and estimating the delivery ratio was not possible due to the limited data. Therefore, upon reviewing the literature, it was decided to use empirical formulas developed for watersheds around the world to estimate the Sediment Delivery Ratio (SDR) for the study area. Details are discussed in the ensuing section 6.2.6 of this chapter.

The estimation of sediment yield is carried out in two stages. First, the annual soil loss (tons/ha/year) is estimated using the RULSE Model. In the second stage, the Sediment Delivery Ratio (SDR) is applied to account for sediment that is eroded but does not reach a stream channel because of retention and sedimentation process (Schulte-Rentrop et al., 2005). The conceptual framework in the form of flow chart for estimation of sediment yield using RUSLE model is illustrated in Figure 6.1.

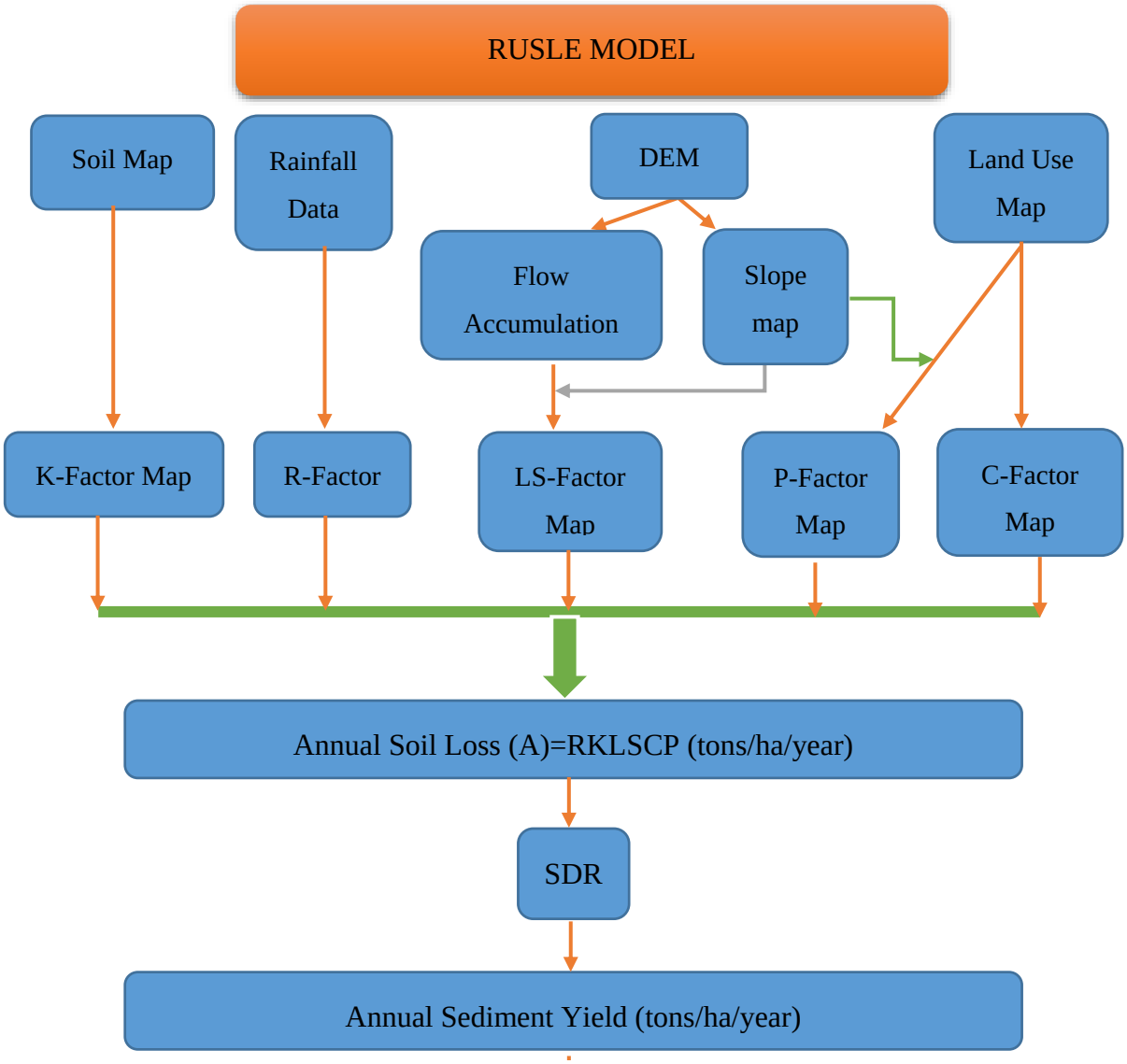

Figure 6.1: Conceptual framework of RUSLE for Sediment yield analysis

6.2 Data & Material Preparation for USLE approach

In this study, the Bunakha catchment was divided into 200m X 200 m grid cell sizes for estimating annual soil loss using ArcMap tool (GIS). The sediment yields were estimated for each grid cell area in order to get the perspective of sediment loss situation of the study.

Renschler et al. (1999) reported that with grid cell size ranging from 200 m to 250 m to be more reasonable while estimating the scale and spatial distribution of soil loss within GIS environment. This indicates that the smaller the grid cell size the better will be the results of soil loss estimation as more detailed information on geomorphological characteristics can be acquired at this scale. Therefore, it was decided to convert the study area into a 200 m x 200 m grid for estimating the annual sediment yield so that the RUSLE model could be used to analyze sediment yield in much more detail in combination with GIS. It was also possible to estimate the sediment yield at sediment gauging station which is located approximately 3 km upstream of the prospective reservoir area of BHEP so that comparisons can be made with gauged sediment rates for further improvement of the model features.

The procedure adopted for determining each factor with use of ArcMap tool is illustrated in the following sections.

6.2.1 Rainfall Erosivity Factor (R)

The rainfall erosivity factor(R) is the product of the annual sum of the rainfall energy and the maximum 30 minute rainfall intensity in each rainfall event of greater or equal to 13 mm per hour (Kitahara et al., 2000). In order to derive a linear relationship between mean annual rainfall and 30-minute rainfall intensity (EI_{30}) to determine R, hourly rainfall data and record of storm event are required. However, such data are not available for the study area. Therefore, a relationship used for the Himalaya region in India by Jain et al. (2001) with respect to their rainfall data has been used to estimate R with the assumption that the rainfall pattern in their region is similar to the study area. Raster map of precipitation was already prepared in Chapter 5 with IDW interpolation method (section 5.2.5 of Chapter 5), the same was used for estimation of R factor. The obtained relation for the R factor is:

$$R_{factor} = 79 + 0.363R_N \qquad \text{Eq. 6.2}$$

where:

RN = Mean annual rainfall (mm)

Using Eq. 6.2, the R factor raster map of the study area was generated using the raster calculator of ArcMap (Figure 6.2).

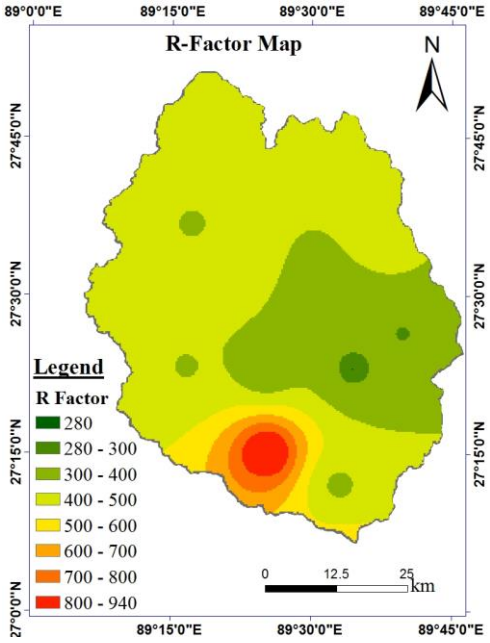

Figure 6.2: R-Factor map for Bunakha Catchment

The R factor map was then converted to vector format and then later spatially joint with the gridded map of the study to estimate the soil in each grid/cells in combination with other factors of RUSLE.

The highest R-values are concentrated in the lower region of the study area due to high intensity of rainfall in that region. The majority of the study area is characterized by R factors ranging between 400-500 MJ mm h^{-1} ha^{-1} $year^{-1}$. However, it is worth mentioning that that rainfall map was produced with the limited gauging stations available in the study area and that a more varied R factor map could be expected if the gauging stations were also densely distributed at the upper stretch of the study area.

6.2.2 Soil Erodibility Factor (K)

The land slope, nature of rainstorm, cover & management has more prominent influence to the soil loss than the inherent properties of the soil. However, it is worth noting that different soils erode differently and some soils are eroded more readily than others even under same conditions of other factors. Therefore, this difference in erodibility characteristics is referred to as soil erodibility (Wischmeier and Smith, 1978).

As reported by Wischmeier and Smith (1978), the K factor can be computed by using a nomograph solution when the silt fraction does not exceed 70% provided appropriate details about the soil are available with algebraic approximation as shown below:

$$100K = 2.73 \times 10^{-6} \times M_{1.14}(12 - a) + 3.25 \times 10^{-2}(b - 2) + 2.5 \times 10^{-2}(c - 3) \quad \text{Eq. 6.3}$$

Where:

M = Particle size diameter

a= Percent organic matter

b = the soil-structure code used in soil classification, and

c = the profile-permeability class

It can be seen that the equation entails the availability of sufficient soil parameters in order to determine the K value. However, from the existing data it is not possible to determine if the silt content fraction exceeds 70% or not, i.e. if the above equation can be applied.

Therefore, owing to the limited soil data available for the study area, as is often the case, in order to estimate the K values, a method proposed in (NCP, 2014) by using Table 6.1 prepared by Roose (1996) was used. It classifies texture classes of the soil based on the value ranges of the soil composition such as sand, silt and clay along with the percentage of organic carbon, thus enabling estimation of K values.

Table 6.1: Estimation of K values based on soil textures and organic matter content

Textural Class	Spanish Texture Class	Soil composition			Mean K (based on % organic material)		
		Sand	Silt	Clay	unknown	< 2%	≥ 2 %
Clay	*Arcilloso*	0-45	0-40	40-100	0.22	0.24	0.21
Sandy Clay	*Arcilloso arenoso*	45-65	0-20	35-55	0.2	0.2	0.2
Silty Clay	*Arcilloso limoso*	0-20	40-60	40-60	0.26	0.27	0.26
Sand	*Arenoso*	86-100	0-14	0-10	0.02	0.03	0.01
Sandy Loam	*Franco arenoso*	50-70	0-50	0-20	0.13	0.14	0.12
Clay Loam	*Franco - arcilloso*	20-45	15-52	27-40	0.3	0.33	0.28
Loam	*Franco*	23-52	28-50	7-27	0.3	0.34	0.26
Loamy Sand	*Franco arenoso*	70-86	0-30	0-15	0.04	0.05	0.04
Sandy Clay Loam	*Franco arenso arcilloso*	45-80	0-28	20-35	0.2	0.2	0.2
Silty Clay Loam	*Franco limoso arcilloso*	0-20	40-73	27-40	0.32	0.35	0.3
Silt	*Limoso*	0-20	88-100	0-12	0.38	0.41	0.37
Silty Loam	*Franco limoso*	20-50	74-88	0-27	0.38	0.41	0.37

The soil characteristics presented in Table 6.2 below were extracted from the raster map obtained from Harmonized World Soil Data Base V 1.2 (FAO/IIASA/ISRIC/ISSCAS/JRC,

2012) which gives composition percentage of sand, silt, clay and organic carbon of soil for the study area. The detail description of the soil and their area coverage in the study area was already discussed in the previous chapter (refer section 5.2.7).

Since the conversion value for organic carbon to organic matter (OM) of the soil layer was not known for the study area the expression below from J.G. Arnold (2012) was used to determine the same. The estimated K value and soil texture classification using Table 6.1 are presented in Table 6.2.

$$OM = 1.72 \times OC \qquad \text{Eq. 6.4}$$

Where: OC = Carbon content of the organic layer (%)

Table 6.2: Soil characteristic and their K factor value

Soil Unit	Sand	Silt	Clay	OC	OM	Texture Class	K-Factor
Orthic Acrisol (Ao)	49	27	24	1	1.72	Sandy Clay Loam	0.24
Dystric Cambisols (Bd)	41	39	20	1.45	2.494	Loam	0.26
Lithosols (l)	43	34	23	1.4	2.408	Loam	0.26

.

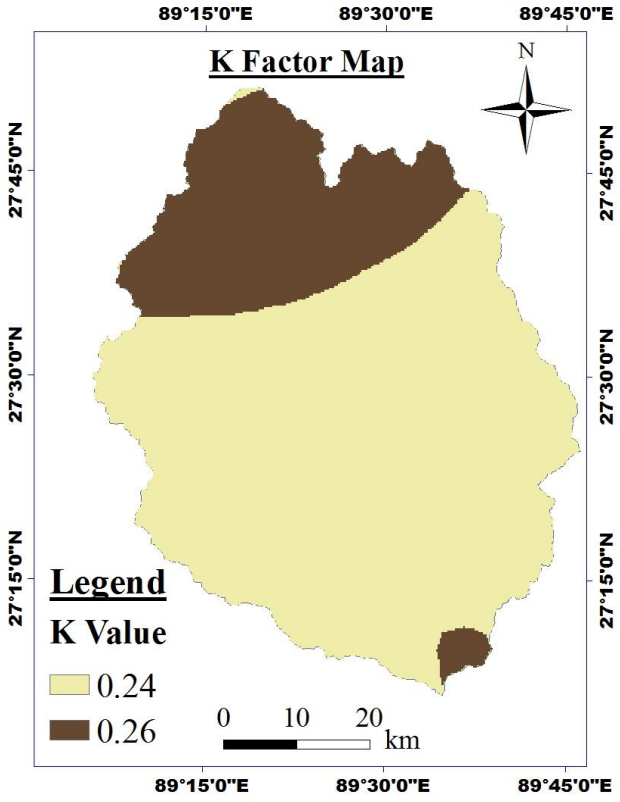

Figure 6.3: k Factor vector Map for the Study area

The soil raster map for the study area extracted from Harmonized World Soil Data Base was converted to vector format. The estimated K factor values were assigned to each soil class and the K factor map was produced as shown in Figure 6.3 above.

The vector format map was spatially joint with the gridded vector (200 m x 200 m) so that each grid/cell holds the K value to get the soil loss in the respective grids in combination with the other factors.

6.2.3 Slope Length Steepness factor (LS)

The LS factor is the expected ratio of soil loss per unit area from a field slope to that from a 22.13 m (or 72 ft.) length of uniform 9 % slope under otherwise identical conditions (Wischmeier and Smith, 1978). These authors developed the expression:

$$LS = \left(\frac{x}{72.6}\right)^{m} \times (65.4 \sin^2 \theta + 4.56\, sin\theta + 0.065) \qquad \text{Eq. 6.5}$$

where:

x = Slope length in feet

θ = angle of slope, and

m = 0.5 if the percent slope is 5 or more, 0.4 on slopes of 3.5-4.5 percent, 0.3 on slopes of 1-3 percent, and 0.2 on uniform gradients of less than 1 percent.

However, it is to be noted that the above expression was derived from conditions viz. under natural rainfall, slope steepness from 3-8 percent and terrain length of about 30-300ft and its accurateness beyond such conditions was not determined (Wischmeier and Smith, 1978).

The LS factor considers also the effect of topography. As the gradient of the slope increases, soil loss increases and the same is the case for the slope length due to the fact that the steeper the slope gradient of the surface, the more amount of soil is carried along by the accumulating overland runoff and its velocity down the hillslope (Amsalu and Mengaw, 2014) and by upslope contributing area (Moore and Burch, 1986). Therefore, an advanced LS factor computation method considering the above contributing factors was suggested by Moore and Burch (1986) as mentioned below and used by Simms et al. (2003), (Zhang et al., 2009, Mitasova et al., 1996).

$$LS = \left(\frac{As}{22.13}\right)^{0.6} \times \left(\frac{sin\theta}{0.0896}\right)^{1.3} \qquad \text{Eq. 6.6}$$

where:

As = Specific catchment area i.e. the upslope contributing area per unit width

θ = the slope angle in degree

The estimation of the LS factor is usually done manually from actual field data by measuring slope length and steepness when it comes to dealing with a field sized area. If a similar manual approach has to be employed for larger catchment scales, which are generally characterized by varying terrains and slope lengths throughout the stretch, it would be labor intensive and hence not feasible for modelling soil erosion. Due to this fact, the application of USLE and RUSLE model has been limited to generate estimates of the LS factor. However, with the use of GIS tools such as ArcMap features, the estimation of the LS factor is possible with DEM raster maps (Van Remortel et al., 2004). Thus, the LS factor can be computed in ArcMap with the raster calculator tool in map algebra with expression mentioned below (Gelagay and Minale, 2016, Parveen and Kumar, 2012, Amsalu and Mengaw, 2014, Jain et al., 2001):

LS = power("flow_accumulation"*cell_size/22.13,0.6)*power(sin(slope* 0.01745)/0.089,1.3) Eq. 6.7

Where flow accumulation represents number of cell contributing for downward flow, slope is the slope gradient in degree and cell size presents the grid/cell size of DEM which is 25 m for the present study area.

In ArcMap, the slope map in degrees (refer Figure 6.5) was produced using 25 m resolution DEM. Similarly, the flow accumulation raster map was generated after carrying out fill (refer Figure 6.4) followed by flow direction in ArcMap. By using Eq. 6.7 in ArcMap with raster calculator, the LS factor map was generated as shown in Figure 6.5. The raster map was then converted to vector format and later spatially join with the gridded map of the study area so that each cell is assigned with LS factor value for estimation of soil loss in combination with other RUSLE factors.

From the produced map it can be seen that majority of the slope ranges (in degrees) falls in between 20 to 40 degree and in some parts of the study area, the slopes are almost close to 90 degree which is attributed to steep terrain of the region (refer Figure 6.5). As pointed out by Wischmeier and Smith (1978), the steeper the slope gradient, the larger the soil loss when coupled with increasing slope length down the hill.

The flow accumulation map has a value as high as 154012 indicating that many numbers of 25 m cell sizes were accumulated into downslope cell in some part of the study area. The output cells with the flow accumulation of zero are local topographic highs and represents ridges in the study area.

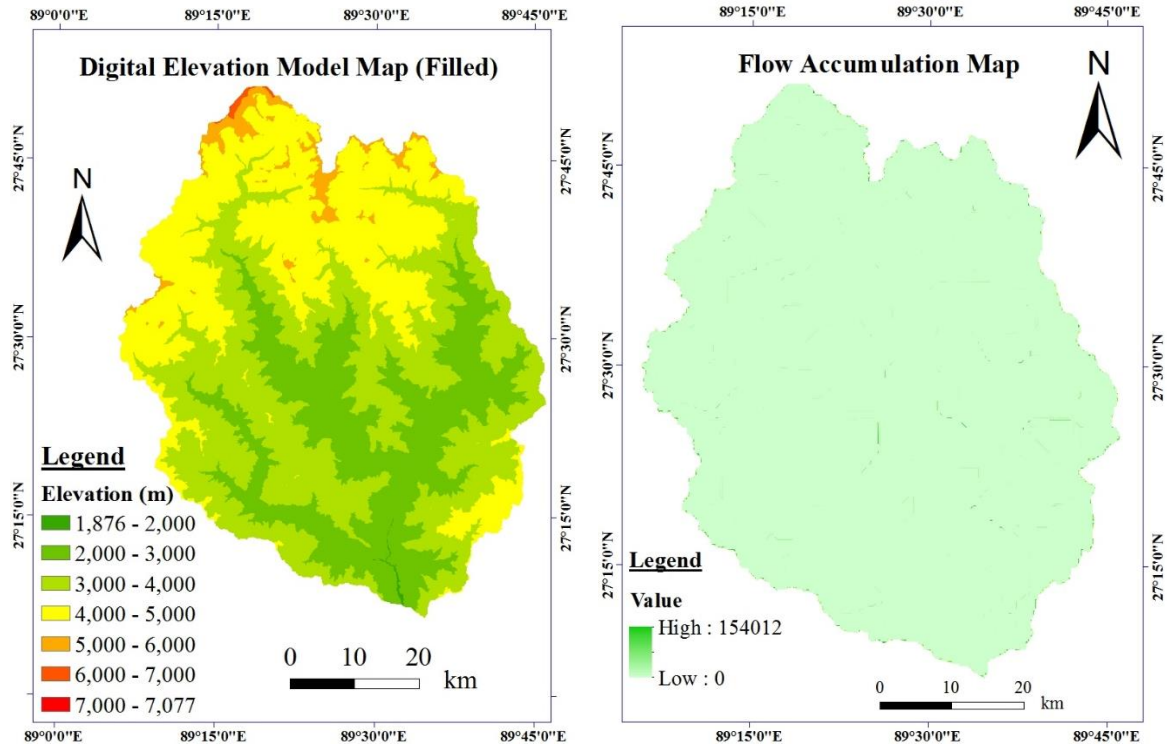

Figure 6.4: Filled Digital Elevation Map (*Left*) & generated flow accumulation map (*Right*) for the study area

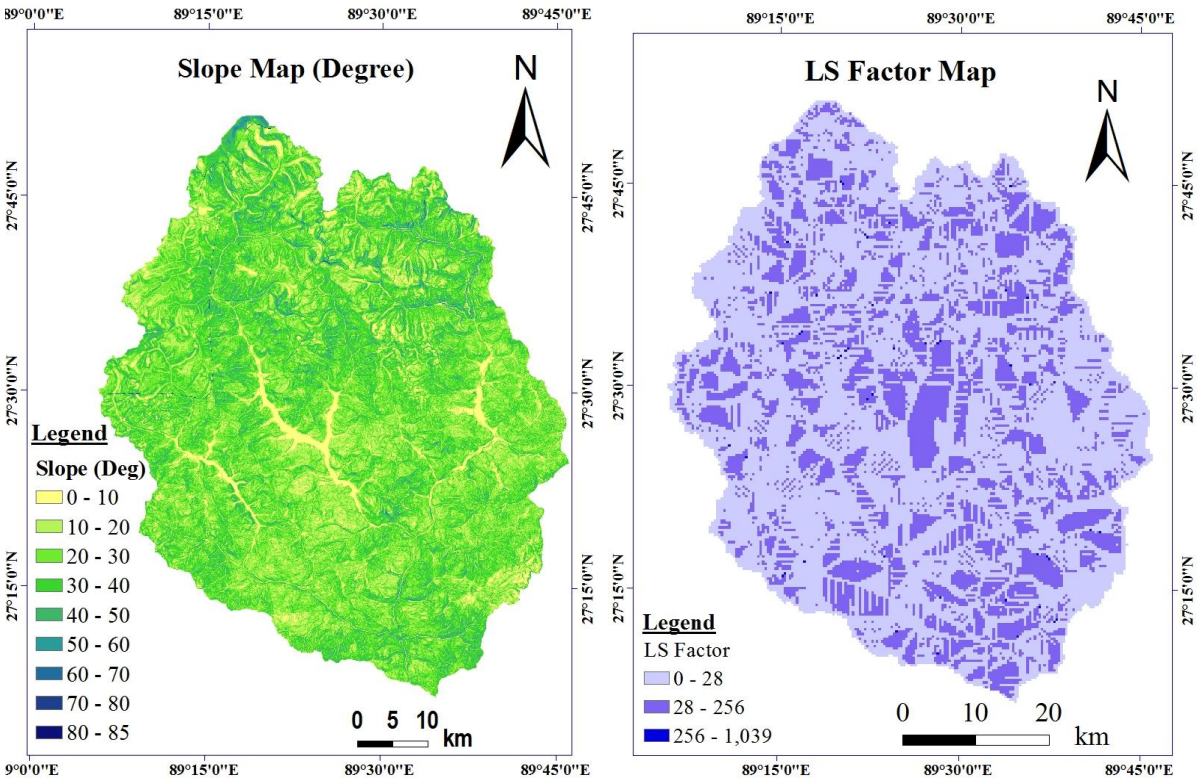

Figure 6.5: Slope map in Degree (*Left*) & LS factor map (*Right*)generated for the study area

6.2.4 Cover & Management Factor (C)

The Cover & Management Factor, denoted as C, ranges from 0 to 1 and is the ratio of soil loss from land cropped under specified continuous fallow conditions. It measures the combined effect of all the interrelated cover and management variables and therefore, as the name depicts, its ratio depends on land use or cover and its management information which influence the sediment yield from the watershed (Wischmeier and Smith, 1978). This factor gives representative values that can be assigned to the RUSLE land cover and management factors corresponding to each land use/cover condition (Pandey et al., 2007)

For the study area, the land cover map prepared by National Soil Service Centre, Department of Agriculture under Ministry of Agriculture and Forest, Bhutan had already C value assigned corresponding to each land cover/use and it is shown in the table below:

Table 6.3: C factor value for corresponding land use/cover of the study area

SN	Land cover/use	C factor
1	Chuzhing[7]	0.2500
2	Kamshing[8]	0.2500
3	Built-up Areas	0.0750
4	Landslides	0.3500
5	Broadleaf Forests	0.0010
6	Broadleaf + Conifer	0.0020
7	Fir	0.0030
8	Mixed Conifer	0.0030
9	Meadows	0.0250
10	Non-Built-up Areas	0.0100
11	Snow and Glaciers	0.0000
12	Rock Outcrops	0.0001
13	Shrubs	0.0040
14	Lakes	0.0000
15	Rivers	0.0000
16	Reservoirs	0.0000
17	Blue pine	0.0040
18	Apple Orchards	0.0030
19	Screes	0.0010
20	Moraines	0.0010

From the above table, the highest C value of 0.35 was assigned to land cover affected by landslide followed by Chuzhing and kamzhing with a factor value of 0.25 due to their high

[7] Chuzing (Bhutanese term) equivalent to Irrigated Cropland and pastures
[8] Kamshing (Bhutanese term) equivalent to Dryland Cropland and pastures

potential of soil loss. The smallest value is that of the water bodies as it is expected that no soil will be lost from the water surface. The area coverage corresponding to each of the land use/cover was already discussed in the previous chapter associated with PSIAC approach of estimating yield (refer section 5.2.6 of Chapter 5).

With each C value assigned to the respective land use/cover, raster map of the C factor was generated (refer Figure 6.6) and then it was converted to vector format, spatially joint with the gridded map of the catchment in order to estimate the soil loss in combination with other factors of RUSLE.

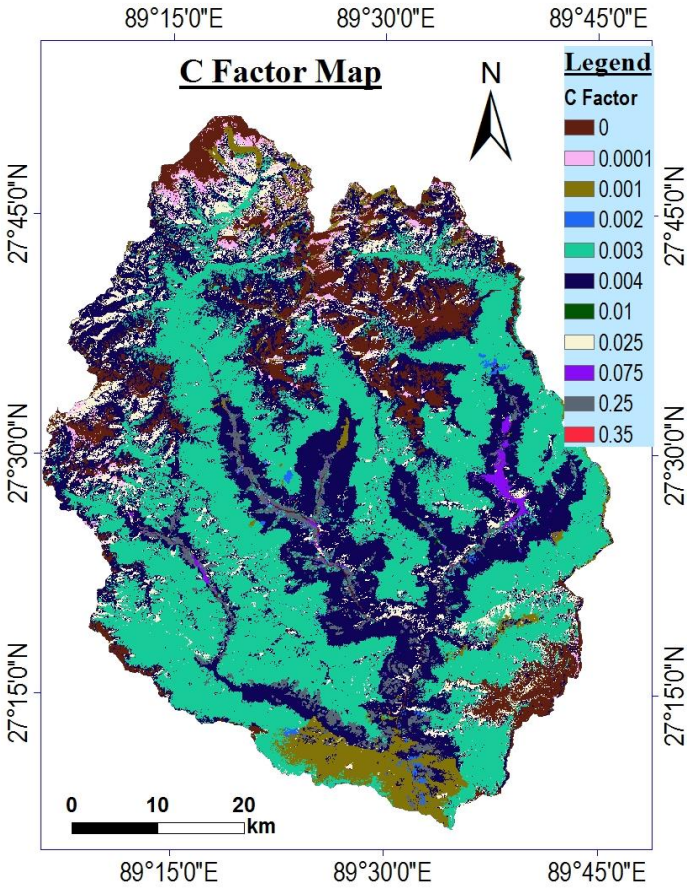

Figure 6.6: C factor raster map of the study area

6.2.5 Support Practice Factor (P)

The support practice factor (P) is the ratio of soil loss with a specific support practice to the corresponding loss with up-and-down culture. Support practices such as improved tillage practices, sod-based crop plant rotations, fertility treatments and larger extents of crop residues left on the cultivation field contribute to control of soil erosion (Wischmeier and Smith, 1978).

For the study area, there is no specific documentation about the support practice put in place. However, as far as the presence of steep terrain landscape is concerned, steep back slope terrace is the common support practice being put in place in most of the farming fields in Bhutan (see

Picture 6.1) and it stands true for the study area as well with 3.13% of the catchment area consisting of agricultural land.

Therefore, for the study area, as suggested by Wischmeier and Smith (1978), the P factor value was assigned by classifying land into agricultural and other land use types. The agricultural land is categorized into six slope classes and p-value to the respective slope classes were assigned since management activities are highly dependent on the slope of the area as shown in Table 6.4.

Picture 6.1: Back slope terrace farming in Bhutan

Table 6.4: P-Factor value for respective land use/cover for the study area.

Land use type	Slope Percent	P-factor	Area %	Reference P factor value
Agricultural land (Chuzing & Kamshing)	0-5	0.1	3.13	(Wischmeier and Smith, 1978)
	5-10	0.12		
	10-20	0.14		
	20-30	0.19		
	30-50	0.25		
	50-100	0.33		
Other lands (Rest of land cover/use except water bodies	All	1.00	87.23	
Water bodies	All	0.00	9.64	(Jain et al., 2001)

After converting the raster land use/cover map into vector format and carrying out spatial join with the gridded map of the study area, the attribute tables which contains land use/cover types in each cells were exported in Excel file format. By using Excel, the P factor values were assigned accordingly and later joint with the gridded attribute table with ArcMap tools and converted back into the raster file format using feature to raster conversion tools of ArcMap to create P factor map as shown in Figure 6.7.

Since the majority of the land use/cover types consists of forests, shrubs, meadows, etc. the raster map produced for P factor shows that 87.23% of the area were assigned a P factor of 1 while 9.64% consisting of water bodies were assigned P = 0. Depending on the slope classes of the agricultural land, the P factor value as mentioned in Table 6.4 was assigned accordingly and, as Figure 6.7 illustrates, P factors less than 1 are mostly concentrated along the river valleys which is due to the fact that most of the agricultural lands are located along the river valleys which are relatively flatter region and more fertile compared to those of surrounding hilly areas.

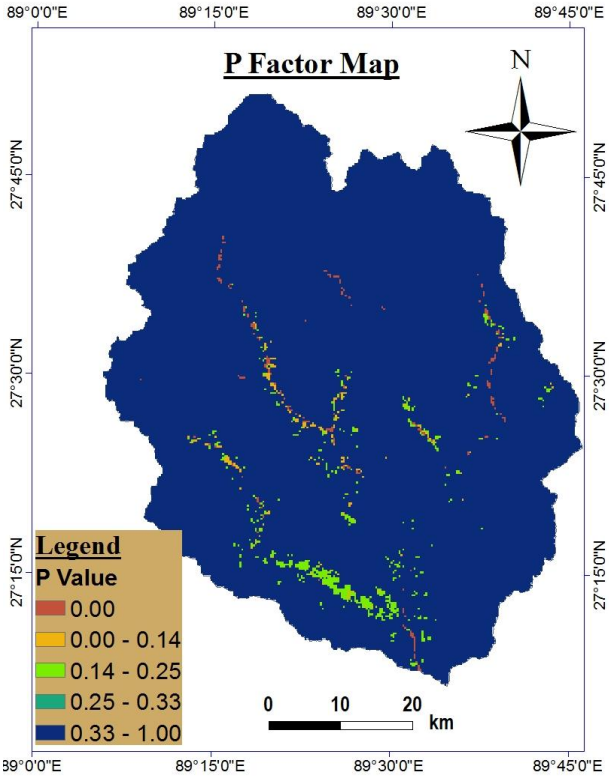

Figure 6.7: P factor raster map for the study area

6.2.6 Sediment Delivery Ratio (SDR)

The soil erosion computed by the use of RUSLE gives the gross soil erosion which is not equivalent to sediment yield as most of the time not all the eroded materials is transported to streams. Soil erosion is the first step towards sediment yield in streams leading to reservoirs and other water bodies. Only a portion of eroded soil are transported into the channel system while the remaining get deposited along the way. Therefore, sediment yield can be quantified from gross soil erosion using Sediment Delivery Ratio (SDR), also referred to as a transmission coefficient, which is fraction of gross soil erosion by water that is delivered to a particular point in the drainage system (Ouyang and Bartholic, 1997). The SDR takes into consideration the sediment deposition that become increasingly significant as the area of catchment increases,

and therefore, determines the relative importance of sediment sources and their delivery down the catchment systems (Lee and Kang, 2013).The SDR is mathematically expressed as:

$$SDR = \frac{Y}{E} \qquad \text{Eq. 6.8}$$

where:

SDR = Sediment Delivery Ratio

Y = Sediment Yield of the Basin

E = Gross Erosion of the Basin

There have been several models developed for SDR to compute the sediment yield from the catchment. As reported by Ouyang and Bartholic (1997), these models can be generally grouped into two categories:

1. Statistical or empirical based on observed data which are found easy to use and computationally efficient
2. Deterministic model based on the hydrological and sedimentological process which may be able to compute temporal and spatial simulation. However, it requires very extensive data and that would be disadvantage to a situation like in the case of the chosen study area.

Out of numerous approaches developed viz. Soil loss-Sediment yield approach, Drainage area and SDR Curves, Rainfall-runoff & SDR Curves, Slope-gradient & Relief-length Ratio and particle size & SDR, Ouyang and Bartholic (1997) suggest the use of drainage area method which is widely used and acceptable to estimate the SDR of a catchment considering its applicability and data availability. Mathematical expressions are listed below including a brief background:

1. Renfro (1975) developed, based on sediment yields observed in 14 watersheds in the Blackland Prairie Area in Texas, the following formula.

$$\log_{10}(SDR) = 1.7935 - 0.14191 \log_{10}(A) \qquad \text{Eq. 6.9}$$

where:

A = drainage area in km^2

2. Vanoni (1975) developed, based on data from 300 watersheds throughout the world, the following relationship which is considered a more generalized one to estimate SDR.

$$SDR = 0.42A^{-0.125} \quad \text{Eq. 6.10}$$

where

A = drainage area in square miles.

3. Boyce (1975) gives, based on the data from the Blackland Prairie, Texas, the following formula:

$$SDR = 0.51A^{-0.11} \quad \text{Eq. 6.11}$$

Where A = drainage area in square miles.

Though all the above empirical formulas (viz. Eq. 6.9, Eq. 6.10 and Eq. 6.11) were developed for the different region outside Bhutan, they had to be used since there are no such general relations developed for Bhutan watershed as well for the Himalaya regions. A detailed analysis of numerous watersheds would have to be carried out with the statistical analysis of their estimated soil loss and their respective observed sediment yields in order to develop such empirical relations which would be more suitable for the mountainous terrain region like in the case of Bhutan.

Since sediment delivery in the watershed involves complex processes, ensuring good estimation of sediment yield with use of SDR of a single model is very difficult (Ouyang and Bartholic, 1997). Therefore, the sediment yield for the study area was estimated by applying the above mentioned equations to get an approximation of the value ranges.

6.3 Estimation of sediment yield with RUSLE

As discussed in the previous sections with regard to the preparation of each RUSLE factors, the product of these factors (i.e. A = R*K*LS*C*P) gives the estimation of soil loss and upon applying the SDR, sediment yield at each grid/cells can be calculated. The results of the RUSLE factors are summarized in Table 6.5 and those for soil loss and sediment yield of the study area based on application of different SDR equations are illustrated in Table 6.6 below:

Table 6.5: RUSLE factor value summary

Parameters	RUSLE Factors				
	R	**K**	**LS**	**C**	**P**
Min.	280.44	0.24	0.00	0.00	0.00
Max.	940.02	0.26	1039.31	0.35	1.00
Avg.	425.35	0.24	22.26	0.01	0.98

Table 6.6: Summary results of Sediment yield estimation using RUSLE approach

Parameters	Soil loss (ton/ha/year)	Soil loss (ton/km^2/year)	Sediment Yield (ton/km^2/year)		
			With SDR **Eq. 6.9**	With SDR **Eq. 6.10**	With SDR **Eq. 6.11**
Minimum	0.00	0.00	0.00	0.00	0.00
Maximum	2719.94	271994.09	69165.94	46298.85	51598.71
Average	14.72	1472.30	451.74	302.39	337.01
Estimation at gauging station	24.26	2425.86	616.88	412.93	460.20

The table showing the detail results of RUSLE factors, soil loss and sediment yield of the study area extracted from the ArcMap is enclosed as Appendix B, Table B1

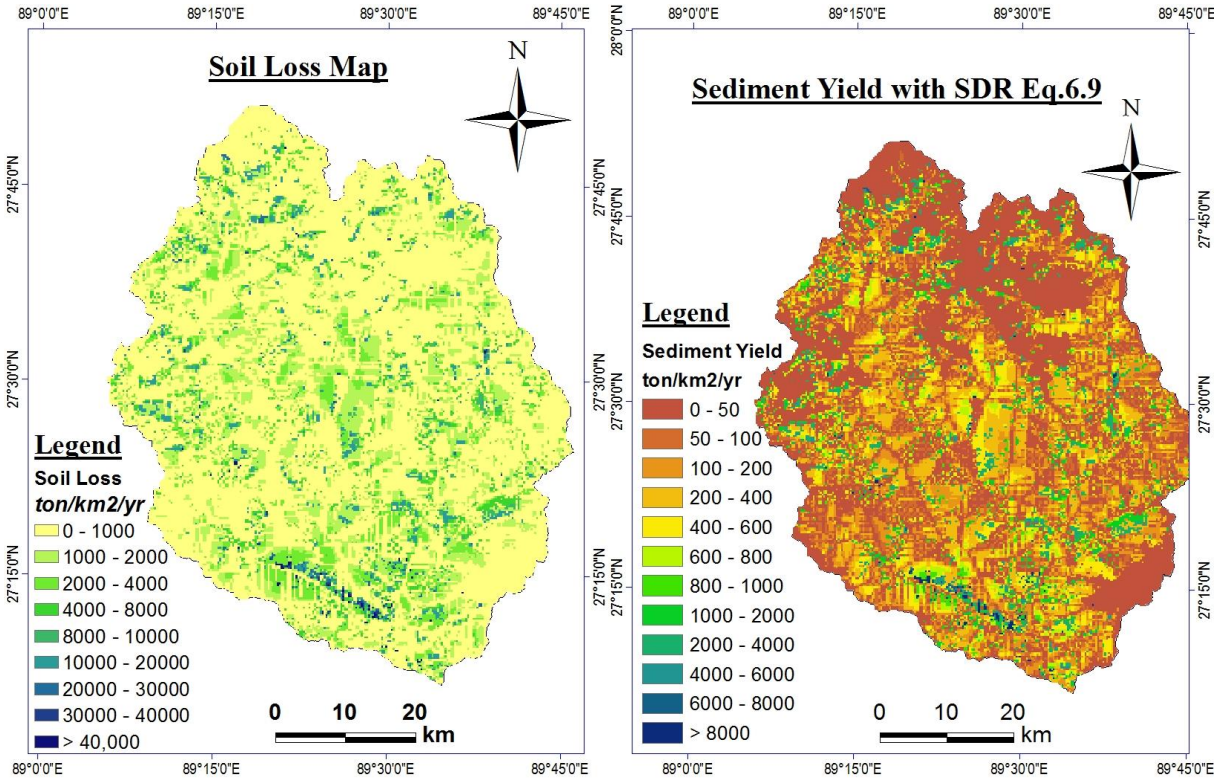

Figure 6.8: Soil loss map (*Left*) and Sediment yield map of the study area produced after application of SDR **Eq. 6.9** (*Right*)

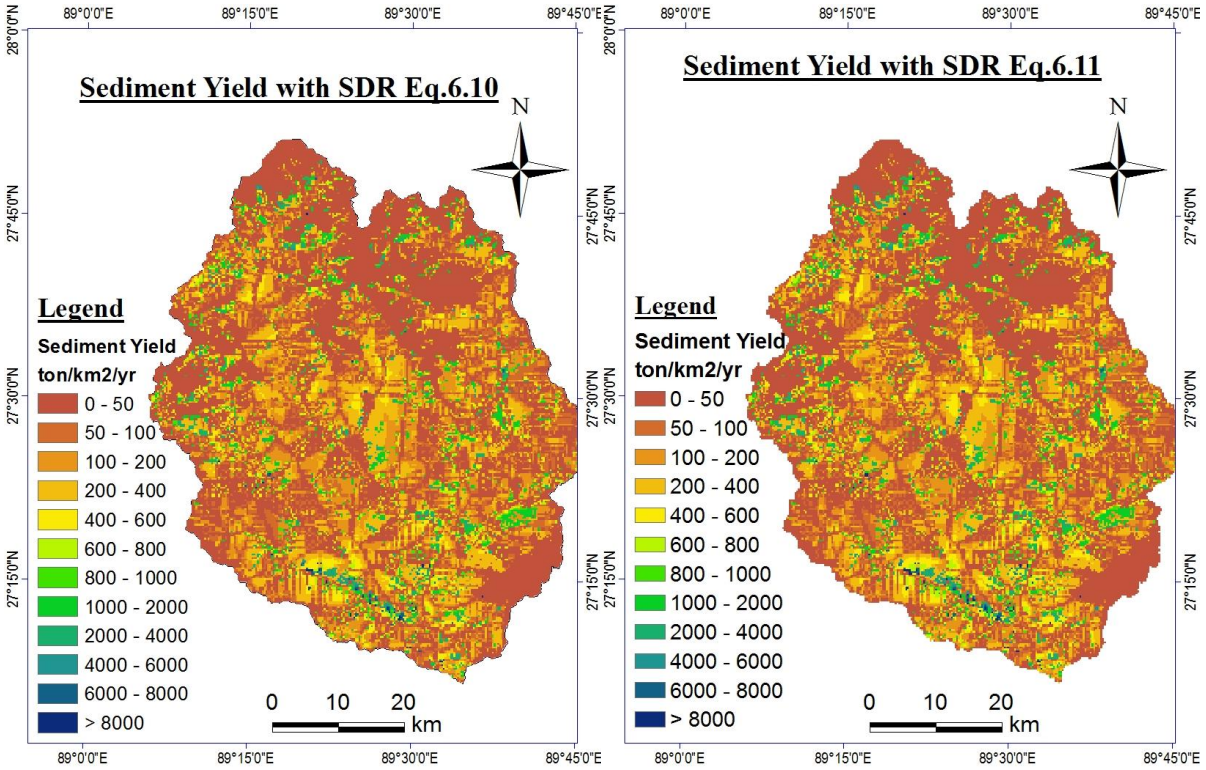

Figure 6.9: Sediment Yield map of the study area produced after using SDR **Eq. 6.10** (*Left*) and Sediment yield map produced after using SDR **Eq. 6.11** (*Right*).

6.4 Discussion

As illustrated in Table 6.5, results of the RULSE factor analysis gives the information that the main influencing factors are rainfall erosivity (R) and slope steepness length (LS) factor followed by soil erodibility factor (K). The other two factors viz. C and P have played very minor part to the soil loss and sedimentation yield of the study area due to their negligible factor values. For the soil loss and sediment yield estimation to be more accurate, estimation of R and LS factors were perceived to be very essential and that would necessitate high density and frequency of rainfall data for R factor and DEM with good resolution for estimating LS factor.

From the tables above, it can be seen that soil loss in the study area is as high as 271994 ton/km^2/year attributed to high LS factor while in some part of the study area, the soil loss is equal to zero in places where there are water bodies and rock outcrops and it may be due to the fact that soil losses do not occur from water surface and hardly from rock outcrops as well. The sediment yield estimated based on SDR Eq. 6.10 gave the lowest value and it probably must be due to the fact that the equation was derived from a generalized condition i.e. considering the study of watershed throughout the world.

Though from maps generated for sediment yield, it is very hard to point out the yield pattern. However, as illustrated in Figure 6.8 (*Right*) and Figure 6.9, the sediment yield of majority of the study area extends from 50 to 600 t/km2/yr. Areas with sediment yield more than 4000 t/km^2/year are sparely scattered and these areas must be located in the very steep terrain coupled with high rainfall impact, absence of support practice and soil surface prone to erosion.

There is relatively high sediment yield zone of small area concentrated in south-west part of the catchment and such outcome is attributed to high rainfall in that region.

CHAPTER 7: ANALYSIS OF SEDIMENT DATA

As already discussed in Chapter 4: the suspended sediment data for the period 2009-2015 is used in the present study to carry out the reservoir sedimentation study of Bunakha. The data is measured at the gauging station Tamchu which is located at about 3 km upstream of the planned reservoir for Bunakha Hydro-electric Project as discussed in section 4.1 of Chapter 4 . In the following, the analysis of the observed suspended sediment data is carried out and, with the use of discharge series, river cross-section and other necessary data, the computation of suspended load and bed loads were also attempted and compared with the observed loads.

7.1 Daily Variability of Sediment Concentration

The data series of suspended sediment concentration (both fines and sand) and discharge measured at Tamchu gauging station were plotted as shown in Figure 7.1. The plot illustrates that larger sediment concentration had occurred during the high flow period. There was an exceptionally very high sediment concentration (both fine and sand) measured on 26th May 2009. The reason for its occurrence is explored and discussed in the next section.

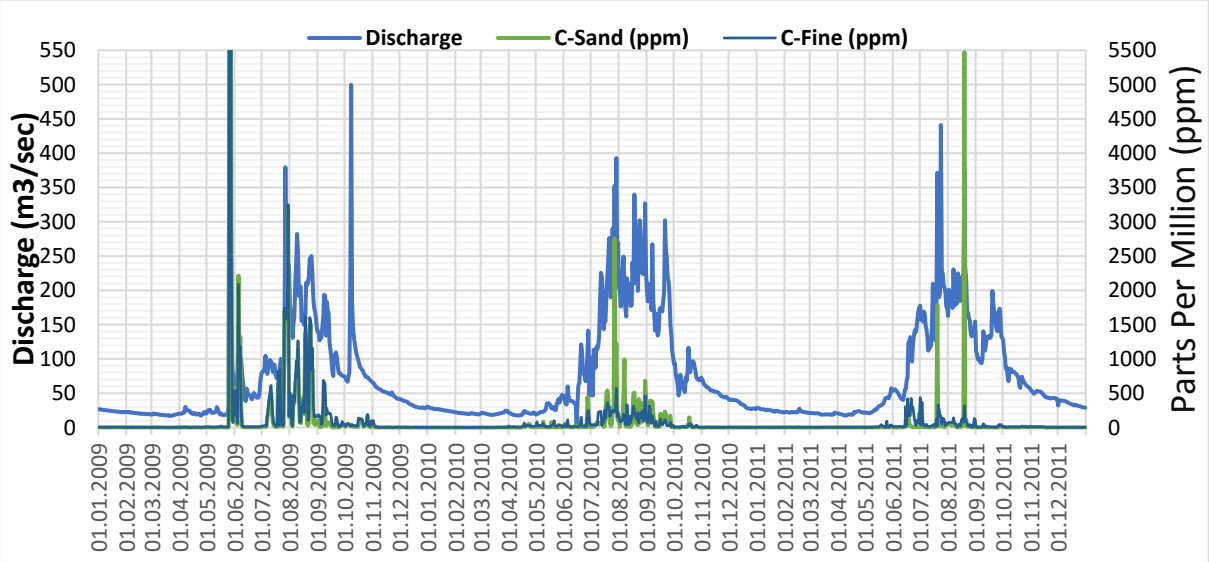

Figure 7.1: Daily variability of suspended sediment concentration (in ppm) along with the discharge for the period 2009-2011.

7.2 Daily Variability of suspended Sediment load

For computing suspended sediment load from its measured concentrations, the equation below was used to transform concentration (ppm) to load (kg/m^3) with the equation (Julien, 2010) mentioned below:

$$C = \rho_s C_v = \frac{\rho \frac{\rho_s}{\rho} C_w}{\frac{\rho_s}{\rho} + \left(1 - \frac{\rho_s}{\rho}\right) C_w} = \frac{\rho \frac{\rho_s}{\rho} C_{ppm} 10^{-}6}{\frac{\rho_s}{\rho} + \left(1 - \frac{\rho_s}{\rho}\right) 10^{-06} C_{ppm}} \quad \text{Eq. 7.1}$$

Where:

ρ_s = Density of sediment (kg/m3)

ρ = Density of water (kg/m3)

C_w = weight concentration

$$= \frac{\text{weight}}{\text{total weight water-sediment mixture}} = \frac{V_s \rho_s}{V_t \rho + V_s(\rho_s - \rho)} \left[\frac{kg}{kg}\right]$$

$$C_v = \text{Volume Concentration} = \text{Sediment} \frac{\text{Volume}}{\text{volume of water-sediment mixture}} = \frac{V_s}{V_t} \left[\frac{m^3}{m^3}\right]$$

C_{ppm} = sediment concentration in parts per million or $\left[\frac{mg}{l}\right]$

Suspended sediment load was estimated from observed suspended sediment concentration data series as a function of discharge and density of sediment and water using Eq. 7.1. From the plot in Figure 7.2, it can be observed that a relatively high load was observed on 26th May 2009. After visual inspection of the discharge data series, it was found that this event was coupled to an extremely large discharge on that day. In order to further validate this event, the discharge upstream and downstream of the gauging station was evaluated to verify if similar magnitude of discharge had occurred. As expected, it was observed that large discharges had been recorded in both the gauging stations (refer Figure 7.4) on the same day.

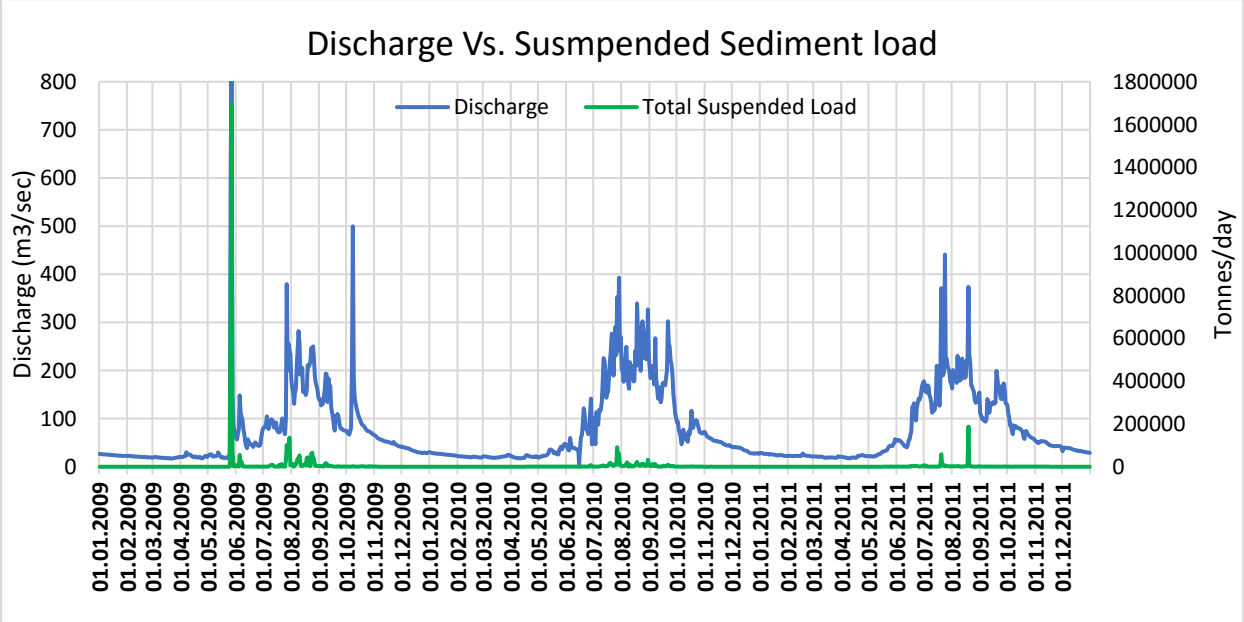

Figure 7.2: Discharge vs. suspended sediment load: Period shown from 2009 to 2011

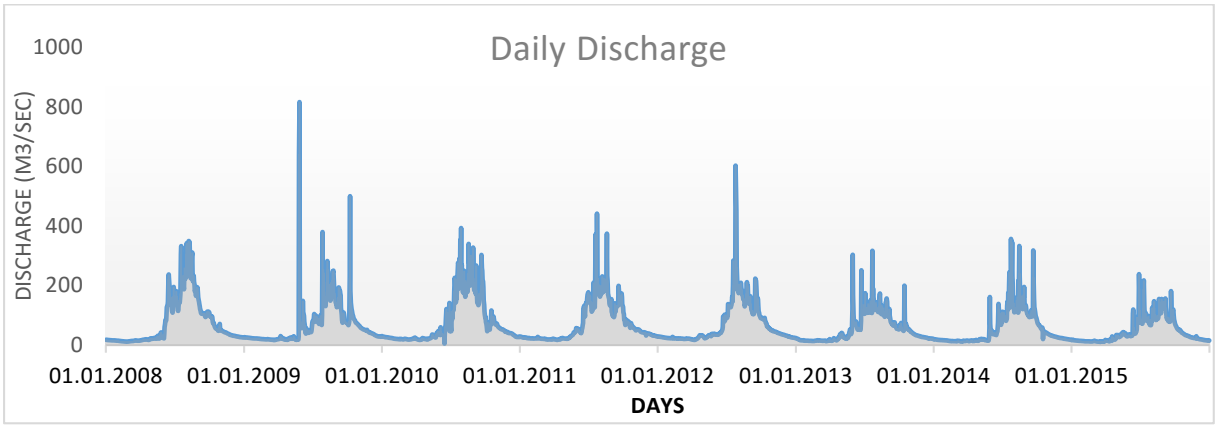

Figure 7.3: Daily discharge variation at sediment gauging station (2008-2015)

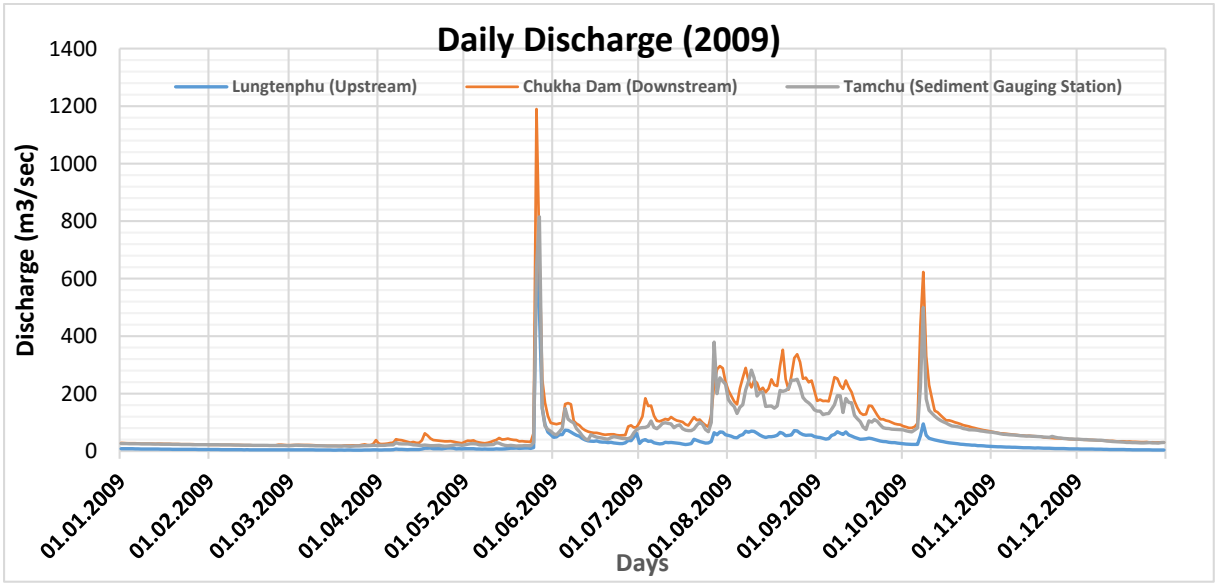

Figure 7.4: Validation of discharge of Tamchu gauging station with other gauging stations located upstream and downstream: 2009

Upon further inquiries, it was found out that this event was due to a flash flood triggered by Cyclone Aila which made its way from Bay of Bengal into the north-eastern Bhutan on 26th May 2009 (GHNC, 2011, RSPN, 2009). Picture 7.1 shows a glance of flash flood occurred on that day.

Picture 7.1: 2009 flash flood captured at the upstream of the sediment gauging station on 26th May 2009

From the picture above, transport of massive sediment load seems inevitable. Therefore, the event of extremely high suspended sediment rates was validated and attributed to the unusual flash flood incidence on that day.

7.3 Monthly Variability of Sediment Concentration

In order to investigate the monthly variability of sediment concentration, both discharge and suspended sediment concentration data series were averaged on a monthly basis and plotted as shown in Figure 7.5. It is obvious from Figure 7.5 that the larger the discharge, the higher the sediment concentration due to the fact that when flow in the channel increases, it entails more turbulence coupled with increased velocity and shear velocity exceeding the settling velocity of the sediment particle, i.e. more sediments are transported in suspension. However, a simple linear regression between the monthly average data of sediment concentration against discharge shows a low correlation (R^2=0.19) indicating that discharge is not the only factor for varying pattern of sediment loads in this complex multivariate system associated to sediment transportation.

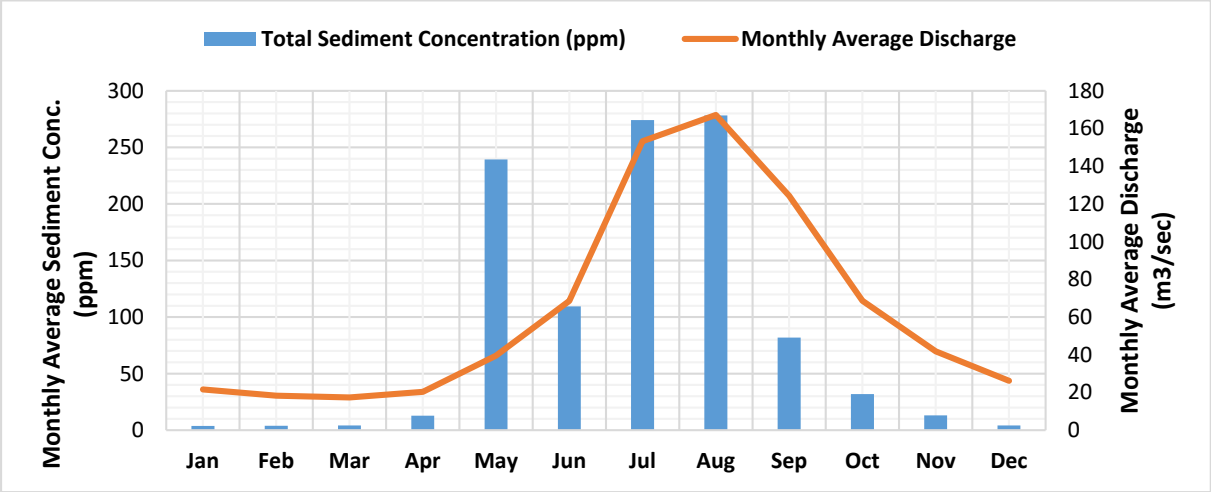

Figure 7.5: Overall monthly average sediment concentration shown along with the overall monthly average discharge

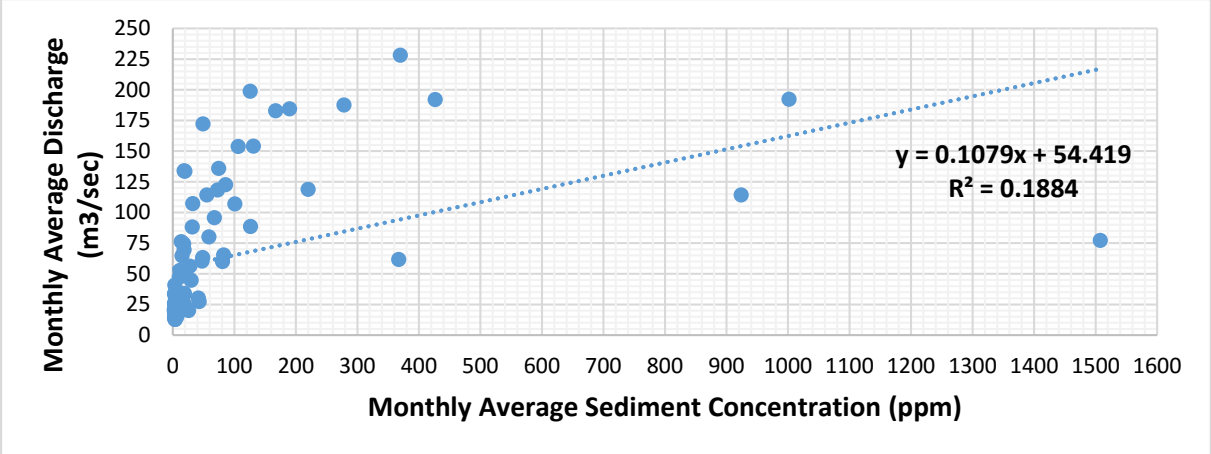

Figure 7.6: Linear regression of monthly average discharge against the monthly average sediment concentration.

7.4 Annual Variability of Sediment Load

The suspended sediment load (both fines and sand) were summed up annually and are presented in Table 7.1 and Figure 7.7 below.

As seen from Figure 7.7, the observed annual suspended loads have a similar order of magnitude except for the year 2009. The reason for such occurrence was due to flash flood incident as already discussed briefly in the previous section (refer 7.2)

Table 7.1: sediment load estimated from observed suspended sediment data

Year	Sand load (tons)	Fine load (tons)	Total suspended load (tons)
2009	1792787	2093852	3886639
2010	415519	269780	685299
2011	269601	131618	401220
2012	56075	85313	141388
2013	35704	71263	106967
2014	64826	120688	185515
2015	22637	75067	97704

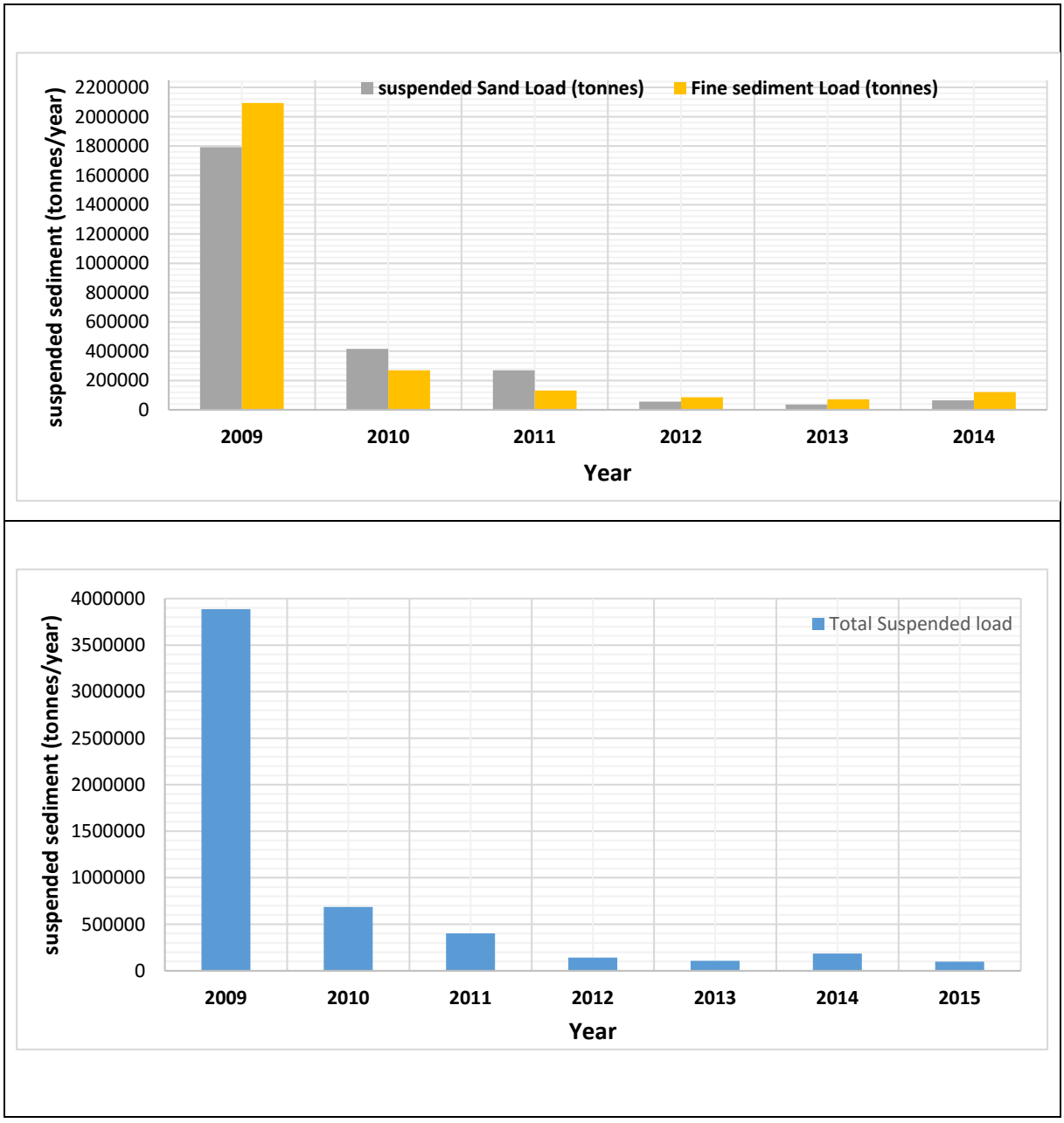

Figure 7.7: Observed total annual suspended sediment load (in tons) for period 2009-2015

7.5 Determination of bed load

The term bed load defines sediment loads which are transported along the river bed in a rolling, sliding, or saltation motion (Van Rijn, 1984). The sediment loads carried by the flow of water are in the form of bed-load and suspended load depending on the flow characteristics and the size of the bed materials. As of now, there is no clear sharp division being established between these two loads and problem is more related to distinguishing between saltation and suspension. However, researchers have developed numerous mathematical expressions to define their layers. The moment of the bed load is initiated when bed-shear velocity exceeds its critical velocity value (Van Rijn, 1984).

The available bed load transport models have a strong empirical character as they are based on data obtained in laboratory experiments and field studies. The further development of these models are hampered due to limited number of accurate laboratory and field studies on bed load transport process. Due to these reasons, there is no universally applicable bed load formula developed so far.

The gauging station in Bunakha Catchment has only suspended sediment load measured while it has assumed 30% of the total suspended load as the bed load. However, it is worth noting that the assumption is not based on any measurement. Therefore, it was felt that the need to estimate the bed load was necessary by taking into consideration of river hydrology, river sections and other necessary assumptions. River cross section at the sediment gauging station (refer Figure 7.9) and discharge-stage curve (refer Figure 7.8) were obtain from Department of Hydrometeorology Services (DHMS), MoEA, Bhutan and it was used while computing the bed load sediment.

Two bed load formulas were used for computation of bed load and their brief descriptions are illustrated below:

i. Meyer-Peter and Müller (1948)

For estimation of bed load proposed by Meyer-Peter and Müller (1948) is an approach based on the bed shear stress concept which considers both median subsurface grain size (d_{50}) and varying size class (d_i). However, for the study area, the approach which utilizes d_{50} is considered for computation of bed load.

The equation is expressed as:

$$q_b = 8\left(Fr_{*,s}\left[\frac{K_{st}}{K_r}\right]^{0.5} - Fr_{*,c}\right)^{1.5}\sqrt{\frac{\rho_s - \rho}{\rho} g d_m^3} \qquad \text{Eq. 7.2}$$

Where:

q_b = volumetric transport rate ($\frac{m^3}{m.s}$)

$Fr_{*,s} = \frac{\rho g R S}{(\rho_s - \rho) g\, dm}$ = Shield-stress

S = bed slope

$Fr_{*,c}$= Critical Shield-stress = 0.047

ρ_s = Density of sediment

ρ = Density of water

K_{st} = Manning roughness value

$\frac{K_{st}}{K_r}$ = Reduction factor condiering bed roughness

K_r= Grain-stickler-number ($K_r = \frac{26}{d_{90}^{\frac{1}{6}}}$)

D_m = mean diamter of sediment grains

ii. Ribberink (1998)

Ribberink (1998) investigated the validity the bed-load transport formula, based on the bed-shear concept of Meyer-Peter and Muller for steady uniform flows with the aim to develop a general bed load transport formula for a wide range of flow and sediment conditions. For that, large set of laboratory data for steady flows were used and arrived to an equation as illustrated below.

For a steady flow, the bed load transport is often represented by non-dimensional parameter as shown below:

$$q_b = \Phi\sqrt{g(s-1)d_{50}^3} \qquad \text{Eq. 7.3}$$

Φ can be calculated by:

$$\Phi = 10.4(\theta_c - \theta_{cr})^{1.67} \qquad \text{Eq. 7.4}$$

Where:

q_b = The volumetric bed load sediment transport rate per unit time and with (m^3/sec/m)

Φ = Non-dimensional parameter

$\theta_c = \frac{\tau_c}{(\rho_s - \rho) g d_{50}}$ = dimensionless bottom shear stress or Shield parameter

$\theta_{Cr} = \frac{0.03}{1+1.2D_*} + 0.055[1 - \exp(-0.02D_*)]$ = Critical Shield's parameter

$D_* = d_{50}\left[\frac{(S-1)g}{\vartheta^2}\right]^{\frac{1}{3}}$ = Dimensionless grain size

g = Gravitational acceleration (m^2/sec)

d_{50} = Median diameter grain

$\tau_c = \rho g R I$ = Shear stress at the bottom of river bed due to current

ρ_s = Density of sediment

ρ = Density of water

S = Ratio of ρ_s to ρ

R = Hydraulic radius

I = River bed slope

ϑ = kinematic viscosity of water = 1.3 x 10^{-6} m^2/sec (at 10 °C)

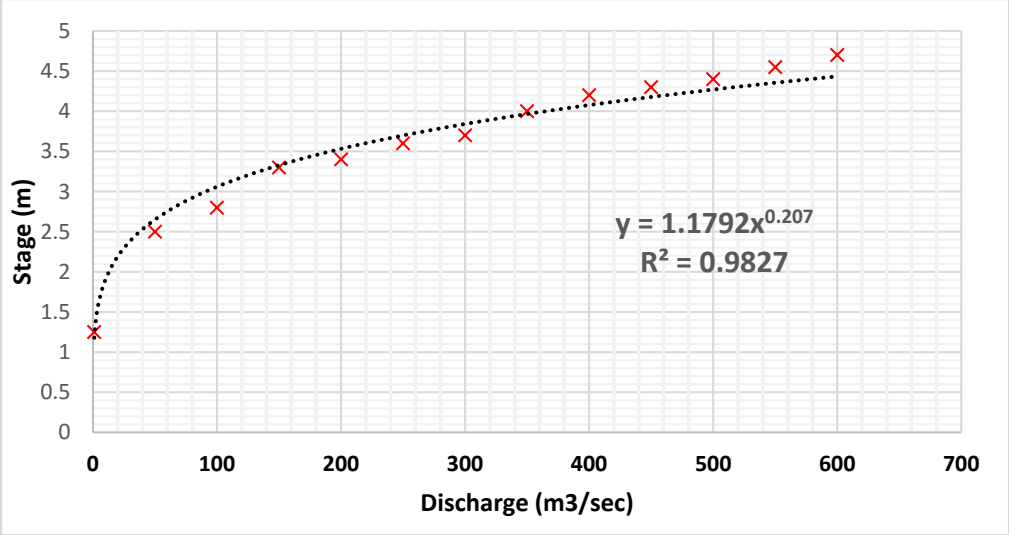

Figure 7.8: Discharge-stage curve of sediment gauging station (Tamchu). Source: DHMS, MoEA, Bhutan. The equation of the curve was used to determine the depth of the river for each corresponding daily discharge series of the river.

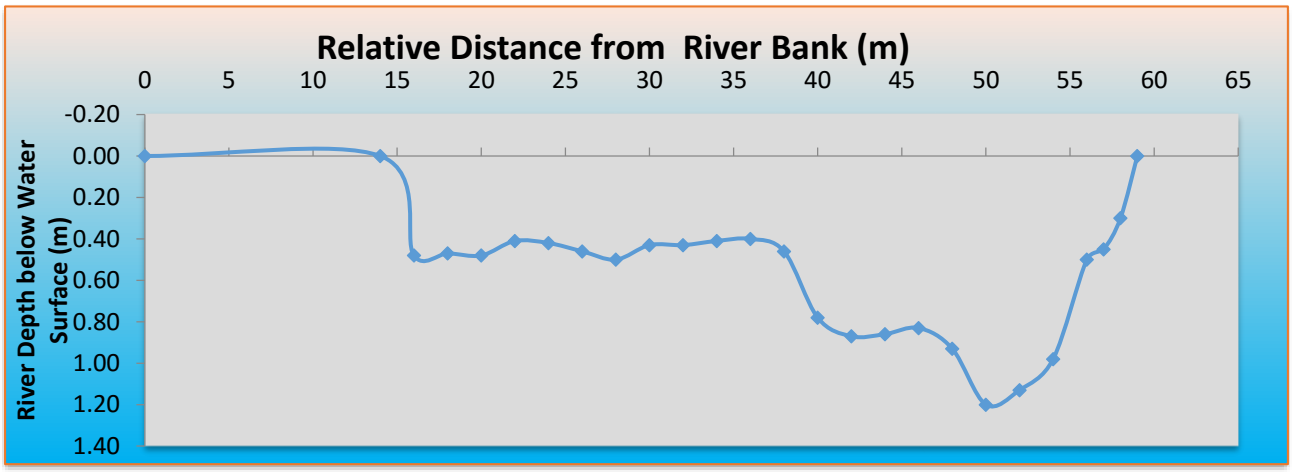

Figure 7.9: River cross section at Sediment gauging station (Tamchu). However, it is to be noted that the cross section was prepared during the lean flow season. From the figure, the maximum river depth from surface is read as 1.2 m, but it is expected the depth and width of the river will increase during the larger flow conditions. (Source: DHMS, MoEA, Bhutan)

By using Eq. 7.2, Eq. 7.3 and Eq. 7.4, the bed load for the Tamchu sediment gauging station was computed using the available data (refer Table 7.2) and some of which were assumed due to lack of data. The results are shown in Figure 7.10.

Table 7.2: Input and assumption data for bed load computation

Parameters	Unit	Value
Strickler-Value, K_{st}	[$M^{1/3}/s$]	35.00
Width of Channel, B	[m]	40.00
Critical Shear Stress, $Fr_{*,c}$	[N/m^2]	0.047
Reduction factor considering bed roughness $\frac{K_{st}}{K_r}$	-	0.95
Density of Sediment, ρ_s	[kg/m^3]	2650.00
Density of Water, ρ	[kg/m3]	1000.00
Mean Diameter of grain, d_{50}	[m]	0.0375
Gravity, g	[m/sec^2]	9.81
Slope of Channel, I	-	0.0012

Though from the river cross section, the width of the river is seen to be wider than 40 m, it was assumed as 40 m in order to compensate the irregular section towards bed level. Despite the fact that its width would change with every change in flow situation, it was considered constant while computing the bed load due to the limited measurement data available for the river cross section.

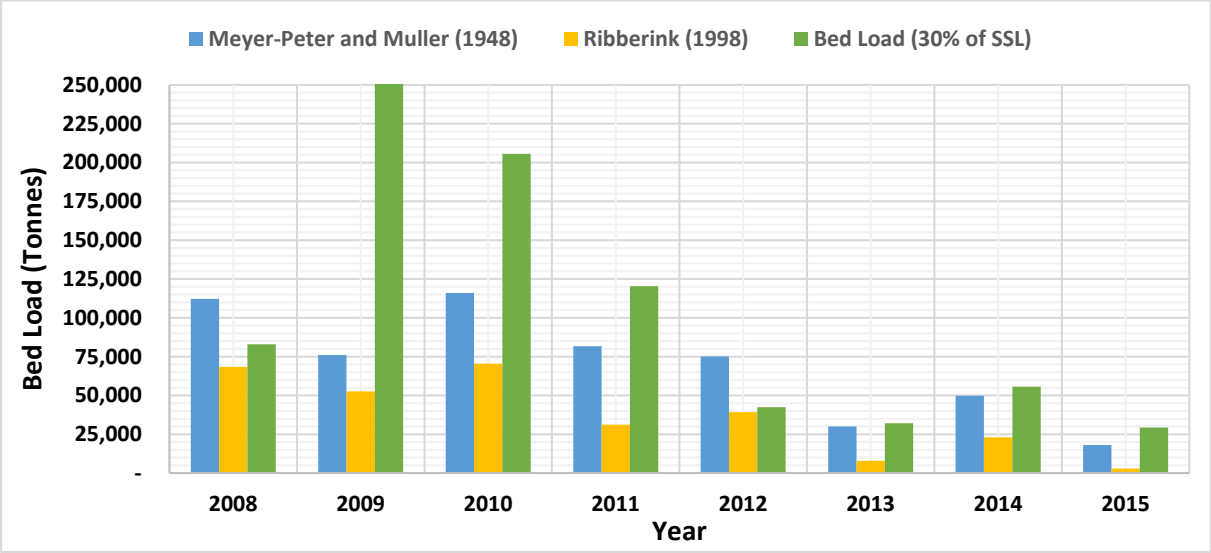

Figure 7.10: Bed load (in tons) computed with Meyer-Perter and Muller (1948), Ribberink (1998) and bed load computed by assuming 30% of suspended sediment load (as practiced in DHMS, MoEA) as the bed load portion .

Table 7.3: Computed annual bed load using Meyer-Peter & Muller (1948) and Ribberink (1998) empirical equations along with the bed load calculated assuming its load as 30% of the suspended sediment load.

year	Bed Loads (tons/year)		
	Meyer-Peter Muller (1948)	**Ribberink (1998)**	**30% of SS (assumed)**
2009	76037	52686	1165992
2010	116041	70457	205590
2011	81747	31245	120366
2012	75158	39246	42416
2013	30071	7906	32090
2014	49884	23011	55654
2015	18147	2970	29311

As illustrated in Figure 7.10, the assumption of bed load considered as 30% of the suspended sediment load does not seems to stand true since it can be seen that in most cases, the bed load calculated with this assumption is higher than the computed bed load using the empirical formulae of Meyer-Peter & Müller (1948) and Ribberink (1998). It is difficult to give a final conclusion since the application of these approaches reequired also some assumptions. However, it can be said that the computed bed loads as per the computation of bed load adopted in this case ranges from 10-25% of the suspended sediment load.

The daily variation of bed load using the methods illustrated above is shown in Figure 7.11.

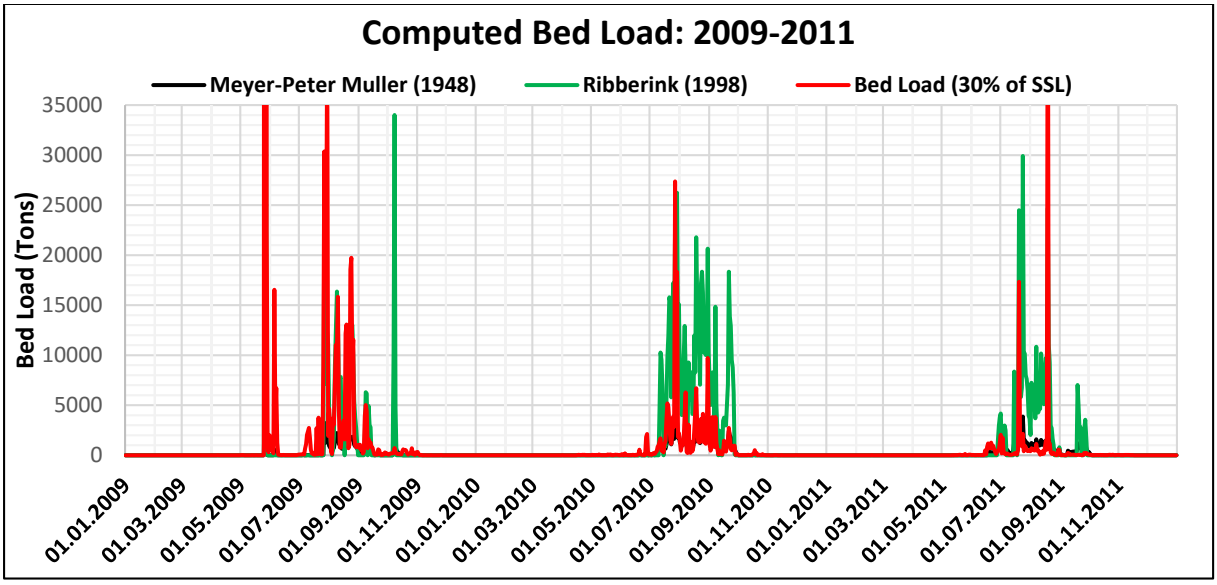

Figure 7.11: Daily variation of bed computed bed load using Meyer-Peter Muller (1948) and Ribberink (1998) empirical equations along with the bed load calculated assuming its load as 30% of the suspended sediment load. However, it is to be noted that some of peak loads are deliberately not shown in the figure above for better visibility of lower values ranges.

Figure 7.11 illustrates that in the lean flow period i.e. during seasons other than monsoon, bed material transport has approached to zero due to the fact that the discharge in those period are too low for the initiation of bed load transports or destroy the existing amour layer of the river bed.

7.6 Determination of Suspended Sediment Load using empirical equation

Though suspended sediment loads were measured in the gauging station, it was nevertheless attempted to compute and subsequently compared with the observed one. For calculation of suspended sediment load, the method presented by Rijn (1984) was used which enables the computation of the suspended load as the depth-integration of the product of the local concentration and flow velocity and it is based on the determination of the reference concentration.

The following equations as illustrated by Rijn (1984) has been used:

$$D_* = d_{50}\left[\frac{(S-1)g}{\vartheta^2}\right]^{\frac{1}{3}} \qquad \text{Eq. 7.5}$$

Where:

D_* = Dimensionless grain diameter;

d_{50} = Median grain diameter (m);

S = Ratio of sediment grain density to water density;

g = Gravitational acceleration (m/s^2);

ϑ = Kinematic viscosity of water (m^2/s)

$$T = \frac{(u_*')^2 - (u_{*,cr})^2}{(u_{*,cr})^2} \qquad \text{Eq. 7.6}$$

Where:

T = Transport stage parameter;

$u_*' = \left(\frac{\sqrt{g}}{C'}\right) u_m$ = Bed-shear velocity related to grains (m/s);

g = Gravitational acceleration (m/s^2);

u_m = mean flow velocity (m/s);

$C' = 18log\left(\frac{12R_b}{3D_{90}}\right)$ = Chezy-Coefficient related to grains;

R_b = Hydraulic radius related to the bed;

$u_{*,cr} = \frac{4w_S}{D_*}$ = Critical Shear velocity (m/s) for $1 < D_* \leq 10$;

D_{90} = Grain diameter at 90% fine

w_s = fall velocity of sediment particle (m/s).

$$Z = \frac{w_s}{\beta \kappa u_*} \qquad \text{Eq. 7.7}$$

Where:

Z = Suspension paramete

w_s = partical fall velocity of suspended sediment (m/s)

β = Coefficient related to diffusion of sediment particles;

κ = constant of Von Karman;

u_* = overall shear velocity (m/s).

$$w_s = 10\frac{\vartheta}{D_s}\left\{\left[1 + \frac{0.01(S-1)gD_s^3}{\vartheta^2}\right]^{0.5} - 1\right\} \qquad \text{Eq. 7.8}$$

Where:

$w_s = particle\ fall\ velocity\ of\ suspended\ sediment$ (m/s);

ϑ = Kinematic viscosity of water (m^2/s)

$D_s = \left(1 + 0.011(\sigma_s - 1)(T - 25)\right)d_{50}$ = parameter which express the representative particle diameter of the suspended sediment particles;

S = Ratio of sediment grain density to water density;

g = Gravitational acceleration (m/s^2);

ϑ = Kinematic viscosity of water (m^2/s)

σ_s = Geometric standard deviation of bed materials;

$$\beta = 1 + 2\left[\frac{w_s}{u_*}\right]^2, for\ 0.1 < \frac{w_s}{u_*} < 1 \qquad \text{Eq. 7.9}$$

Where:

$\beta =$ Coefficient related to diffusion of sediment particles known as $\beta - factor$;

u_* = overall shear velocity (m/s);

$$Z' = Z + \varphi \qquad \text{Eq. 7.10}$$

Where:

Z' = The modified suspension number;

Z = suspension number according to Eq. 7.7;

φ = Overall correction factor representing all additional effects such as volume occupied by particles, reduction of particle fall velocity and damping of turbulence according to Eq. 7.11;

$$\varphi = 2.5\left[\frac{w_s}{u_*}\right]^{0.8}\left[\frac{C_a}{C_0}\right]^{0.4} for\ 0.01 \leq \frac{w_s}{u_*} \leq 1 \qquad \text{Eq. 7.11}$$

Where:

C_a = Reference concentration;

C_0 = maximum volumetric bed concentration = 0.65;

$$a = 0.5\Delta, or\ a = K_s, (with\ a_{min} = 0.01d \qquad \text{Eq. 7.12}$$

Where:

a = reference level (m);

Δ= height of bed form (m);

K_s =equivalent roughness height of Nikuradse;

$d = \text{depth of water(m)}$

$$C_a = 0.015\left(\frac{D_{50}}{a}\right)\left(\frac{T_{1.5}}{D_*^{0.3}}\right) \quad \text{Eq. 7.13}$$

The parameters of the equations are already defined in aforementioned equations.

$$\frac{D_s}{D_{50}} = 1 + 0.011(\sigma_s - 1)(T - 25) \quad \text{Eq. 7.14}$$

The parameters of the equations are already defined in aforementioned equations

$$F = \frac{\left[\frac{a}{d}\right]^{Z'} - \left[\frac{a}{d}\right]^{1.2}}{\left[1 - \frac{a}{d}\right]^{Z'}[1.2 - Z']} \quad \text{Eq. 7.15}$$

Where:

F = F-factor;

$$q_s = Fu_m dC_a \quad \text{Eq. 7.16}$$

Where:

$q_s = \text{suspended load transport per unit width } (\frac{m_3}{sec*m})$

$u_m = \text{mean flow velocity } \left(\frac{m}{s}\right)$

$d = \text{Flow depth (m)}$

$C_a = \text{Reference concentration;}$

Therefore, as proposed by Van Rijn (1984), the complete method to estimate the suspended sediment load (volume) per unit width was followed as specified below:

1. Computation of particle diameter, D_* — By Eq. 7.5
2. Computation of critical bed-shear velocity — According to shields, $u_{*,cr}$
3. Computation of transport stage parameter, T — By Eq. 7.6
4. Computation of reference level, a — By Eq. 7.12
5. Computation of reference concentration, Ca — By Eq. 7.13
6. Computation of particle size of suspended sediment, Ds — By Eq. 7.14
7. Computation of fall velocity of suspended sediment, w_s — By Eq. 7.8
8. Computation of β-factor — By Eq. 7.9

9. Computation of overall shear velocity $u_* = \sqrt{gdI}$
10. Computation of φ-factor By Eq. 7.11
11. Computation of suspension parameter, Z By Eq. 7.7
12. Computation of modified suspension parameter, Z' By Eq. 7.10
13. Computation of F-factor By Eq. 7.15
14. Computation of suspended load transport, q_s By Eq. 7.16

Shown below are the data and assumptions used to enable computation of suspended sediment load using equations specified above:

Table 7.4: Input and assumption data for suspended sediment load computation

Parameters	**Units**	**Values**
Width of River, B	[m]	40
River Bed slope, I	-	0.0012
Median grain diameter, d_{50}	[m]	0.0005
Kinematic Viscosity of water	[m^2/sec]	1.30E-06
Strickler roughness value, Kst		35
Density of water, ρ	[kg/$m^{3]}$	1000
Density of sediment, ρ_s	[kg/$m^{3]}$	2650
Acceleration due to gravity, g	[m/sec^2]	9.81
Ratio of ρ_s to ρ, S	-	2.65
Dimensionless grain size dia., D_*	-	12.65
Geometric Standard Deviation, σ_s	-	1.5
Grain Diameter, d_{90}	[m]	0.0006
Von Karman Constant, k	-	0.4

Table 7.5: Computed, observed suspended sediment load (tones) and their discrepancy ratio (r).

Year	COMPUTED Suspended Sediment load (tones)	OBSERVED Suspended Sediment load (tones)	r
2009	3159683	3886639	0.81
2010	3324663	685299	4.85
2011	3256550	401220	8.12
2012	3155262	141388	22.32
2013	2830616	106967	26.46
2014	2786683	185515	15.02
2015	2617514	97704	26.79

The accuracy of the computed to observed sediment loads were given in terms of discrepancy ratio (r) which is defined as:

$$r = \frac{q_{s_{computed}}}{q_{s_{observed}}} \qquad \text{Eq. 7.17}$$

As seen from Table 7.5 where (r) value ranges from 0.8 to 26.79 indicating that the predicted suspended sediment load using prescribed method gives very high discrepancy (also refer Figure 7.12) except for the year 2009. This may be due to the following reasons:

1. There is no grain size distribution data available for the sediment gauging station. Therefore, standard deviation of river bed gran geometry and median grain size reported by Choden (2009) for a river in Bhutan were used for the computation. However, when evaluated closely, the grain size distribution plotted depicts that the suspended sediment grain sizes are very much finer than what is expected in the rapid rivers of Bhutan, thereby yielding much larger suspended sediment loads compared to the observed value. The grain size distribution used may not stand true for the sediments of river channel of the Bunakha catchment.
2. The width of the river was kept constant throughout the computation and that has failed to capture the high flow situations (monsoon season) which is expected to produce more sediment load than predicted, thereby yielding less sediment load compared to the observed one in those periods. However, in the period of low flow situations, the predicted values are much larger than the observed sediment loads (refer Figure 7.13) due to the assumptions of constant width of river while in actual condition it may be much lesser than the assumed width. Cumulatively, the predicted loads are much larger in many folds than the observed loads except for the year 2009.

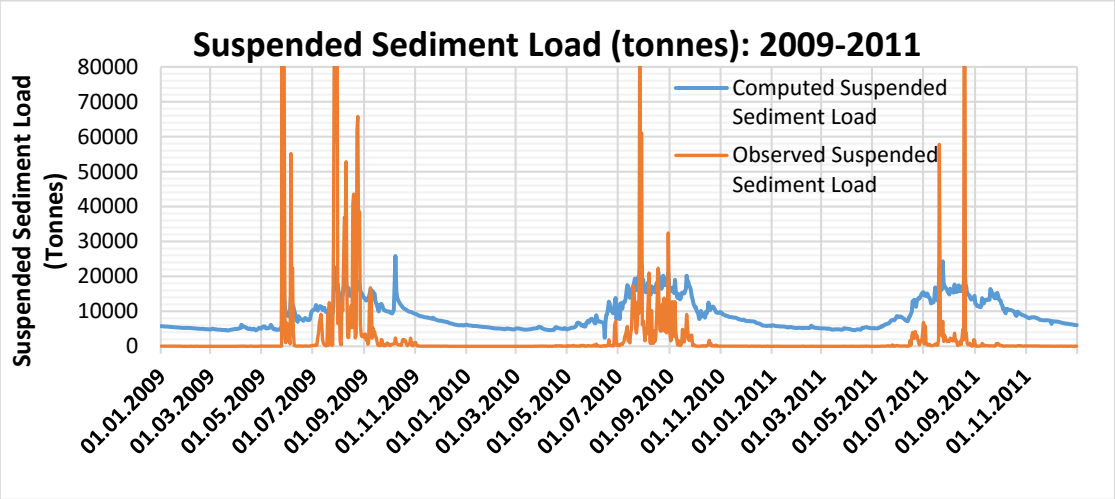

Figure 7.12: Computed and observed sediment load (in tons) for the period 2009-2011. Some of peak loads are deliberately not shown in the figure above for better visibility of lower values ranges

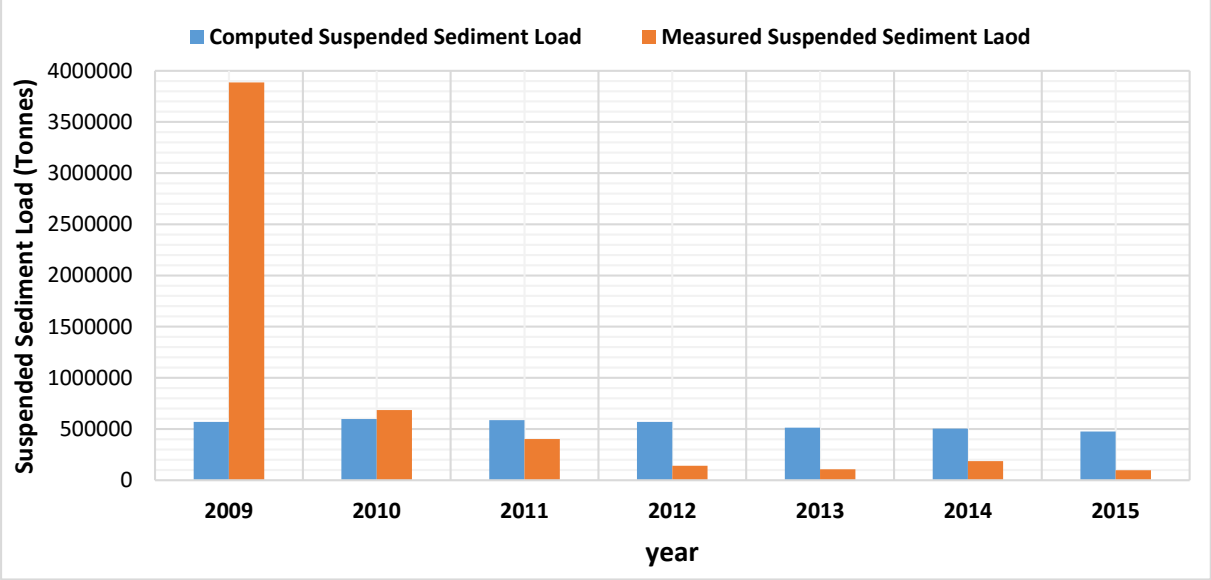

Figure 7.13: Revised computed and observed sediment load (in tons) for the period 2009-2011. Some of peak loads are deliberately not shown in the figure above for better visibility of lower values ranges.

Therefore, the computation was tested with larger grain size for d_{50} (2 mm) and d_{90} (1 mm) to produce the computed value as close as the observed one. The revised computed suspended sediment load is shown in Table 7.6 along with the observed load and it illustrates that the discrepancy ratio is drastically reduced ranging from 0.15 to 4.8 indicating that the computed SSL has fairly replicated the observed values except for the year 2009 where the computed value is too low as also illustrated in Figure 7.13. Though, the annual accumulation of bed load were of the same magnitude of order, there were variation both in terms of spatial and temporal

which may be due to the assumptions of constant river width maintained owing to lack of details.

Table 7.6: Revised computed suspended sediment load with discrepancy ration r

Year	Computed Suspended Sediment load (tones)	Observed Suspended Sediment load (tones)	r
2009	569571	3886639	0.15
2010	597171	685299	0.87
2011	586598	401220	1.46
2012	569202	141388	4.03
2013	512781	106967	4.79
2014	503398	185515	2.71
2015	475055	97704	4.86

However, it is to be noted that the grain size was assumed, it cannot be ascertained if grain size used actually represents the grain characteristics of the sediment gauging station. Nevertheless, the result obtained with this changed in parameter was carried forward for further analysis of reservoir sedimentation study while the former computed values were neglected/discarded.

7.7 Summary of data analysis & estimation from PSIAC and RUSLE approach

The ensuing tables in this section illustrates the summary of results arrived from sediment data analysis for the period 2009-2015. The results obtained from PSIAC and RUSLE approaches are also summarized.

The result obtained as illustrated in the tables, irrespective of the approaches, seems to provide sedimentation rate of similar order of magnitude. The total load determined by combining observed sediment load (SSL) and various bed load calculation approaches (refer Table 7.7) viz. with the assumptions of bed load portion as 30 % of the SSL as adopted at DHMS, MoEA, Bhutan and with the use of Meyer-Peter Muller (1948) and Ribberink (1998) show that the assumptions considered by DHMS seem to be conservative and the obtained results are comparatively larger than those computed by using the empirical equations. The computed bed load with these equations ranged from 10-25% of the suspended sediment load. The specific sediment yield (tons/km^2/year) derived from the overall average of the sediment of the whole period are 454, 376 and 366 respectively, as presented in Table 7.8.

Table 7.7: Total suspended load (observed and computed) and total bed load (with assumption & empirical equations

Year	Total suspended load (tons)		Total Bed load (tons)		
	Observed	Computed Rijn (1984)	Assumption (30 % of SSL)	Meyer-Peter Muller (1949)	Ribberink (1998)
2009	3886639	569571	1165992	76037	52686
2010	685299	597171	205590	116041	70457
2011	401220	586598	120366	81748	31245
2012	141388	569202	42417	75158	39246
2013	106967	512781	32090	30071	7906
2014	185515	503398	55654	49883	23011
2015	97704	475055	29311	18147	2970

Table 7.8: Total sediment load:- Combination of OBSERVED suspended sediment load and selected bed load calculation approaches

Year	Total Sediment load (tons/year) with observed SSL		
	With 30 % of SSL	With MPM (1949)	With Ribberink (1998)
2009	5,052,630	3,962,676	3,939,325
2010	890,888	801,340	755,756
2011	521,585	482,967	432,464
2012	183,804	216,546	180,634
2013	139,057	137,038	114,873
2014	241,169	235,399	208,525
2015	127,015	115,851	100,674
Overall average	1,022,307	850,259	818,893
Overall specific sediment yield (ton/ km^{2}/yr)	454.36	377.89	363.95

Table 7.9:Total sediment load:- Combination of COMPUTED suspended sediment load and selected bed load calculation approaches.

Year	Total Sediment load (tons/year) with COMPUTED SSL		
	with 30 % bed load	With MPM (1949)	With Ribberink (1998)
2009	1735563	645608	622257
2010	802761	713212	667628
2011	706964	668346	617843
2012	611618	644360	608448
2013	544871	542852	520687
2014	559052	553282	526408
2015	504366	493202	478024
Overall average	780742	608694	577328
Overall specific sediment yield (tons/km^{2}/yr)	347	271	257

The annual average sediment yield estimated from PSIAC and RULSE approaches both gives comparable results compared to the observed and computed loads.

The sedimentation rate in terms of mm/year resulted from all approaches ranges from 0.13 to 0.63 which are in the ranges reported in earlier studies carried out in other rivers of Bhutan. The porosity of the sediment was assumed as 30% indicating that accumulated volume of the sediment in the reservoir would be increased by the factor of 1.3. The highest value can be considered as the upper limit for evaluating the reservoir sedimentation of the study area. However, for predicting the reservoir sedimentation, mean value of 0.5 mm/year was used after taking into consideration the safety factor of 1.3 to take into account the extreme event of landslide due to glacier lake outburst.

Table 7.10: Sediment yield- PSIAC approach with GIS integration

	(S1)[9] & (S1)[10]	(S2)[11] & (S2)[12]	(S3)[13] & (S3)[14]
Sediment Yield estimation at Gauging station (ton/km^2/year)	**805**	**365**	**1293**

Table 7.11: Sediment yield- RUSLE approach with GIS integration

	Sediment Yield (ton/km^2/year)		
	With SDR **Eq. 6.9**	With SDR **Eq. 6.10**	With SDR **Eq. 6.11**
Estimation at gauging station	**617**	**413**	**460**

[9] Considering Scenario 1 of the channel erosion parameter
[10] Considering Scenario 1 of the upland erosion parameter
[11] Considering Scenario 2 of the channel erosion parameter
[12] Considering Scenario 2 of the upland erosion parameter
[13] Considering Scenario 3 of the channel erosion parameter
[14] Considering Scenario 3 of the upland erosion parameter

Table 7.12: Sedimentation rate (mm/year) derived from the results of approaches used

Approach	With 30 % Bed load assumed (tons)	With MPM (1948)	With Ribberink (1998)
With Observed SSL[15]: Sedimentation rate (mm/year)	0.22	0.19	0.18
With Computed SSL: Sedimentation rate (mm/year)	0.17	0.13	0.13
PSIAC Approach	(S1) & (S1)	(S2) & (S2)	(S3) & (S3)
Sedimentation rate (mm/year)	0.40	0.18	0.63
RUSLE Approach	With SDR **Eq. 6.9**	With SDR **Eq. 6.10**	With SDR **Eq. 6.11**
Sedimentation rate (mm/year)	0.303	0.203	0.226

[15] Suspended sediment load

CHAPTER 8: PREDICTING SEDIMENT DISTRIBUTION IN THE RESERVOIR

The inflow of sediment into the reservoir gets deposit in the due course of time and bed level of the reservoir rises up and sets a new bed level which is referred to as New Zero-capacity Elevation (NZE). This rising of bed level due sediment deposition causes the live storage capacity to shrink. Therefore, it is necessary to predict the NZE for different time horizons to assess the revised reservoir capacity and its corresponding area (BIS, 1994).

There are two widely used empirical methods viz. (i) Area-Increment method; (ii) Empirical Area Reduction method to predict the sediment distribution in the reservoir developed by U.S Bureau of Reclamation and also has been recommended in IS 5477 (Part 2): 1994 of the India Stand Code of practice, which consist of four steps as briefly outlined below (Morris and Fan, 1998):

1. Determination of amount of sediment to be distributed.
2. Selection of the appropriate empirical curve for sediment distribution on the basis of the site characteristics.
3. Determination of New Zero-capacity Elevation (NZE) which is the height of the sediment accumulation at the dam after certain years.
4. Distribution of sediment as a function of depth above NZE with the use of selected empirical curve.

Out of the two empirical method, the Empirical Area Reduction Method is adopted in the present study.

Therefore, reservoir detail and data for reservoir storage and area were obtained. They are mentioned below (DHPS, 2013).

The salient features of reservoir include:

Full Reservoir Level (FRL)	2006 m.a.s.l
Minimum Draw Down Level (MDDL)	1950 m.a.s.l
Maximum Flood Level	2008 m.a.s.l
Gross Storage Volume at FRL	329.16 mil. m^3
Gross Storage volume at MDDL	78.54 mil. m^3
Live Storage Volume	250.62 mil. m^3
Surface Area at FRL	6.82 km^2
Length of the Reservoir at FRL	17.253 km

Table 8.1: Reservoir Stage storage and area

Elevation (m)	Area (ha)	Area (km^2)	Gross Storage ($mil.m^3$)	Live Storage ($mil.m^3$)
1850	0.4	0.004	0	
1860	6.08	0.0608	0.2683	
1870	14.42	0.1442	1.2637	
1880	27.52	0.2752	3.3258	
1890	40.87	0.4087	6.7233	
1900	56.47	0.5647	11.5694	
1910	75.12	0.7512	18.1267	
1920	117.72	1.1772	27.6893	
1930	143.54	1.4354	40.731	
1940	185.7	1.857	57.1478	
MDDL 1950	243.47	2.4347	78.5412	0
1960	308.02	3.0802	106.0525	27.511
1970	376.58	3.7658	140.2252	61.684
1980	453.97	4.5397	181.6925	103.151
1990	542	5.42	231.426	152.885
2000	627.98	6.2798	289.8723	211.331
FRL 2006	681.92	6.8192	329.1582	250.617
2008	699.94	6.9994	342.9764	
2010	720.07	7.2007	357.176	
2014	765.28	7.6528	386.8784	

Source: Detail Project Report of Bunakha Hydro-electric Project, 2013

By using the above data, the reservoir capacity and area elevation curve was plotted as shown in Figure 8.1 below:

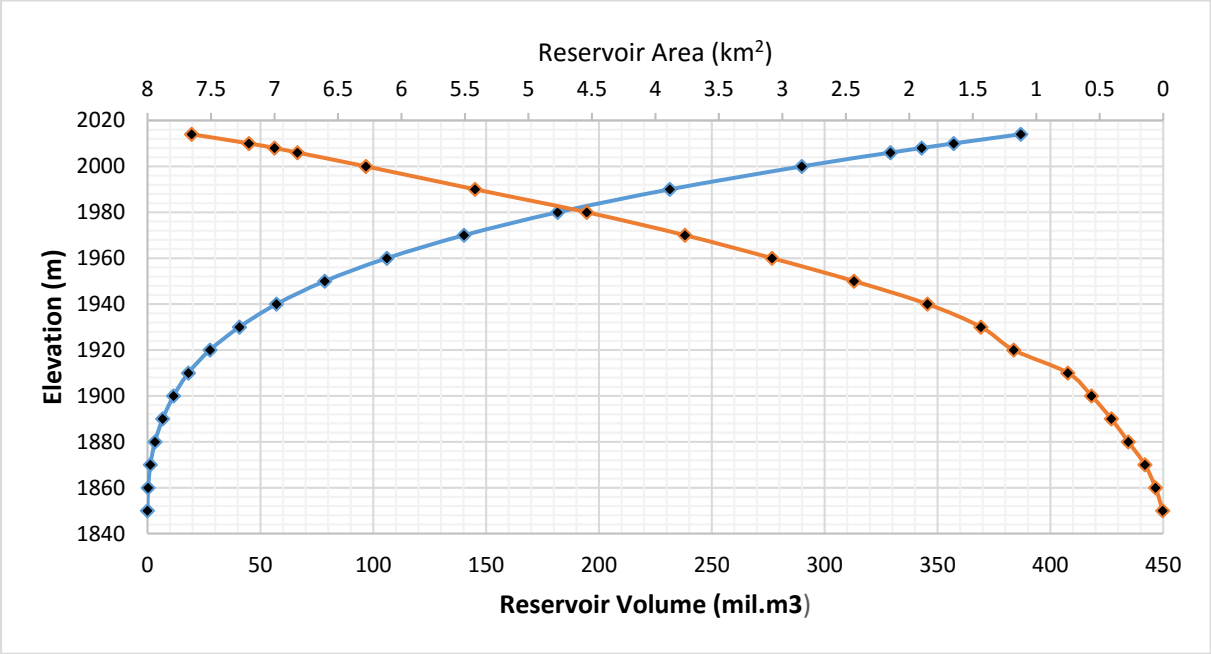

Figure 8.1: Reservoir capacity and area elevation curve

8.1.1 Empirical Area Reduction Method

The deposition of sediment over the due course of time makes the reservoir shrinks thereby causing the stage-capacity curve to shift up. As mentioned above, there are two widely used empirical methods and for the current study, the Empirical Area Reduction Method was used which was developed to distribute sediment deposits within a reservoir as a function of depth. It projects the shift in the stage-storage curve as a result of sediment deposit. However, it comes with some limitations as well. The method does not identify the specify which location within the reservoir will be impacted due to sediment (Morris and Fan, 1998).

The basic equation used in this method is:

$$A_p = Cp^m(1-p)^n \qquad \text{Eq. 8.1}$$

Where:

A_p = A non-dimensional relative area at relative distance 'p' above the stream bed level

$C, m \,\&\, n$ = non-dimensional constants which have been fixed depending on the type of reservoir

In this method, reservoirs are classified into four types based on their shapes as tabulated below and their respective M values are also shown:

Table 8.2: Reservoir classification based on their shapes and their respective M values

Reservoir shape	Type	M
Gorge	IV	1 to 1.5
Hill & Gorge	III	1.5 to 2.5
Flood plains & foothills	II	2.5 to 3.5
Lake	I	3.5 to 4.5

As stated in the previous section (refer Chapter 7: section 7.7), the sedimentation rate of 0.5 mm/year is considered for predicting the reservoir sediment for the present study.

Computation of expected Sediment volume

In order to determine the amount of sediment that will be trapped in the reservoir, Brune's curve developed by (Brune, 1953) was used as prescribed in Indian Standard Code IS: 12182-1987 and sediment that will be accumulated in period of years was calculated as illustrated in Table 8.3.

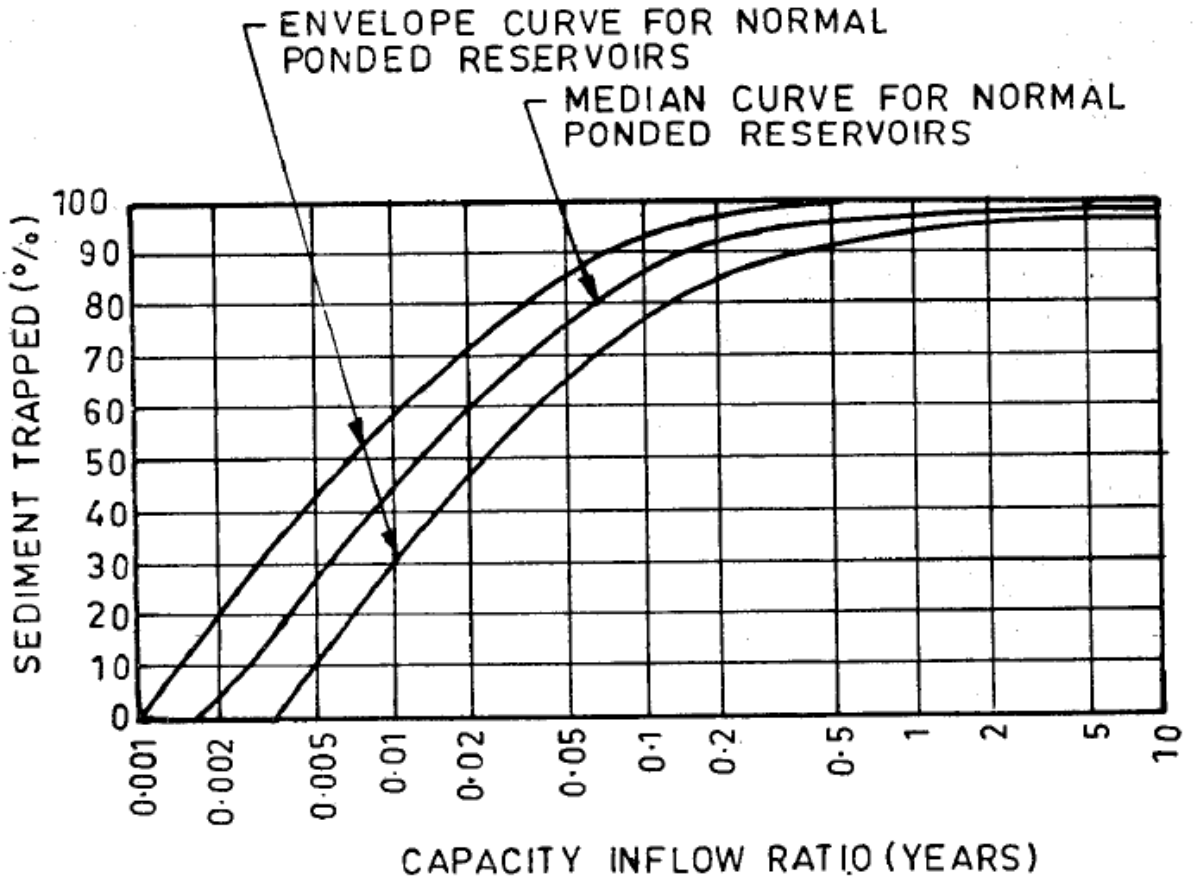

Figure 8.2: Brune's Curve for estimating sediment trapping in the reservoir (Brune, 1953)

Table 8.3: Calculation of sediment accumulation volume in various periods

Gross Capacity at F.R.L (C)=			329.15	[MCM]			
Annual Inflow (I)=			2619	[MCM]			
Sedimentation Rate (r)=			0.5	[mm/year]			
Catchment Area (A)=			3558	[km^2]			
Bed level at Dam site=			1850	[m]			
F.R.L elevation =			2006	[m]			
Average annual sediment volume (A*r)=			1.779	[MCM]			
Year	**Capacity (MCM)**	**Capacity inflow Ratio (C/I)**	**Trap. Efficiency as per IS 12182**	**Sediment inflow in 10 years (MCM)**	**Sediment trapped in 10 years**	**Revised capacity after 10 years**	**Accumulated Sediment volume (MCM)**
1 to 10	329.1582	0.126	88%	17.79	15.66	313.50	15.66
10 to 20	313.50	0.120	87%	17.79	15.48	298.03	31.13
20 to 30	**298.03**	**0.114**	**86%**	**17.79**	**15.30**	**282.73**	**46.43**
30 to 40	282.73	0.108	85%	17.79	15.12	267.60	61.55
40 to 50	**267.60**	**0.102**	**85%**	**17.79**	**15.12**	**252.48**	**76.67**
50 to 60	252.48	0.096	84%	17.79	14.94	237.54	91.62
60 to 70	**237.54**	**0.091**	**84%**	**17.79**	**14.94**	**222.60**	106.56
30 years expected sediment volume=				46.43	MCM		
50 years expected sediment volume=				61.55	MCM		
70 years expected sediment volume=				76.67	MCM		

MCM=Million Cubic Meter

In order to determine the type of reservoir for the present study, as prescribed by Morris and Fan (1998), the elevation (depth) and reservoir capacity were transformed into log and depth-capacity ratio and plotted as presented in Figure 8.3. The value M is determined from the reciprocal of the slope of the depth vs. reservoir capacity plot which determines the type of reservoir for selecting curve type for the reservoir. It is clear from the figure that the slope does not plot as a straight line. Based on the M value computed, the slope of the lower end indicate the reservoir is Type II which corresponds to flood plains and foothills reservoir shape type while slope of the higher end of the plot indicates Type III which corresponds to Hill & Gorge shape type reservoir. Since it is more likely that reservoir of the present study would represent the later one, Type III classification is chosen. Thus, corresponding empirical equation for calculating the relative sediment area A_p as shown below:

$$A_p = 16.967p^{1.15}(1-p)^{2.32} \qquad \text{Eq. 8.2}$$

Where:

p = relative depth

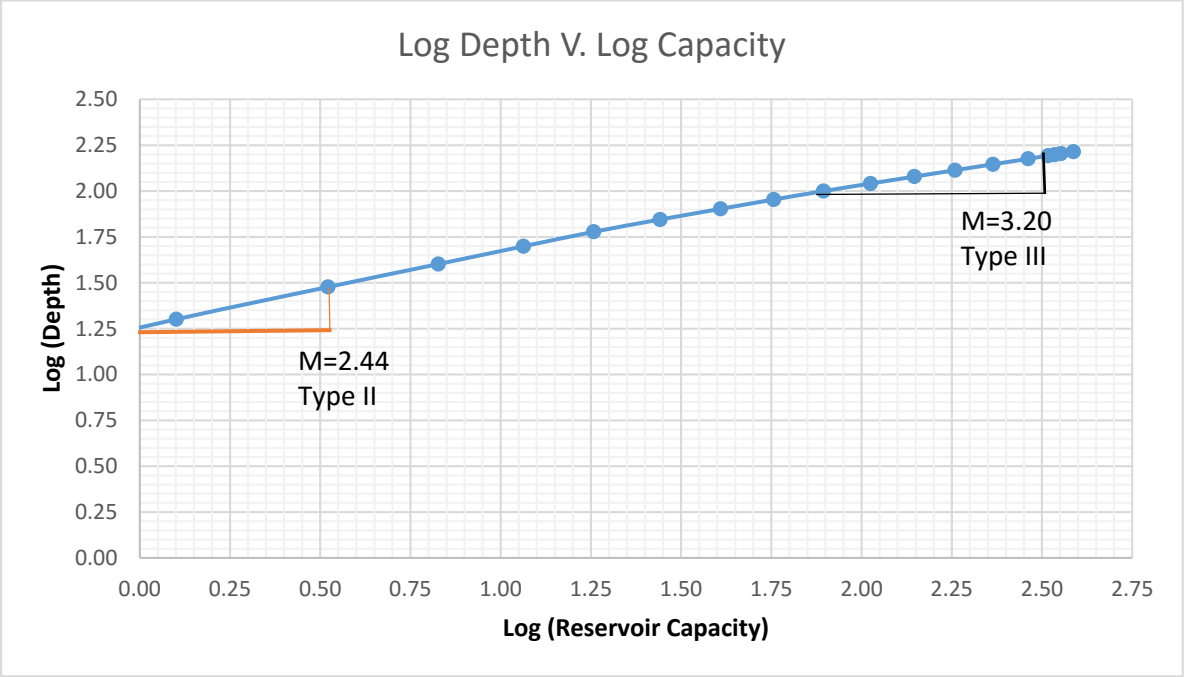

Figure 8.3: Depth Capacity relationship for computing M value

New Zero-Capacity Elevation

The dimensionless function F at different elevation was calculated using the original elevation-area and capacity curves with:

$$F = \frac{S - V_h}{HA_h} \qquad \text{Eq. 8.3}$$

Where:

S = Total sediment deposition

V_h = Reservoir capacity (m^3) at corresponding elevation h

H = Original depth of the reservoir below normal pool.

A_h = Reservoir area (m^2) at its corresponding elevation h

Relative depth p is calculated as:

$$p = \frac{h - h_{min.}}{H} \qquad \text{Eq. 8.4}$$

Where:

$h_{min.}$ = river bed elevation at dam

When F and P value are plotted in type curve, the intersection of the plotted F values with the type curve for reservoir defines P_0 value with which the NZE was determined as:

$$NZE = (P_0 H + h_{min.}) \quad \text{Eq. 8.5}$$

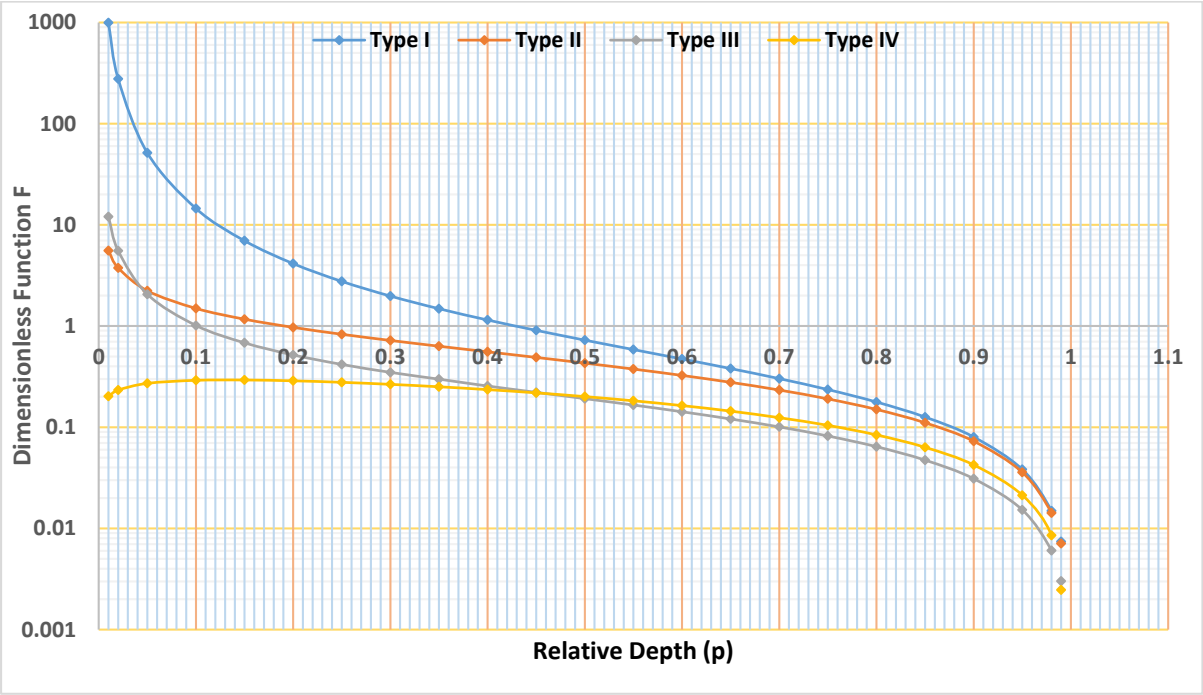

Figure 8.4: Type curves for determining the NZE depth at the dam based dimensionless F function based on the values developed by Strand and Pemberton (1987). Source: (Morris and Fan, 1998)

Thus, the New Zero-capacity Elevation after 30, 50 and 70 years of sedimentation was estimated using Empirical Area Reduction method. The results are as shown in Table 8.4 below:

Table 8.4: New Zero-capacity elevation for various time horizons.

New Zero-capacity Elevation		
After 30 years	After 50 years	After 70 years
1908 m	1926 m	1944 m

The corresponding revised reservoir capacity and reservoir area is presented in the figures that follow:

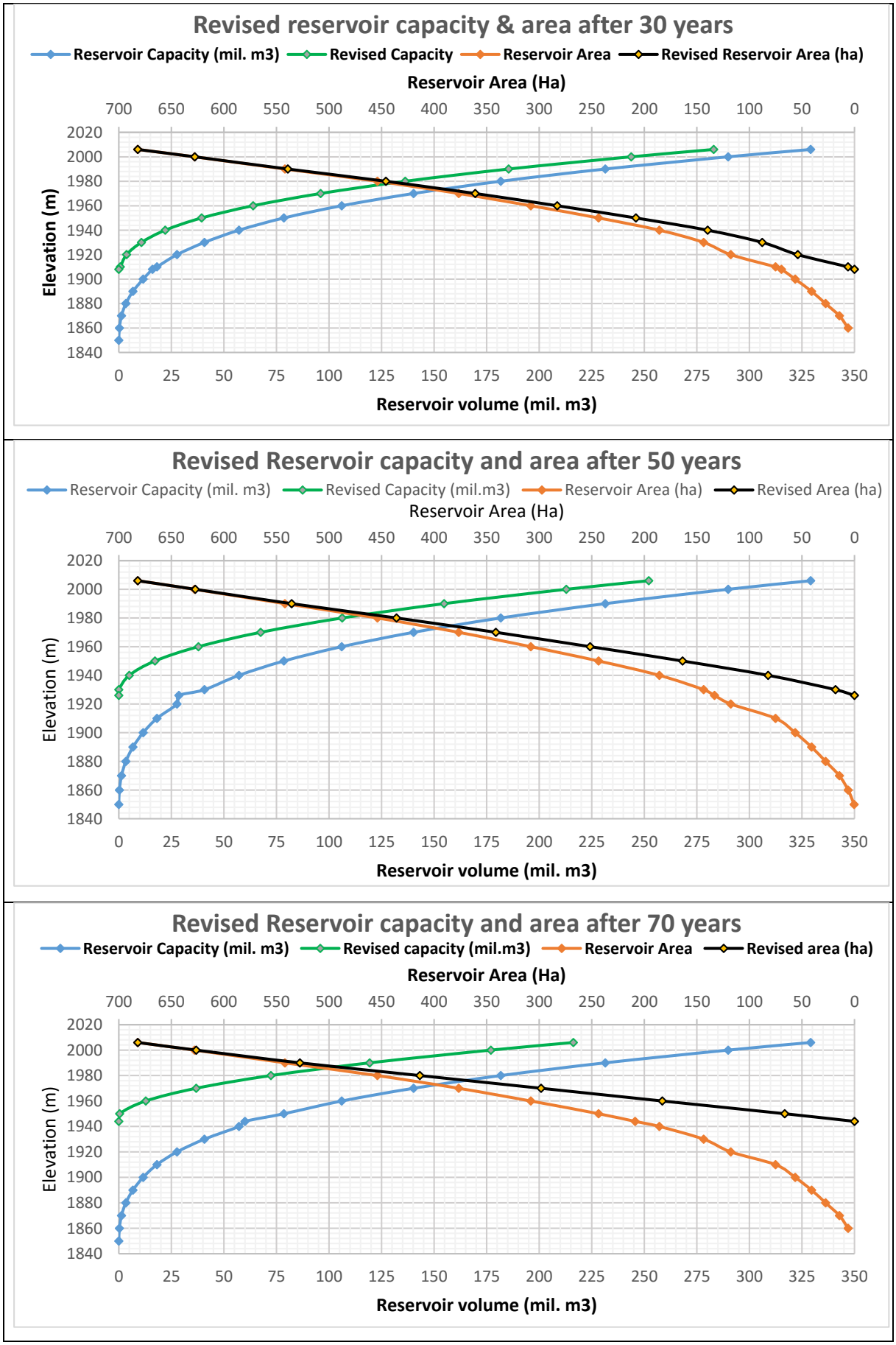

Figure 8.5: Revised capacity and area curve with sediment accumulation after various years

The detailed calculations sedimentation studies along with the various data used is presented as **Appendix B.**

As illustrated in Table 8.4, NZE of the reservoir predicted at different time horizons of 30, 50 and 70 years as 1908 m.a.s.l, 1926 m.a.s.l and 1944 m.a.s.l indicates that even after 70 years of reservoir operation, the sediment deposit level will be well below the MDDL (1950 m.a.s.l) without taking into account the flushing of the sediments from reservoir.

However, Bunakha reservoir is proposed to flushed out its sediment deposit each year in monsoons with its low level spillway sluice that will be installed at elevation of 1915 m.a.s.l, thereby ideally, the long term sediment deposit will not rise up beyond 1915 m.a.s.l. The intake level is set at an elevation 1940 m indicating that with the provision of flushing that will be implemented as mentioned above, the sediment built up will be maintained 25 m below the intake level (DHPS, 2013)

As per the calculation with Empirical Area Reduction method, it would take about 81 years for the sediment deposit to reach at MDDL (1950 m.a.s.l) without taking into account the flushing of the sediments from reservoir. Though it is understood that once the sediment deposit reaches at par with the MDDL, the plant would practically become inoperative due to the submergence of intake, exhaustion period of the live storage was also estimated by computing NZE beyond 70 years as shown in Figure 8.6. By using the trend line equation, it was estimated that, it would take 273 years (flushing of sediment is not considered) for the live storage to get fully exhausted when the sediment deposit would reach at FRL of the dam.

Year	NZE (m.a.s.l)
30	1908
50	1926
70	1944
90	1953
110	1963
130	1972
150	1979
170	1985
190	1990
210	1992
230	2000

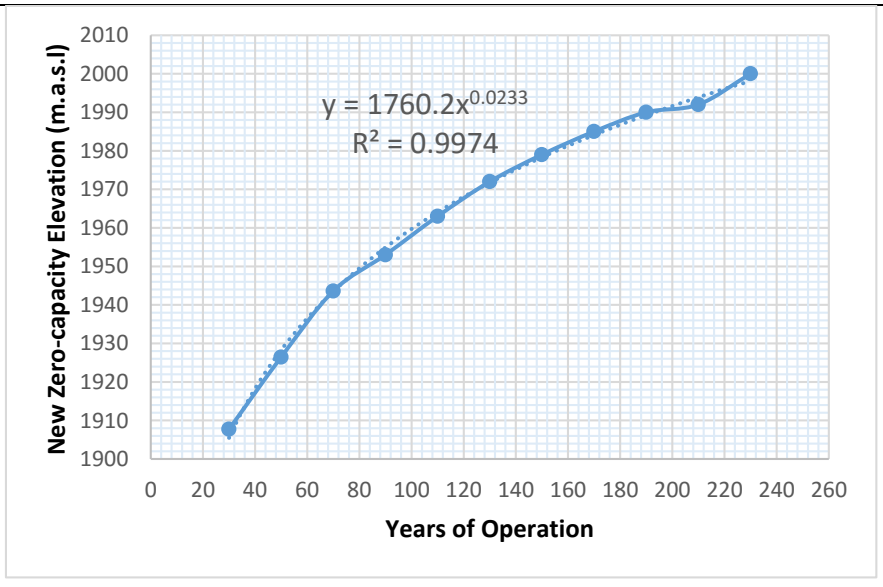

Figure 8.6: New Zero-capacity Elevation (NZE) at various time horizons.

8.2 Prospect of long term changes in sediment Yield due to disturbances

Human activities within a watershed such as change of land use, damming of rivers, deforestation, urbanization may have the potential to effect the sediment yield from the watershed (Wright and Schoellhamer, 2004). Wangchu Basin within which Bunakha catchment is located is the most populous part of the country with about 3/5 of the population living in 1/5 of the basin area (Xue et al., 2013) and over the past one and half decades, there have been vast expansion of infrastructures in these region. Due to rapid urbanization in the area, most of the agricultural land were converted into settlement. There has been numerous bank protection works being carried out in this region. In Bhutan, with its policy to maintain 60% of the country under forest cover for all time to come, more or less there have been negligible deforestation in the region. As it can be seen from the Figure 8.7, considering 2009 years as the exceptional one which huge flash flood has contributed a substantial amount of sediment load occurred during that period, nevertheless, there is a decreasing trend in the observed suspended sediment load even after 2009. Such decreasing trend may be attributed to rapid conversion of agricultural land for expansion of infrastructural and also due to adoption of river bank protection measures.

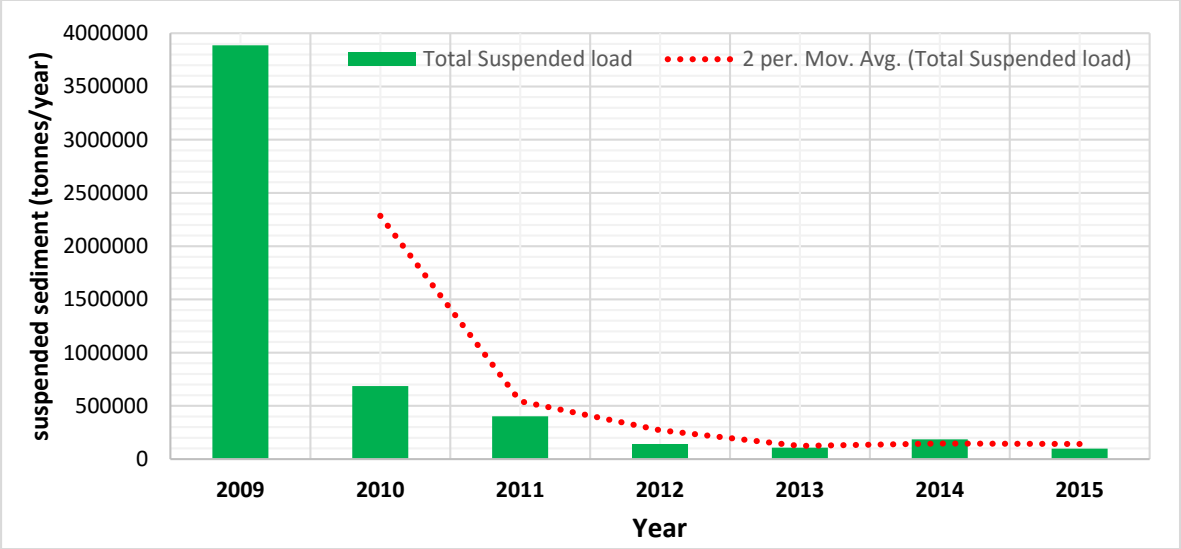

Figure 8.7: Decreasing trend of observed suspended sediment load

Similar occurrence had been reported by Wright and Schoellhamer (2004) in their study titled, "*Trends in the Sediment Yield of the Sacramento River, California, 1957 – 2001*" where they have observed decreasing trend of suspended sediment discharge in the Sacramento River about one-half over the time period due to several disturbances in the watershed including increase in agricultural land conversion for urban uses, increased numbers of dams and reservoirs and bank protection measures put in place in the region.

Though, suspended sediment data analysis of the study area shows the decreasing trend over the period, it would be difficult to conclude that such similar trend would persist in the times to come. It may reach to an equilibrium state when the erodible materials in the catchment get exhausted until some major gemological changes occur.

8.3 Impact of reservoir to the downstream plants

Located about 3.5 km to the downstream of the planned Bunakha Hydro-electric Project are the two existing power plants namely 336 MW Chukha Hydro-electric Plant and 1020 Tala Hydro-electric Plant and further downstream towards the border with India, just after the confluence of Piping River and Wangchu River, there is another planned 600 MW Wangchu Hydro-electric Project. Their relative locations are shown in Figure 8.8

With regard to the cascading hydropower projects seen being developed and planned, the impact to sediment yield downstream of the Bunakha catchment is inevitable.

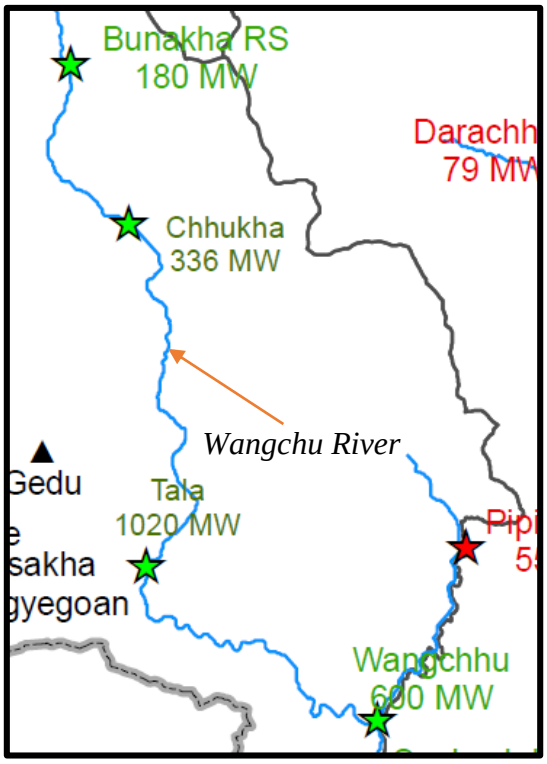

Figure 8.8: Relative locations of planned and exiting hydropower plants and projects along the Wangchu River

Each dam of the hydropower along the Wangchu River will play the role of check dam thereby trapping sediment which otherwise would have been freely transported by the natural river systems. As reported in Chapter 2: section 2.3, the sediment loads measured downstream of the existing Chukha Dam was found to be considerably low which gives an indication that dam

may have intercepted the sediment transportation. However, there can be other factor as well. It may also depend upon time when the data are measured in those stations. It is understood that Chukha Hydro-electric Plant has incorporated sediment flushing facilities and the accumulated sediment deposits are flushed at regular interval for maintaining good operation of the plant and hence, it is expected that there will not be significant change in the sediment load downstream even though spatial and temporal variation of the sediments will occur. However, it might be the case that in the period of data measurement in those stations, the sediment deposits are not flushed yet. Therefore, observed sediment load may depart significantly from the true condition giving the false indication in the long run.

It has been observed that damming of river cuts off the supply of bed material and it creates favorable conditions for the sand fraction of the bed material to be transported faster than the gravels causing the degradation of bed and due to which formation of amour layer is initiated. It was found that amour layer can provide more stability to the bed downstream of the dam compared to the condition of before impoundment provided that peak discharges are reduced during the dam operation so as to maintain the amour layer (Morris and Fan, 1998).

Considering the future Bunakha reservoir which has relatively bigger storage capacity than those plants in the Wanchu River System, it is understood that all the sediment deposit cannot be flushed out even with the low level spillway incorporated for flushing the sediment deposit. The river downstream of the Bunakha would torrent down as sediment deficit and create amour layer situation as reported by Morris and Fan (1998). However, it would be advantageous for the downstream hydropower plants since they will have to deal with less sediment deposit and its related problem.

The operation of reservoir would lead to an increase flow in the river during lean season and dampen the flood peaks during the rainy season. However, such change of the downstream hydrological regime would have negative impact on the riverine habitats (Kummu and Varis, 2007).

CHAPTER 9: CONCLUSIONS

9.1 Critical discussion of the results

Reservoir being the key parameter for storage scheme hydropower plant, it is very important to study its sedimentation characteristics and one of the principal inputs for that is the rate of sediment load inflow into the reservoir to predict its sedimentation in the due course of its operational period. Therefore, inflow rate which is also referred as sediment yield were determined through two independent studies viz. i) Application of PSIAC and RUSLE approach coupled with Geographic Information System (GIS), ii) Data analysis of available suspended sediment data of Tamchu gauging station which is located about 3 km upstream of the planned location of Bunakha reservoir. It was fascinating to observe that irrespective of these independent estimation method, the results obtained for sediment inflow rate were in the order of same magnitude.

9.1.1 PSIAC Approach

While applying the PSIAC approach to determine the sediment yield for the Bunakha Catchment/Watershed, all the required data were readily available except for the two factors namely upland and channel erosions for which these factors had to be accounted by considering different boundary conditions and that had also led to indirectly testing their sensitiveness towards estimation of sediment yield. It is worth noting that these two factors share 38% of the total PSIAC rating. Therefore, when worst case scenario was considered, the sediment yield estimated were relatively higher than that of other approaches particularly for value obtained for gauging station and upper limit yield value obtained from this approach clearly reflects this case. The average sediment yields for the Bunakha catchment/watershed estimated with PSIAC approach were 182 tons/km^2/year, 279 tons/km^2/year and 363 tons/km^2/year for scenario 1, scenario 2 and scenario 3 respectively. It is to be noted that these scenarios considered, excluding scenario 1 for upland erosion which is based on limited available mapped landslide data in the vicinity of reservoir area, are in increasing order of sediment yield levels. However, sediment yield estimated at the location of gauging station were obtained as 805 tons/km^2/year, 365 tons/km^2/year and 1293 tons/km^2/year which translate to sediment rate of 0.4 mm/year 0.18 mm/year and 0.63 mm/year for scenario 1, scenario 2 and scenario 3 respectively which are slightly higher than that of average sediment yield value.

9.1.2 RUSLE Approach

The determination of sedimentation rates based on the RUSLE approach was implemented in a GIS and estimated in two stages. First, the annual soil loss was determined using the RUSLE Model and in the second stage, Sediment Delivery Ratio (SDR) was applied to account for sediment that is eroded but does not reach a stream channel because of retention and sedimentation process. Results of its factor analysis illustrates that the main influencing factors are rainfall erosivity (R) and slope steepness length (LS) factor followed by soil erodibility factor while other factors namely Cover & Management factor (C) and Support Practice factor (P) have the minimum role to play towards soil loss and sediment yield contribution due to their least values. Therefore, it entails the requirement of high density rainfall data along with storm records for R-factor and high resolution DEM raster map for LS-factor to increase the accuracy of the RUSLE model. Furthermore, SDR which determines sediment yield from soil loss resulted from RUSLE, must be studied in detail. As far as availability of journal and article publications are concerned, there is not a single study being carried out to determine the SDR suitable for any region of Bhutan. Hence, widely used and acceptable empirical formulas for SDR (viz. Eq. 6.9, Eq. 6.10 and Eq. 6.11) were used. From the sediment yield thematic map generated (refer Figure 6.8 (*Right*), it illustrates that majority of the sediment yield value for the study area extend from 50 to 600 tons/km^2/year and few of those areas with extremely high yield are concentrated south-west region where there is comparatively high rainfall intensity.

The average annual sediment yields for the Bunakha catchment/watershed estimated with RUSLE approach were 452 tons/km^2/year, 302 tons/km^2/year and 337 tons/km^2/year using SDR Eq. 6.9, Eq. 6.10 and Eq. 6.11 respectively. However, average annual sediment yield estimated at the location of gauging station were obtained as 616 tons/km^2/year, 413 tons/km^2/year and 460 tons/km^2/year which translate to sediment rate of 0.303 mm/year 0.203 mm/year and 0.226 mm/year using SDR Eq. 6.9, Eq. 6.10 and Eq. 6.11 respectively.

By applying RUSLE, lumped empirical method and PSIAC approach which is semi-quantitative method, it is learnt that the sediment yield in the desired watershed can be estimated provided that the study area has sufficient information about geology, soil, rainfall, runoff, well developed DEM and erosion prone areas.

9.1.3 Analysis of observed suspended sediment data

Two approaches were employed in estimating the total sediment load. In the first approach, observed suspended sediment load was combined with bed load estimated from various computational approach. In the second approach, in lieu of using observed suspended sediment

data, the suspended sediment load was computed using parameter such as river cross section, discharge series, grain size distribution and other necessary data and combined with bed load estimated from various computational approach.

First approach-The total load determined by combining observed sediment load (SSL) and bed load estimated from various computation approaches (refer Table 7.7) viz. i) 30% of the SSL as adopted at DHMS, MoEA, Bhutan, ii) using Meyer-Peter Muller (1949) and iii) using Ribberink (1998) show that the assumptions considered by DHMS seems very conservative and results obtained are comparatively larger than those obtained by using the empirical equations. Therefore, as far as method adopted for bed load computations are concerned, it was observed that bed loads were in the range of 10-25% of the suspended sediment load. And the specific sediment yield arrived from the overall average of the sediment of the whole period are 454 tons/km^2/year, 376 tons/km^2/year and 366 tons/km^2/year which translate to sedimentation rate as 0.22 mm/year, 0.19 mm/year and 0.18 mm/year.

Second approach- The total sediment load determined by combing with computed suspended sediment load and bed load estimated as discussed above are 347 tons/km^2/year, 271 tons/km^2/year and 257 tons/km^2/year which corresponds to sedimentation rate as 0.17 mm/year, 0.13 mm/year and 0.13 mm/year with bed load as 30% of SSL, Meyer-Peter Muller (1948) equation, and Ribberink (1998) equation respectively.

It was seen that there is a decreasing trend in the observed suspended sediment load over period of 2009-015. Such a decreasing trend may be attributed to rapid conversion of agricultural land for expansion of infrastructural and also due to adoption of river bank protection measures.

9.1.4 Predicting reservoir sedimentation

Outcome of all the approaches illustrates that the sedimentation rate ranges from 0.13 to 0.63 mm/year. However, for predicting the reservoir sedimentation, mid value of 0.50 mm/year was used after taking into consideration the safety factor of 1.3 to take into account the extreme event of landslide due to glacier lake outburst. For predicting the reservoir sedimentation, Empirical area reduction was used and NZE after 30, 50 and 70 years were 1908 m, 1926 m and 1944 m respectively. Even after 70 years of operation without accounting the flushing of sediment, the reservoir bed level will be well below the start of the live storage level. The intake level is set at an elevation 1940 m (DHPS, 2013), but with the provision of low level spillway sluice at 1915 m for flushing out sediments incorporated, its deposit level is planned to maintain at 1915 m level throughout the plants operation period. Upon further calculation, it was predicted that the sediment deposit would take 81 years to reach at MDDL (1950 m.a.s.l) and 273 years to completely exhaust the live storage without considering the flushing of sediments.

9.1.5 Comments on sedimentation rate used for in DPR of BHEP

The sedimentation rate estimated from approaches used in this current study reveals that its value ranges from 0.13 to 0.63 mm/year. Moreover, data analysis carried in the different DPRs of the hydropower projects in Bhutan has their computed rates ranging up to 0.56 mm/year. However, in most cases, a sediment rate of 1mm/year was often adopted for the design of headworks and assessment of sediment inflow into the reservoir related to sediment yield studies of tributary rivers of Brahmaputra river which descends from other Himalaya regions. However, the assumption that this value can be used generally for the rivers of Bhutan has not been validated so far. Nevertheless, the rate of 1 mm/year has been used as the design input for almost all the hydropower projects and hence, this might have caused over/under design of the headword components and dam structures associated with sediments.

9.2 Limitation of Study

Listed below are few points that may cause limitation to the current study:

1. The shortcoming of the PSIAC approach concerns the fact the rating system suggested by PSIAC (1968) appears very subjective since range of ratings adopted for different sediment yield level would mean different to different users and might vary from region to region.
2. Use of soil map of scale 1:5000000 extracted from DSMW and HSMD might not represent the actual soil characteristics of the soil found in the study area and that may have affected the accurateness.
3. Assumption had to be made for the channel erosion and upland erosions factor for PSIAC approach due to limited or unavailability of data. Therefore, sediment yield resulted from such assumptions may not reflect the true sediment characteristic of the study area.
4. The limited rainfall data available had led to using the R-factor relation adopted in another Himalayan region, and application of empirical equation for SDR with regard to the RUSLE approach may have reduced the accuracy of sediment yield estimation of the study area.
5. Suspended sediment load computation used for the current study proposed by Rijn (1984) may not be applicable for Himalayan rivers which are generally characterized by steep torrent flows.

9.3 Recommendations

i. Similar studies in different catchment areas of Bhutan need to be carried out to find their sedimentation rate in order to further validate the measured sediment data and also validate the use of 1 mm/year used in all hydropower projects.

ii. Number of sediment measuring gauging stations need to be increased to enable such studies in the future.

iii. To validate and compare the findings of this study, similar studies in other catchments of Bhutan needs to be carried out.

iv. Sediment Delivery Ratio equation application for watersheds of Bhutan needs to be developed through statistical analysis of soil loss and their corresponding measured sediment yield, particularly for RUSLE Model.

REFERENCES

AMSALU, T. & MENGAW, A. 2014. GIS based soil loss estimation using rusle model: the case of jabi tehinan woreda, ANRS, Ethiopia. *Natural Resources,* 2014.

AREKHI, S., NIAZI, Y. & KALTEH, A. M. 2012. Soil erosion and sediment yield modeling using RS and GIS techniques: a case study, Iran. *Arabian Journal of Geosciences,* 5**,** 285-296.

ARNOLD, J. G., SRINIVASAN, R., MUTTIAH, R. S. & WILLIAMS, J. R. 1998. Large area hydrologic modeling and assessment part I: Model development1. Wiley Online Library.

BELDRING, S. & VOKSØ, A. 2011. Climate change impacts on the flow regimes of rivers in Bhutan and possible consequences for hydropower development: Report No. 4: Norwegian Water Resources and Energy Directorate (NVE), Norway.

BIS 1994. IS 5477 (Part 2): Indian Standard-Fixing the Capacities of Reservoir-Methods Part 2 Dead Storage.

BOYCE, R. C. 1975. Sediment routing with sediment delivery ratios. *Present and prospective technology for predicting sediment yields and sources***,** 61-65.

BRUNE, G. M. 1953. Trap efficiency of reservoirs. *Eos, Transactions American Geophysical Union,* 34**,** 407-418.

CHODEN, S. 2009. Sediment transport studies in Punatsangchu River, Bhutan. *Master's Thesis, Department of Building and Environmental Technology, Lund University, Sweden*.

COLLINS, D. N. & HASNAIN, S. I. 1995. Runoff and sediment transport from glacierized basins at the Himalayan scale. *IAHS Publications-Series of Proceedings and Reports-Intern Assoc Hydrological Sciences,* 226**,** 17-26.

CORNWELL, K., NORSBY, D. & MARSTON, R. 2003. Drainage, sediment transport, and denudation rates on the Nanga Parbat Himalaya, Pakistan. *Geomorphology,* 55**,** 25-43.

DANESHVAR, M. R. M. & BAGHERZADEH, A. 2012. Evaluation of sediment yield in PSIAC and MPSIAC models by using GIS at Toroq Watershed, Northeast of Iran. *Frontiers of Earth Science,* 6**,** 83-94.

DE VENTE, J., POESEN, J. & VERSTRAETEN, G. 2005. The application of semi-quantitative methods and reservoir sedimentation rates for the prediction of basin sediment yield in Spain. *Journal of Hydrology,* 305**,** 63-86.

DHPS 2013. Detail Project Report (DPR) of Bunakha Hydro Electric Project 180 MW (3X60 MW), Department of Hydropower and Power System, Ministry of Economic Affairs, Thimphu, Bhutan

DHPS 2014. Detail Project Report (DPR), Hydrology of Wangchu Hydro-electric Project, 570 MW (4 X 142.5 MW), Chukha: Department of Hydropower & and Power System, Ministry of Economic Affairs, Thimphu, Bhutan. III.

FAO-UNESCO 1977. FAO-UNESCO Soil Map of the World. VII-South Asia.

FAO/IIASA/ISRIC/ISSCAS/JRC 2012. Harmonized World Soil Database (version 1.2). FAO, Rome, Italy and IIASA, Laxenburg, Austria.

GABET, E., BURBANK, D., PRATTSITAULA, B., PUTKONEN, J. & BOOKHAGEN, B. 2008. Modern erosion rates in the High Himalayas of Nepal. *Earth and Planetary Science Letters,* 267**,** 482-494.

GARG, V. & JOTHIPRAKASH, V. 2011. Sediment Yield Assessment of a Large Basin using PSIAC Approach in GIS Environment. *Water Resources Management,* 26**,** 799-840.

GELAGAY, H. S. & MINALE, A. S. 2016. Soil loss estimation using GIS and Remote sensing techniques: A case of Koga watershed, Northwestern Ethiopia. *International Soil and Water Conservation Research*.

GHNC 2011. Bhutan National Human Development Report 2011: Sustaining progress-Rising to the climate change.

HASNAIN, S. I. 1996. Factors controlling suspended sediment transport in Himalayan glacier meltwaters. *Journal of hydrology,* 181**,** 49-62.

J.G. ARNOLD, J. R. K., R. SRINIVASAN, J.R. WILLIAMS, E.B. HANEY, S.L. NEITSCH 2012. Soil and Water Assessment Tool: Input/Output Documentation Version 2012. 307.

JAIN, S. K., KUMAR, S. & VARGHESE, J. 2001. Estimation of soil erosion for a Himalayan watershed using GIS technique. *Water Resources Management,* 15**,** 41-54.

JULIEN, P. Y. 2002. *River mechanics*, Cambridge University Press.

JULIEN, P. Y. 2010. *Erosion and sedimentation*, Cambridge University Press.

KEBLOUTI, M., OUERDACHI, L. & BOUTAGHANE, H. 2012. Spatial interpolation of annual precipitation in Annaba-Algeria-comparison and evaluation of methods. *Energy Procedia,* 18**,** 468-475.

KITAHARA, H., OKURA, Y., SAMMORI, T. & KAWANAMI, A. 2000. Application of universal soil loss equation (USLE) to mountainous forests in Japan. *Journal of Forest Research,* 5**,** 231-236.

KUENZA, K., DORJI, Y. & WANGDA, D. 2004. Landslides in Bhutan. *Country Report, Department of Geology and Mines, Royal Government of Bhutan, Thimpu*.

KUMMU, M. & VARIS, O. 2007. Sediment-related impacts due to upstream reservoir trapping, the Lower Mekong River. *Geomorphology,* 85**,** 275-293.

LANE, E. & BORLAND, W. 1951. Estimating bed load. *Eos, Transactions American Geophysical Union,* 32**,** 121-123.

LEE, S. & KANG, S. 2013. Estimating the GIS-based soil loss and sediment delivery ratio to the sea for four major basins in South Korea. *Water Science & Technology,* 68.

LONG, S., MCQUARRIE, N., TOBGAY, T., GRUJIC, D. & HOLLISTER, L. 2011. Geologic map of Bhutan. *Journal of Maps,* 7**,** 184-192.

MAHMOOD, K. 1987. "Reservoir Sedimentation: Impact, Extent, Mitigation," World Bank Technical Report

No. 71, Washington, D.C.

MEYER-PETER, E. & MÜLLER, R. Formulas for bed-load transport. 1948. IAHR.

MITASOVA, H., HOFIERKA, J., ZLOCHA, M. & IVERSON, L. R. 1996. Modelling topographic potential for erosion and deposition using GIS. *International Journal of Geographical Information Systems,* 10**,** 629-641.

MOORE, I. & BURCH, G. 1986. Modelling erosion and deposition: topographic effects. *Transactions of the ASAE,* 29**,** 1624-1630.

MORGAN, R., QUINTON, J., SMITH, R., GOVERS, G., POESEN, J., AUERSWALD, K., CHISCI, G., TORRI, D. & STYCZEN, M. 1998. The European Soil Erosion Model (EUROSEM): a dynamic approach for predicting sediment transport from fields and small catchments. *Earth surface processes and landforms,* 23**,** 527-544.

MORRIS, G. L. & FAN, J. 1998. *Reservoir sedimentation handbook: design and management of dams, reservoirs, and watersheds for sustainable use*, McGraw Hill Professional.

NCP 2014. Sediment Retention: Avoided Dredging and Water Purification.

NDOMBA, P. M. 2013. Validation of PSIAC Model for Sediment Yields Estimation in Ungauged Catchments of Tanzania. *International Journal of Geosciences,* 04**,** 1101-1115.

NOORI, M. J., HASSAN, H. H. & MUSTAFA, Y. T. 2014. Spatial Estimation of Rainfall Distribution and Its Classification in Duhok Governorate Using GIS. *Journal of Water Resource and Protection,* 6**,** 75.

OUYANG, D. & BARTHOLIC, J. Predicting sediment delivery ratio in Saginaw Bay watershed. Proceedings of the 22nd National Association of Environmental Professionals Conference, 1997. 659-671.

PALMIERI, A., SHAH, F., ANNANDALE, G. & DINAR, A. 2003. Reservoir conservation volume I: the RESCON approach economic and engineering evaluation of alternative strategies for managing sedimentation in storage reservoirs. *A contribution to promote conservation of water storage assets worldwide, The International Bank for Reconstruction and Development/The World Bank, Washington, DC, USA.*

PANDEY, A., CHOWDARY, V. & MAL, B. 2007. Identification of critical erosion prone areas in the small agricultural watershed using USLE, GIS and remote sensing. *Water resources management,* 21**,** 729-746.

PARVEEN, R. & KUMAR, U. 2012. Integrated approach of Universal Soil Loss Equation (USLE) and geographical information system (GIS) for soil loss risk assessment in Upper South Koel Basin, Jharkhand.

PRATT-SITAULA, B., GARDE, M., BURBANK, D. W., OSKIN, M., HEIMSATH, A. & GABET, E. 2007. Bedload-to-suspended load ratio and rapid bedrock incision from Himalayan landslide-dam lake record. *Quaternary Research,* 68**,** 111-120.

PSIAC 1968. Factors Effecting Sediment Yield and Measure for the Reduction of Erosion and Sediment Yield.

RENARD, K. G., FOSTER, G. R., WEESIES, G., MCCOOL, D. & YODER, D. 1997. *Predicting soil erosion by water: a guide to conservation planning with the Revised Universal Soil Loss Equation (RUSLE),* US Department of Agriculture, Agricultural Research Service Washington.

RENFRO, G. 1975. Use of erosion equations and sediment delivery ratios for predicting sediment yield. *Present and Prospective Technology for predicting sediment yields and sources***,** 33-45.

RENSCHLER, C., DIEKKRÜGER, B. & MANNAERTS, C. 1999. Regionalization in surface runoff and soil erosion risk evaluation. *IAHS Publication(International Association of Hydrological Sciences)***,** 233-241.

RIBBERINK, J. S. 1998. Bed-load transport for steady flows and unsteady oscillatory flows. *Coastal Engineering,* 34**,** 59-82.

RIJN, L. C. V. 1984. Sediment transport, part II: suspended load transport. *Journal of hydraulic engineering,* 110**,** 1613-1641.

RSPN 2009. Flash flood in Thimphu (26 May 2009).

SCHULTE-RENTROP, A., KOLL, K., ABERLE, J. & DITTRICH, A. 2005. Sediment budget of a heathland sand-bed river. *Acta Geophysica Polonica,* 53**,** 553.

SHANKER, R., KUMAR, G. & SAXENA, S. 1989. Stratigraphy and sedimentation in Himalaya: a reappraisal. *Geology and tectonics of the Himalaya.*

SIMMS, A., WOODROFFE, C. & JONES, B. 2003. Application of RUSLE for erosion management in a coastal catchment, southern NSW. *Faculty of Science-Papers***,** 34.

STØLE, H. 1993. Withdrawal of water from Himalaya rivers-sediment contral at Intake.

STRAND, R. & PEMBERTON, E. 1987. Design of small dams. *United States Department of the Interior, Bureau of Reclamation. Chap. Reservoir sedimentation***,** 529-564.

TAMRAKAR, B. & ALFREDSEN, K. 2013. Satellite-Based Precipitation Estimation for Hydropower Development. *Hydro Nepal: Journal of Water, Energy and Environment,* 12**,** 52-58.

TANGESTANI, M. H. 2006. Comparison of EPM and PSIAC models in GIS for erosion and sediment yield assessment in a semi-arid environment: Afzar Catchment, Fars Province, Iran. *Journal of Asian earth sciences,* 27**,** 585-597.

VAN REMORTEL, R. D., MAICHLE, R. W. & HICKEY, R. J. 2004. Computing the LS factor for the Revised Universal Soil Loss Equation through array-based slope processing of digital elevation data using a C++ executable. *Computers & Geosciences,* 30**,** 1043-1053.

VAN RIJN, L. C. 1984. Sediment transport, part I: bed load transport. *Journal of hydraulic engineering,* 110**,** 1431-1456.

VANONI, V. A. 1975. Sedimentation engineering, ASCE manuals and reports on engineering practice—No. 54. *American Society of Civil Engineers, New York, NY.*

WALLING, D. 1977. Limitations of the rating curve technique for estimating suspended sediment loads, with particular reference to British rivers. *Erosion and solid matter transport in inland waters***,** 34-48.

WISCHMEIER, W. H. & SMITH, D. D. 1978. Predicting rainfall erosion losses-A guide to conservation planning. *Predicting rainfall erosion losses-A guide to conservation planning*.

WOIDA, K., MOINES, D. & CLARK, K. A GIS application of PSIAC for predicting sediment-yield rates. Proceedings of Seventh Federal Interagency Sedimentation Conference. USGS, Reno, NV, X-25–X-32, 2001.

WRIGHT, S. A. & SCHOELLHAMER, D. H. 2004. Trends in the sediment yield of the Sacramento River, California, 1957–2001. *San Francisco Estuary and Watershed Science,* 2.

XIAOQING, Y. & YANG, X. 2003. *Manual on sediment management and measurement,* Secretariat of the World Meteorological Organization.

XUE, X., HONG, Y., LIMAYE, A. S., GOURLEY, J. J., HUFFMAN, G. J., KHAN, S. I., DORJI, C. & CHEN, S. 2013. Statistical and hydrological evaluation of TRMM-based Multi-satellite Precipitation Analysis over the Wangchu Basin of Bhutan: Are the latest satellite precipitation products 3B42V7 ready for use in ungauged basins? *Journal of Hydrology,* 499**,** 91-99.

ZHANG, Y., DEGROOTE, J., WOLTER, C. & SUGUMARAN, R. 2009. Integration of Modified Universal Soil Loss Equation (MUSLE) into a GIS framework to assess soil erosion risk. *Land Degradation & Development,* 20**,** 84-91.

APPENDICES

Appendix A. Sediment yield estimation with PSIAC Approach

Table A1: Factors of PSIAC and their individual rating as per PSIAC (1968)

Factor	Rating	Main Characteristic
Surface geology	0	(a) Massive hard formation
	5	(a) Rocks of medium hardness, (b)moderately weathered, (c)moderately fractured
	10	(a) Marine shales and related mudstones and siltstone
Soils	0	(a) High percentage of rock fragments, (b) aggregated clays, (c)high in organic matters
	5	(a) Medium texture, (b) Occasional rock fragments, (c) caliche layers
	10	(a) Fine texture, easily dispersed, saline-alkaline high shrink-swell characteristics, (b) single grain silts and fine sands
Climate	0	(a) Humid climate with rainfall of low intensity, (b) precipitation in the form of snow, (c) arid climate with low intensity storms, (d) arid climate with rare convective storms
	5	(a) Storm of moderate duration and intensity, (b) infrequent convective storms
	10	(a) Storms of several days duration with short periods of intense rainfall, (b) frequent intense convective storms, (c) freeze-thaw occurrence
Runoff	0	(a) Low peak flows, (b) low volume of runoff per unit area, (c) rare runoff events
	5	Moderate peak flows, (b) Moderate volume of runoff per unit area
	10	High peak flows, (b) large volume of flow per unit area
Topography	0	(a) Gentle upland slopes (<5%), (b) extensive alluvial planes
	10	(a) Moderate upland slopes (<20%), (b) moderate floodplain development
	20	(a)Steep upland slopes (>30%), high relief, little or no floodplain development
Ground Cover	-10	(a) Completely protect by vegetation, rock fragments, litter. Little opportunity for rainfall to reach erodible material
	0	(a) Cover <40%,; noticeable litter, (b) if trees present understory not well developed
	10	(a) Ground cover <20%, vegetation sparse, little or no litter, (b) no rock in surface soil
Land Use	-10	(b) No cultivation, (b) no recent logging, (c) low intensity grazing

	0	(a) <25% cultivated, (b) 50% or less recently logged, (c) <50% intensively grazed, (d) ordinary road land and other construction
	10	(a) >50% cultivated, (b) almost all the area intensively grazed, (c) all of the area recently burnt
Upland erosion	0	(a) No apparent signs of erosion
	10	(a) About 25% of the area characterized by rill and gully or landslide erosion, (b) wind erosion with deposition in stream channels.
	25	(a) >50% of the area characterized by rill and gully or landslide erosion
Channel erosion and sediment transport	10	(a) Moderate flow depths medium flow duration with occasionally eroding banks or bed
	25	Eroding banks continuously or at frequent intervals with large depths and long flow duration, (b) active head cuts and degradation in tributary channels
After adding all the individual factors which gives total PSIAC index that can be translated to sediment yield	PSIAC Index	Estimated Sediment Yield ranges (tons/ha/year) based on region- Pacific Southwest USA
	>100	>18.3
	75-100	6.1-18.3
	50-75	3.0-6.1
	25-50	1.2-3.0
	0-25	<1.2

Table A2: PSIAC rating and the sediment yield summary including yield at gauging station

Particular	**PSIAC Rating**		
Minimum	-2	8	23
Maximum	107	90	120
Average	**33.61**	**41.60**	**58.69**
Catchment : Average Sediment Yield (t/ha per year)	**1.82**	**2.79**	**3.63**
Catchment: Average t Sediment Yield t/km2 per year	**181.97**	**279.17**	**362.58**
PSIAC Index at gauging Station	79	59	89
Sediment Yield at Station (t/ha per year)	**8.05**	**3.65**	**12.93**
Sediment Yield at Station (t/km2 per year)	**805.2**	**364.80**	**1293.2**

Table A3: PSIAC Rating of each factor in each grid (1 km x 1 km) as extracted from ArcMap

		PSIAC Rating											
		1	2	3 & 4	5	6	7			8			9
FID	Shape *	Runoff	Precipit-ation	Groundcover cum Land use	Topography	Geology	Channel Erosion (MS=15 & MB=2) (S1)	Channel Erosion (S2)**	Channel Erosion (S3)**	Upland Erosion(Data) (S1)*	Upland Erosion (S2)*	Upland Erosion (S3)*	Soil
0	Polygon	7	10	-10	20	2	0	0	0	0	10	25	5
1	Polygon	7	10	-20	10	2	0	0	0	0	10	25	5
2	Polygon	9	4	-20	20	2	0	0	0	0	10	25	5
3	Polygon	9	10	-20	20	2	2	0	0	0	10	25	5
4	Polygon	8	10	-20	20	2	2	0	0	0	10	25	5
5	Polygon	7	10	-16	20	2	2	0	0	0	10	25	5
6	Polygon	5	4	-16	20	0	0	0	0	0	10	25	4
7	Polygon	6	4	-16	20	2	0	0	0	0	10	25	5
8	Polygon	6	10	-20	10	2	0	0	0	0	10	25	5
9	Polygon	7	10	-20	20	2	2	0	0	0	10	25	5
10	Polygon	7	10	20	20	2	15	10	25	25	10	25	5
11	Polygon	7	10	-20	0	2	15	10	25	0	10	25	5
12	Polygon	7	10	-12	20	2	2	0	0	0	10	25	5
13	Polygon	7	10	-20	20	2	2	0	0	0	10	25	5
14	Polygon	5	10	-20	20	2	2	0	0	0	10	25	5
15	Polygon	5	10	-16	20	2	0	0	0	0	10	25	4
16	Polygon	5	4	-8	20	0	0	0	0	0	10	25	4
17	Polygon	5	4	-16	10	2	0	0	0	0	10	25	5
18	Polygon	6	10	-16	20	2	0	0	0	0	10	25	5

19	Polygon	7	10	-20	20	2	0	0	0	0	10	25	5
20	Polygon	7	10	-20	10	2	2	0	0	0	10	25	5
Continued till		Continued till			Continued till				Continued till			Continued till	
3720	Polygon	5	9	0	10	2	0	0	0	0	10	25	6
3721	Polygon	5	9	0	10	0	0	0	0	0	10	25	6
3722	Polygon	5	4	0	10	2	0	0	0	0	10	25	0
3723	Polygon	5	9	0	0	2	0	0	0	0	10	25	0
3724	Polygon	5	9	0	20	2	2	0	0	0	10	25	6
3725	Polygon	5	9	0	20	2	2	0	0	0	10	25	6
3726	Polygon	5	9	0	20	2	2	0	0	0	10	25	6
3727	Polygon	5	9	0	20	2	0	0	0	0	10	25	6
3728	Polygon	5	4	0	20	2	0	0	0	0	10	25	6
3729	Polygon	5	4	-20	10	0	0	0	0	0	10	25	0
3730	Polygon	5	9	0	20	2	0	0	0	0	10	25	0
3731	Polygon	5	9	0	20	2	0	0	0	0	10	25	0
3732	Polygon	5	9	0	20	2	0	0	0	0	10	25	6
3733	Polygon	5	9	0	20	2	0	0	0	0	10	25	6

NB:

- FID denotes field identity of GRID cell of 1km by 1km. Therefore, the last FID number i.e 3733 indicate that there are 3733 such grid covering Bunakha catchment
- The whole grid table is not shown

Table A4: Total PSIAC Rating in each GRID cell for different scenarios accounted

FID	Total PSIAC Rating in each GRID (S1) & (S1)	Total PSIAC Rating in each GRID (S2) & (S2)	Total PSIAC Rating in each GRID (S3) & (S3)
0	34	44	59
1	14	24	39
2	20	30	45
3	28	36	51
4	27	35	50
5	30	38	53
6	17	27	42
7	21	31	46
8	13	23	38
9	26	34	49
10	104	84	114
11	19	24	54
12	34	42	57
13	26	34	49
14	24	32	47
15	25	35	50
16	25	35	50
17	10	20	35
18	27	37	52
19	24	34	49
20	16	24	39
	Continued till	Continued till	Continued till
3720	32	42	57
3721	30	40	55
3722	21	31	46
3723	16	26	41
3724	44	52	67
3725	44	52	67
3726	44	52	67
3727	42	52	67
3728	37	47	62
3729	-1	9	24
3730	36	46	61
3731	36	46	61
3732	42	52	67
3733	42	52	67

Table A5: Classification of geology into different class and their corresponding PSIAC rating allocation

Map Units	Description	Classification	Allotted PSIAC Rating	Remarks
Ghlml	Lower metasedimentary unit (Neoproterozoic-Cambrian) – Dominantly amphibolite-facies (Gansser, 1983; Grujic et al., 2002; Danier et al., 2003) metasedimentary rocks, including quartzite, and biotite-muscovite-garnet schist and paragneiss often exhibiting kyanite, sillimanite, or staurolite, and partial melt textures (long and McQuarrie,2010). Orthogneiss intervals locally split out. Up to ~50 km thick; thickens toward Western Bhutan.	Moderate-Strong	2	Source: https://www.esci.umn.edu/courses/1001/minerals/amphibole.shtml Hardness Value: 5 or 6
Ghlmu	Upper metasedimentary unit (Neoproterozoic-Ordoviciann)- Variable metamorphic grade; dominantly amphibolite facies (Gansser, 1983, partial melt- and often kyanite-, sillimanite-, or staurolite-bearing paragneiss, schist, and quartzite in east (Grujic et al., 2002) and near base in west-Central Bhutan	Moderate-Strong	2	Source: https://www.esci.umn.edu/courses/1001/minerals/amphibole.shtml Hardness Value: 5 or 6
Ghlo	Orthogneiss unit (Cambrian-Ordovician) – Cliff-forming, massive-weathering, granite-composition orthogneiss; generally, exhibits leucosomes**and abundant feldspar augen (Long and McQuarrie, 2010; Long et al., 2011B). Paragneiss, schist, and quartzite intervals locally split out. Interpreted as deformed Cambrian-Ordovician granite plutons that intruded Greater Himalayan sedimentary protoliths (Long and McQuarrie, 2010). 1.5-8.0 km-thick; thickens toward eastern Bhutan (Long et al., 2011B).	Slight-Moderate	7	Granitic rock but has massive weathering

Tgr	Leucogranite (Miocene) – Massive to foliated, syn-Himalayan leucogranite plutons. Leucogranite intrudes the structurally-higher and structurally-lower Greater Himalayan sections, as well as Tethyan Himalayan rocks near the STDl in the Lingshi region (Gansser, 1983).	Strong	0	Due to Leucogranite (type of granite) which contains quartz (33-40 vol. %); Hardness of Quartz = 7
Thu	Undifferentiated (Paleozoic-Eocene) – Limestone, sandstone, shale, and locally marble, quartzite, slate, and phyllite above STDh in Tibet and parts of northernmost Bhutan (Wu et al., 1998; Edwards et al., 1999).	Slight	10	Due to presence of marble, slate, phylitte, limestone, shale (phylite (1-2) & shale are very soft rocks) Source: (Phyllite: http://www.comparerocks.com/en/properties-of-phyllite/model-38-6; Limestone: http://www.mineralszone.com/stones/limestone.html:
Tr-Jru	Triassic-Jurassic, undifferentiated – Dark-gray, tan weathering shale, and fine-grained sandstone (Gansser, 1983). Forms diagnostic tan slopes. Equivalent to lower part of Lingshi Formation of Tangri and Pande (1995). Ca. 2,000 m-thick.	Slight-Moderate	7	Due to weather shale stone (laminated in nature)

Pzu	Paleozoic, undifferentiated – In Lingshi region: medium-gray, cliff-forming, thin-bedded, silt lamination-rich, fossiliferous limestone (Gansser,1983) equivalent to Barshong Formation (Early-Middle Cambrian) of Tangri and Pande (1995)	Moderate	5	Medium hardness of Limestone (3.5-4) Source: http://www.rockbreaker.com/equipment/rockbreakersystemsmain/26-products/booms/702-rockhardness.html Or http://www.mineralszone.com/stones/limestone.html
Pzc	Dominated by tan, cliff-forming marble, with lesser gray phyllite and dark-gray phyllitic quartzite in Lingshi region (Gansser, 1983). Dominantly upper greenschist facies (Gansser, 1983). 2.2-4.0 km-thick (Long et al., 2011B).	Slight	10	Due to presence of phyllite Hardness: 1-2 Source: http://www.comparerocks.com/en/properties-of-phyllite/model-38-6
Pzpu/ m3	Upper unit (Cambrian-Ordovician) – Tan to gray, very coarse-grained, thin- to medium-bedded, cliff-forming, biotite-rich quartzite, interbedded with biotite-muscovite-garnet schist (Tobgay et al., 2010). Marble marker bed (m3; 250 m-thick) is divided out. 1,600 m-thick total (Tobgay et al., 2010).	Slight-Moderate	7	Biotite Hardness: 2.5 to 3 Source: http://geology.com/minerals/biotite.shtml Hardness: 2.5 to 3, contains quartz
Pzpm /m2/m1	Middle unit (Cambrian-Ordovician) – Gray to tan, thin-bedded, fine-grained, micaceous quartzite, interbedded with biotite-garnet-muscovite schist (Tobgay et al., 2010), rare calc-silicate rocks, and marble. Contact with schist of lower unit is gradational. Two white to gray,	Slight-Moderate	7	Biotite Hardness: 2.5 to 3 Source: http://geology.com/minerals/biotite

	mediumcrystalline marble marker beds (m1, 10 m-thick; m2, 100-200 m-thick) are divided out. 2,000 m-thick total (Tobgay et al., 2010)			.shtml Hardness: 2.5 to 3, contains quartz
Pzo	Orthogneiss (Ordovician) - Concordant, foliated leucogranite and granitic orthogneiss bodies within middle and upper unit, interpreted as deformed Ordovician granite plutons (Tobgay et al., 2010). Kyanite- and sillimanite-bearing schist locally present in country rock adjacent to intrusions (Tobgay et al., 2010)	Strong	0	Due to Leucogranite (type of granite) which contains quartz (33-40 vol. %); Hardness of Quartz = 7; Granite hardness hard to define; depents on miniral content Source: http://www.newworldencyclopedia.org/entry/Mohs_scale_of_mineral_hardness
Pzpl	Lower unit (Neoproterozoic-Ordovician) - Muscovite-biotite-garnet-staurolite schist, with kyanite present within quartz veins (Tobgay et al.,2010). Quartzite interbeds become more common upsection. 600 m-thick (Tobgay et al., 2010).	Slight-Moderate	7	Biotite Hardness: 2.5 to 3 Source: http://geology.com/minerals/biotite.shtml Hardness: 2.5 to 3, contains quartz

Figure A1: Conceptual framework of PSIAC model

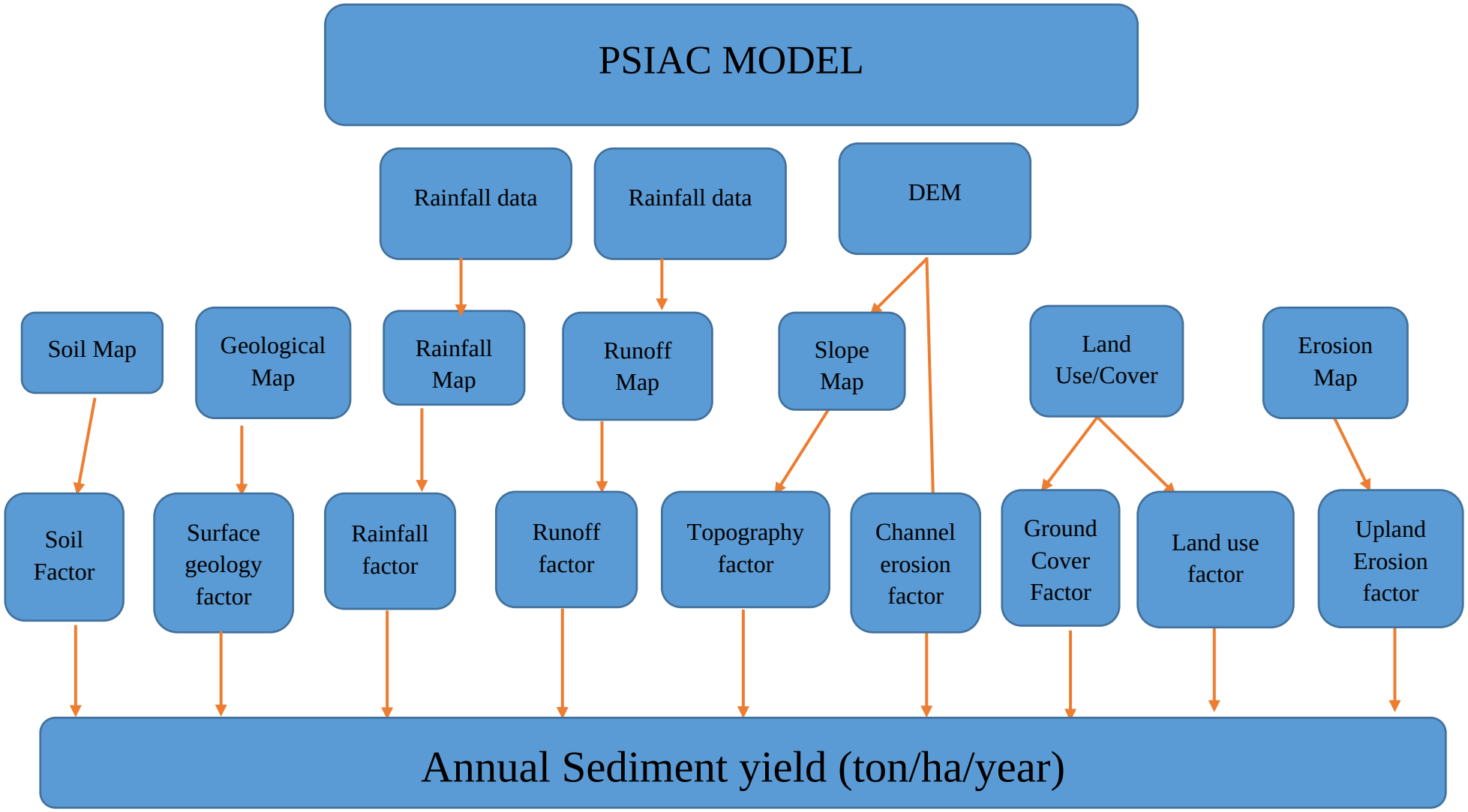

Appendix B. sediment yield estimation with RUSLE Model

Table B1: Sediment yield estimation in each grid cell (200 m x 200 m) using RUSLE model and the results obtained for each grid is shown as extracted from ArcMap

FID	Long.	Lat.	R-Factor	K-Factor	LS-Factor	C-Factor	P-Factor	Soil loss (ton/km2/year)	Sediment Yield (ton/km2/year)		
									with SDR Eq.6.9	with SDR Eq.6.10	with SDR Eq.6.11
0	208059	3000059	571.93	0.24	3.76	0.00	1.00	154.82	39.37	26.35	29.37
1	208219	3000007	571.93	0.24	3.76	0.03	1.00	1290.13	328.07	219.61	244.75
2	208336	2999986	571.93	0.24	3.76	0.03	1.00	1290.13	328.07	219.61	244.75
3	207626	3000257	565.60	0.24	11.34	0.00	1.00	153.88	39.13	26.19	29.19
4	207819	3000222	565.60	0.24	22.12	0.00	1.00	900.64	229.02	153.31	170.86
5	208007	3000189	571.93	0.24	22.12	0.00	1.00	910.71	231.59	155.02	172.77
6	208206	3000188	571.93	0.24	3.76	0.00	1.00	206.42	52.49	35.14	39.16
7	208367	3000205	564.23	0.24	3.76	0.00	1.00	203.64	51.78	34.66	38.63
8	207472	3000415	558.65	0.24	11.34	0.00	1.00	151.99	38.65	25.87	28.83
9	207606	3000388	565.60	0.24	11.34	0.00	1.00	153.88	39.13	26.19	29.19
10	207806	3000388	565.60	0.24	22.12	0.00	1.00	900.64	229.02	153.31	170.86
11	208006	3000388	565.60	0.24	22.12	0.03	1.00	7505.30	1908.54	1277.55	1423.80
12	208206	3000388	565.01	0.24	6.04	0.03	1.00	2047.17	520.58	348.47	388.36
13	208405	3000389	564.23	0.24	6.04	0.00	1.00	327.09	83.18	55.68	62.05
14	208553	3000430	564.23	0.26	2.52	0.00	1.00	147.75	37.57	25.15	28.03
15	207089	3000686	551.06	0.24	23.64	0.00	1.00	312.68	79.51	53.22	59.32
16	207230	3000677	558.65	0.24	39.59	0.00	1.00	2122.98	539.86	361.37	402.74
17	207423	3000601	558.65	0.24	39.59	0.00	1.00	2122.98	539.86	361.37	402.74
18	207606	3000588	558.65	0.24	31.42	0.00	1.00	421.20	107.11	71.70	79.90
19	207806	3000588	558.35	0.24	27.64	0.00	1.00	370.35	94.18	63.04	70.26
20	208006	3000588	558.35	0.24	27.64	0.00	1.00	1111.06	282.53	189.12	210.77
	Continued till		Continued till		Continued till			Continued till		Continued till	
89857	181206	3081988	412.45	0.24	23.34	0.00	1.00	23.11	5.88	3.93	4.38

89858	181406	3081988	412.39	0.24	16.00	0.00	1.00	15.84	4.03	2.70	3.00
89859	181606	3081988	412.39	0.24	15.95	0.00	1.00	0.00	0.00	0.00	0.00
89860	181806	3081988	412.33	0.24	15.95	0.00	1.00	0.00	0.00	0.00	0.00
89861	182006	3081988	412.26	0.24	27.10	0.00	1.00	0.00	0.00	0.00	0.00
89862	182206	3081988	412.26	0.24	27.10	0.00	1.00	0.00	0.00	0.00	0.00
89863	182406	3081988	412.20	0.24	32.19	0.00	1.00	0.00	0.00	0.00	0.00
89864	182606	3081988	412.14	0.24	59.63	0.00	1.00	0.00	0.00	0.00	0.00
89865	182806	3081988	412.14	0.24	59.63	0.00	1.00	0.00	0.00	0.00	0.00
89866	183006	3081988	412.07	0.24	16.11	0.00	1.00	15.93	4.05	2.71	3.02
89867	183206	3081988	412.01	0.26	16.11	0.00	1.00	17.26	4.39	2.94	3.27
89868	183406	3081988	412.01	0.26	17.21	0.00	1.00	0.00	0.00	0.00	0.00
89869	183606	3081988	411.95	0.26	29.77	0.00	1.00	0.00	0.00	0.00	0.00
89870	183806	3081988	411.89	0.26	29.77	0.00	1.00	0.00	0.00	0.00	0.00
89871	183999	3081982	411.89	0.26	0.00	0.00	1.00	0.00	0.00	0.00	0.00
89872	184134	3081922	411.76	0.26	0.00	0.00	1.00	0.00	0.00	0.00	0.00
89873	180704	3082089	412.52	0.24	8.82	0.00	1.00	0.00	0.00	0.00	0.00
89874	180841	3082136	412.52	0.24	0.00	0.00	1.00	0.00	0.00	0.00	0.00
89875	181008	3082170	412.45	0.24	0.00	0.00	1.00	0.00	0.00	0.00	0.00
89876	181207	3082178	412.45	0.24	0.00	0.00	1.00	0.00	0.00	0.00	0.00
89877	181407	3082185	412.39	0.24	10.61	0.00	1.00	10.50	2.67	1.79	1.99
89878	181606	3082188	412.39	0.24	21.19	0.00	1.00	20.97	5.33	3.57	3.98
89879	181806	3082188	412.33	0.24	21.19	0.00	1.00	20.97	5.33	3.57	3.98
89880	182006	3082188	412.26	0.24	0.00	0.00	1.00	0.00	0.00	0.00	0.00
89881	182206	3082188	412.26	0.24	0.00	0.00	1.00	0.00	0.00	0.00	0.00
89882	182406	3082188	412.20	0.24	10.67	0.00	1.00	0.00	0.00	0.00	0.00
89883	182606	3082188	412.14	0.24	9.31	0.00	1.00	9.21	2.34	1.57	1.75
89884	182806	3082188	412.14	0.24	9.31	0.00	1.00	9.21	2.34	1.57	1.75
89885	183006	3082188	412.07	0.24	22.00	0.00	1.00	21.75	5.53	3.70	4.13
89886	183206	3082188	412.01	0.24	22.00	0.00	1.00	21.75	5.53	3.70	4.13
89887	183406	3082188	412.01	0.24	12.36	0.00	1.00	0.00	0.00	0.00	0.00
89888	183606	3082188	411.95	0.24	11.00	0.00	1.00	0.00	0.00	0.00	0.00

89889	183803	3082184	411.89	0.26	11.00	0.00	1.00	0.00	0.00	0.00	0.00
89890	183951	3082151	411.89	0.26	11.00	0.00	1.00	0.00	0.00	0.00	0.00
89891	181493	3082289	412.39	0.24	10.61	0.00	1.00	0.00	0.00	0.00	0.00
89892	181626	3082293	412.39	0.24	21.19	0.00	1.00	0.00	0.00	0.00	0.00
89893	181810	3082296	412.33	0.24	21.19	0.00	1.00	0.00	0.00	0.00	0.00
89894	182009	3082298	412.26	0.24	0.00	0.00	1.00	0.00	0.00	0.00	0.00
89895	182209	3082301	412.26	0.24	0.00	0.00	1.00	0.00	0.00	0.00	0.00
89896	182408	3082303	412.20	0.24	10.67	0.00	1.00	0.00	0.00	0.00	0.00
89897	182608	3082305	412.14	0.24	9.31	0.00	1.00	9.21	2.34	1.57	1.75
89898	182808	3082307	412.14	0.24	9.31	0.00	1.00	9.21	2.34	1.57	1.75
89899	183008	3082310	412.07	0.24	22.00	0.00	1.00	21.75	5.53	3.70	4.13
89900	183208	3082312	412.01	0.24	22.00	0.00	1.00	0.00	0.00	0.00	0.00
89901	183412	3082330	412.01	0.24	12.36	0.00	1.00	0.00	0.00	0.00	0.00
89902	183576	3082306	411.95	0.24	11.00	0.00	1.00	0.00	0.00	0.00	0.00
89903	183724	3082291	411.95	0.24	11.00	0.00	1.00	0.00	0.00	0.00	0.00

NB:

- FID denotes field identity of GRID cell (200 m by 200m). Therefore, the last FID number is 89903 which indicate that there are 89903 such grid covering Bunakha catchment. Each grid has its RULSE factor assigned and the product of these factors results the sediment yield estimation of that particular grid.

Appendix C. Sediment data analysis

It is to be noted that full table of data computation is not shown deliberately to avoid unnecessary pages.

Table C1: Computation of bed load with Meyer-Peter Muller (1948) equation

Average Discharge (m3/sec)	m3/sec	64.41859
K_{st}	-	35
Width of Channel, B	[m]	40
Critical Shear Stress, Fr^*_c	[N/m^2]	0.047
Reduction factor considering bed roughness, [Kst/Kr]	-	0.95
Density of Sediment, Ps	[kg/m^3]	2650
Density of Water, Pw	[kg/m^3]	1000
Mean Diameter of grain, d_{50}	[m]	0.0375
Gravity, g	[m/sec^2]	9.81
Slope of Channel, S	-	0.0012

Date	Discharge (m3/s)	Stage (m)	Hydraulic Radius	Shield Stress	Volumetric Bed load rate (qb) (m3/sec/m	Total Bed load (tons)
01.01.2009	26.483	2.32349465	2.081659	0.040372	0.00	0.00
02.01.2009	26.483	2.32349465	2.081659	0.040372	0.00	0.00
03.01.2009	26.222	2.318735941	2.077838	0.040297	0.00	0.00
04.01.2009	25.788	2.310739171	2.071414	0.040173	0.00	0.00
05.01.2009	25.788	2.310739171	2.071414	0.040173	0.00	0.00
06.01.2009	25.631	2.307820036	2.069068	0.040127	0.00	0.00
07.01.2009	25.474	2.304886687	2.06671	0.040082	0.00	0.00
08.01.2009	25.317	2.301938966	2.06434	0.040036	0.00	0.00
09.01.2009	25.159	2.298957799	2.061942	0.039989	0.00	0.00
10.01.2009	25.002	2.295980757	2.059547	0.039943	0.00	0.00
11.01.2009	24.845	2.292988854	2.057139	0.039896	0.00	0.00
12.01.2009	24.688	2.289981921	2.054719	0.039849	0.00	0.00
13.01.2009	24.531	2.286959785	2.052285	0.039802	0.00	0.00
14.01.2009	24.374	2.283922271	2.049839	0.039754	0.00	0.00
15.01.2009	24.217	2.280869203	2.047379	0.039707	0.00	0.00
16.01.2009	24.06	2.277800398	2.044906	0.039659	0.00	0.00
17.01.2009	23.903	2.274715672	2.042419	0.039611	0.00	0.00
18.01.2009	23.746	2.271614836	2.039919	0.039562	0.00	0.00
19.01.2009	23.589	2.2684977	2.037405	0.039513	0.00	0.00
20.01.2009	23.432	2.265364068	2.034877	0.039464	0.00	0.00
21.01.2009	23.275	2.262213742	2.032335	0.039415	0.00	0.00
22.01.2009	23.118	2.259046519	2.029778	0.039365	0.00	0.00
11.03.2009	18.347	2.153502787	1.944165	0.037705	0.00	0.00
12.03.2009	18.347	2.153502787	1.944165	0.037705	0.00	0.00

13.03.2009	18.347	2.153502787	1.944165	0.037705	0.00	0.00
14.03.2009	17.867	2.141717372	1.934554	0.037519	0.00	0.00
15.03.2009	17.799	2.14002753	1.933175	0.037492	0.00	0.00
16.03.2009	17.799	2.14002753	1.933175	0.037492	0.00	0.00
17.03.2009	17.799	2.14002753	1.933175	0.037492	0.00	0.00
18.03.2009	17.759	2.139031113	1.932362	0.037476	0.00	0.00
19.03.2009	17.261	2.126474224	1.922109	0.037277	0.00	0.00
20.03.2009	17.937	2.143451597	1.935969	0.037546	0.00	0.00
21.03.2009	17.073	2.121659115	1.918174	0.037201	0.00	0.00
22.03.2009	16.936	2.11812368	1.915283	0.037145	0.00	0.00
23.03.2009	17.31	2.127722389	1.923128	0.037297	0.00	0.00
24.03.2009	17.683	2.137133005	1.930813	0.037446	0.00	0.00
25.03.2009	18.057	2.146412107	1.938384	0.037593	0.00	0.00
26.03.2009	18.431	2.155540031	1.945825	0.037737	0.00	0.00
27.03.2009	18.805	2.164522235	1.953141	0.037879	0.00	0.00
28.03.2009	19.178	2.173340417	1.960318	0.038018	0.00	0.00
29.03.2009	19.552	2.182046727	1.967399	0.038156	0.00	0.00
30.03.2009	19.912	2.190303269	1.974108	0.038286	0.00	0.00
31.03.2009	20.352	2.200235355	1.982173	0.038442	0.00	0.00
01.04.2009	19.988	2.192031163	1.975512	0.038313	0.00	0.00
02.04.2009	20.13	2.195245684	1.978122	0.038364	0.00	0.00
03.04.2009	20.278	2.198576948	1.980827	0.038416	0.00	0.00
04.04.2009	21.104	2.2168228	1.995625	0.038703	0.00	0.00
05.04.2009	21.972	2.235396032	2.010664	0.038995	0.00	0.00
06.04.2009	21.864	2.233117123	2.008821	0.038959	0.00	0.00
07.04.2009	30.133	2.386432975	2.132035	0.041349	0.00	0.00
08.04.2009	25.618	2.307577689	2.068873	0.040124	0.00	0.00
09.04.2009	25.025	2.29641781	2.059898	0.03995	0.00	0.00
10.04.2009	25.19	2.29954388	2.062413	0.039998	0.00	0.00
11.04.2009	25.025	2.29641781	2.059898	0.03995	0.00	0.00
12.04.2009	24	2.276623411	2.043957	0.03964	0.00	0.00
13.04.2009	21.486	2.225069977	2.002306	0.038833	0.00	0.00
14.04.2009	21.104	2.2168228	1.995625	0.038703	0.00	0.00
15.04.2009	19.851	2.18891262	1.972979	0.038264	0.00	0.00
16.04.2009	19.97	2.191622397	1.97518	0.038307	0.00	0.00
17.04.2009	21.104	2.2168228	1.995625	0.038703	0.00	0.00
18.04.2009	19.988	2.192031163	1.975512	0.038313	0.00	0.00
19.04.2009	19.191	2.173645292	1.960566	0.038023	0.00	0.00
20.04.2009	18.977	2.1686056	1.956465	0.037944	0.00	0.00
21.04.2009	19.736	2.186281661	1.970841	0.038222	0.00	0.00
22.04.2009	20.36	2.200414356	1.982318	0.038445	0.00	0.00
23.04.2009	18.562	2.158702515	1.948402	0.037787	0.00	0.00
24.04.2009	17.267	2.126627211	1.922234	0.03728	0.00	0.00
25.04.2009	17.945	2.143649452	1.93613	0.037549	0.00	0.00
14.09.2009	123.924	3.197942444	2.757091	0.053471	0.00	269.36
15.09.2009	112.564	3.134925111	2.710123	0.05256	0.00	145.78

16.09.2009	102.248	3.073165992	2.663844	0.051662	0.00	51.80
17.09.2009	83.825	2.949346499	2.57031	0.049848	0.00	0.00
18.09.2009	75.193	2.88374062	2.52034	0.048879	0.00	0.00
19.09.2009	105.414	3.092626103	2.678453	0.051946	0.00	77.98
20.09.2009	100.842	3.064370344	2.657233	0.051534	0.00	41.17
21.09.2009	109.541	3.117308959	2.696948	0.052304	0.00	115.88
22.09.2009	103.695	3.082118544	2.670568	0.051793	0.00	63.41
23.09.2009	91.499	3.003313405	2.611201	0.050641	0.00	0.00
24.09.2009	81.189	2.929903991	2.555531	0.049562	0.00	0.00
25.09.2009	79.123	2.914312633	2.543661	0.049332	0.00	0.00
26.09.2009	78.637	2.910598133	2.540831	0.049277	0.00	0.00
27.09.2009	76.452	2.89366974	2.527921	0.049026	0.00	0.00
28.09.2009	75.515	2.88629255	2.522289	0.048917	0.00	0.00
29.09.2009	75.057	2.882660182	2.519515	0.048863	0.00	0.00
30.09.2009	74.745	2.880175653	2.517617	0.048827	0.00	0.00
01.10.2009	74.28	2.876457441	2.514775	0.048771	0.00	0.00
02.10.2009	70.794	2.847978694	2.492981	0.048349	0.00	0.00
03.10.2009	68.266	2.826622379	2.476602	0.048031	0.00	0.00
04.10.2009	66.8	2.813948846	2.466867	0.047842	0.00	0.00
05.10.2009	73.506	2.870227282	2.510012	0.048679	0.00	0.00
06.10.2009	80.851	2.927374918	2.553607	0.049524	0.00	0.00
07.10.2009	225.048	3.618332126	3.064003	0.059423	0.00	1538.16
08.10.2009	499.583	4.267752785	3.517221	0.068213	0.00	4397.93
09.10.2009	181.916	3.462427962	2.951466	0.057241	0.00	995.26
10.10.2009	142.271	3.29065659	2.825731	0.054802	0.00	490.33
11.10.2009	131.902	3.239511353	2.787934	0.054069	0.00	363.22
12.10.2009	121.949	3.18732513	2.749196	0.053318	0.00	246.87
13.10.2009	113.865	3.142391218	2.715701	0.052668	0.00	159.11
14.10.2009	106.966	3.101996775	2.685479	0.052082	0.00	91.79
15.10.2009	101.707	3.069793027	2.66131	0.051613	0.00	47.63
Continued till		Continued till		continued till		
31.12.2015	15.223	2.071882021	1.877395	0.03641	0.00	0.00

Table C2: Computation of bed load with Riberink (1998) Equation

Gravity, g	9.81	m2/sec
median grain size, d_{50}	0.04	m
Slope, I	0.00	
Density of water, ρ	1000.00	kg/m^3
Density of sediment grain, ρ_s	2650.00	kg/m^3
Kinematic Viscosity of water, v	1E-06	m^2/sec
Relative Density, S	2.65	
Critical Shear Parameter, θ_{cr}	0.06	

Date	Discharge (m3/s)	Stage (m)	Hydraulic Radius	Non-dimensional parameter of bed load (φ)	Volumetric Bed Load, q_b (m^3/sec/m)	Total Bed load (tons)
01.01.2009	26.483	2.32349465	2.081659	0	0	0
02.01.2009	26.483	2.32349465	2.081659	0	0	0
03.01.2009	26.222	2.318735941	2.077838	0	0	0
04.01.2009	25.788	2.310739171	2.071414	0	0	0
05.01.2009	25.788	2.310739171	2.071414	0	0	0
06.01.2009	25.631	2.307820036	2.069068	0	0	0
07.01.2009	25.474	2.304886687	2.06671	0	0	0
08.01.2009	25.317	2.301938966	2.06434	0	0	0
09.01.2009	25.159	2.298957799	2.061942	0	0	0
10.01.2009	25.002	2.295980757	2.059547	0	0	0
11.01.2009	24.845	2.292988854	2.057139	0	0	0
12.01.2009	24.688	2.289981921	2.054719	0	0	0
13.01.2009	24.531	2.286959785	2.052285	0	0	0
14.01.2009	24.374	2.283922271	2.049839	0	0	0
15.01.2009	24.217	2.280869203	2.047379	0	0	0
16.01.2009	24.06	2.277800398	2.044906	0	0	0
17.01.2009	23.903	2.274715672	2.042419	0	0	0
18.01.2009	23.746	2.271614836	2.039919	0	0	0
19.01.2009	23.589	2.2684977	2.037405	0	0	0
20.01.2009	23.432	2.265364068	2.034877	0	0	0
21.01.2009	23.275	2.262213742	2.032335	0	0	0
22.01.2009	23.118	2.259046519	2.029778	0	0	0
23.01.2009	22.961	2.255862193	2.027207	0	0	0
24.01.2009	22.804	2.252660554	2.024621	0	0	0
26.05.2009	639.486	4.491531978	3.667824	0.015994314	0.0014636	13404.268
27.05.2009	815.12	4.722917194	3.82068	0.020678949	0.00189228	17330.295
28.05.2009	150.512	3.329236855	2.854133	6.78059E-06	6.2048E-07	5.6825731
Continued till		Continued till		Continued till		Continued till
31.12.2015	15.223	2.071882021	1.877395	0	0	0

Table C3: Computation of total suspended sediment load from observed data and bed load as 30% of the total suspended sediment load

Day	Daily Discharge	C-sand (ppm)	Susp. sediment conc. c-sand (kg/kg	Susp. sediment conc. c-sand (kg/m^3)	Sand load (Ton/day)	C-Fine (ppm)	Susp. sediment conc. c-Fine (kg/kg	Susp. sediment conc. c-Fine (kg/m^3)	Fine load (Ton/day)	Total Susp. Load (tons/day)	Total Bed load (30% assumed (tons/day)
01.01.2009	26.483	1.622	1.622E-06	0.002	3.711	4.671	4.671E-06	0.005	10.69	14.40	4.32
02.01.2009	26.483	1.622	1.622E-06	0.002	3.711	4.671	4.671E-06	0.005	10.69	14.40	4.32
03.01.2009	26.222	1.594	1.594E-06	0.002	3.611	4.607	4.607E-06	0.005	10.44	14.05	4.21
04.01.2009	25.788	1.548	1.548E-06	0.002	3.449	4.502	4.502E-06	0.005	10.03	13.48	4.04
05.01.2009	25.788	1.548	1.548E-06	0.002	3.449	4.502	4.502E-06	0.005	10.03	13.48	4.04
06.01.2009	25.631	1.532	1.532E-06	0.002	3.392	4.464	4.464E-06	0.004	9.88	13.28	3.98
07.01.2009	25.474	1.515	1.515E-06	0.002	3.335	4.426	4.426E-06	0.004	9.74	13.08	3.92
08.01.2009	25.317	1.499	1.499E-06	0.001	3.279	4.388	4.388E-06	0.004	9.60	12.88	3.86
09.01.2009	25.159	1.483	1.483E-06	0.001	3.223	4.350	4.350E-06	0.004	9.46	12.68	3.80
10.01.2009	25.002	1.466	1.466E-06	0.001	3.168	4.312	4.312E-06	0.004	9.32	12.48	3.74
11.01.2009	24.845	1.450	1.450E-06	0.001	3.113	4.275	4.275E-06	0.004	9.18	12.29	3.69
12.01.2009	24.688	1.434	1.434E-06	0.001	3.059	4.237	4.237E-06	0.004	9.04	12.10	3.63
13.01.2009	24.531	1.418	1.418E-06	0.001	3.006	4.200	4.200E-06	0.004	8.90	11.91	3.57
14.01.2009	24.374	1.402	1.402E-06	0.001	2.953	4.163	4.163E-06	0.004	8.77	11.72	3.52
15.01.2009	24.217	1.387	1.387E-06	0.001	2.901	4.126	4.126E-06	0.004	8.63	11.53	3.46
16.01.2009	24.06	1.371	1.371E-06	0.001	2.850	4.089	4.089E-06	0.004	8.50	11.35	3.40
17.01.2009	23.903	1.355	1.355E-06	0.001	2.799	4.052	4.052E-06	0.004	8.37	11.17	3.35
18.01.2009	23.746	1.340	1.340E-06	0.001	2.749	4.015	4.015E-06	0.004	8.24	10.99	3.30
19.01.2009	23.589	1.324	1.324E-06	0.001	2.699	3.978	3.978E-06	0.004	8.11	10.81	3.24
20.01.2009	23.432	1.309	1.309E-06	0.001	2.650	3.941	3.941E-06	0.004	7.98	10.63	3.19
21.01.2009	23.275	1.293	1.293E-06	0.001	2.601	3.905	3.905E-06	0.004	7.85	10.45	3.14
22.01.2009	23.118	1.278	1.278E-06	0.001	2.553	3.868	3.868E-06	0.004	7.73	10.28	3.08
23.01.2009	22.961	1.263	1.263E-06	0.001	2.506	3.832	3.832E-06	0.004	7.60	10.11	3.03

24.01.2009	22.804	1.248	1.248E-06	0.001	2.459	3.795	3.795E-06	0.004	7.48	9.94	2.98
25.01.2009	22.646	1.233	1.233E-06	0.001	2.412	3.759	3.759E-06	0.004	7.35	9.77	2.93
26.01.2009	22.489	1.218	1.218E-06	0.001	2.366	3.723	3.723E-06	0.004	7.23	9.60	2.88
27.01.2009	22.489	1.218	1.218E-06	0.001	2.366	3.723	3.723E-06	0.004	7.23	9.60	2.88
28.01.2009	22.489	1.218	1.218E-06	0.001	2.366	3.723	3.723E-06	0.004	7.23	9.60	2.88
29.01.2009	22.489	1.218	1.218E-06	0.001	2.366	3.723	3.723E-06	0.004	7.23	9.60	2.88
30.01.2009	22.489	1.218	1.218E-06	0.001	2.366	3.723	3.723E-06	0.004	7.23	9.60	2.88
31.01.2009	22.489	0.932	9.320E-07	0.001	1.811	2.796	2.796E-06	0.003	5.43	7.24	2.17
01.02.2009	22.489	0.946	9.460E-07	0.001	1.838	1.892	1.892E-06	0.002	3.68	5.51	1.65
02.02.2009	22.489	0.944	9.440E-07	0.001	1.834	1.887	1.887E-06	0.002	3.67	5.50	1.65
03.02.2009	22.489	0.933	9.330E-07	0.001	1.813	1.865	1.865E-06	0.002	3.62	5.44	1.63
04.02.2009	22.489	1.025	1.025E-06	0.001	1.992	3.075	3.075E-06	0.003	5.97	7.97	2.39
05.02.2009	21.942	0.983	9.830E-07	0.001	1.864	2.949	2.949E-06	0.003	5.59	7.45	2.24
06.02.2009	21.864	0.908	9.080E-07	0.001	1.715	8.815	8.815E-06	0.009	16.65	18.37	5.51
07.02.2009	21.864	0.947	9.470E-07	0.001	1.789	2.842	2.842E-06	0.003	5.37	7.16	2.15
08.02.2009	21.634	0.928	9.280E-07	0.001	1.735	3.711	3.711E-06	0.004	6.94	8.67	2.60
09.02.2009	21.25	0.910	9.100E-07	0.001	1.671	2.731	2.731E-06	0.003	5.01	6.68	2.01
10.02.2009	21.25	0.907	9.070E-07	0.001	1.665	3.629	3.629E-06	0.004	6.66	8.33	2.50
11.02.2009	21.25	0.954	9.540E-07	0.001	1.752	2.861	2.861E-06	0.003	5.25	7.00	2.10
12.02.2009	20.723	1.908	1.908E-06	0.002	3.416	4.770	4.770E-06	0.005	8.54	11.96	3.59
13.02.2009	20.648	1.956	1.956E-06	0.002	3.489	3.913	3.913E-06	0.004	6.98	10.47	3.14
14.02.2009	20.648	0.965	9.650E-07	0.001	1.722	2.894	2.894E-06	0.003	5.16	6.88	2.07
15.02.2009	20.648	0.916	9.160E-07	0.001	1.634	2.749	2.749E-06	0.003	4.90	6.54	1.96
16.02.2009	20.13	0.947	9.470E-07	0.001	1.647	2.840	2.840E-06	0.003	4.94	6.59	1.98
17.02.2009	20.056	1.011	1.011E-06	0.001	1.752	2.022	2.022E-06	0.002	3.50	5.26	1.58
18.02.2009	20.056	1.823	1.823E-06	0.002	3.159	3.746	3.746E-06	0.004	6.49	9.65	2.90
19.02.2009	20.056	0.969	9.690E-07	0.001	1.679	3.877	3.877E-06	0.004	6.72	8.40	2.52
20.02.2009	20.056	0.990	9.900E-07	0.001	1.716	2.970	2.970E-06	0.003	5.15	6.86	2.06
21.02.2009	20.056	0.990	9.900E-07	0.001	1.716	1.970	1.970E-06	0.002	3.41	5.13	1.54
31.12.2015	15.223	1.033	1.003E-06	0.001	1.359	2.063	2.063E-06	0.002	2.71	4.07	1.22

Table C4: Computation of Suspended Sediment Load with the method specified by Rijn (1984)

Width of River	40	[m]
River Bed slope	0.0012	
Median grain diameter, d_{50}	0.002	[m]
Kinematic Viscosity of water	1E-06	[m^2/sec]
Manning Roughness value, Kst	35	
Density of water, ρ_w	1000	[kg/$m^{3]}$
Density of sediment, ρ_s	2650	[kg/$m^{3]}$
Acceleration due to gravity, g	9.81	[m^2/sec]
Relative density, S	2.65	
Geometric Standard Deviation, σ_s	2.5	
Grain Diameter, d_{90}	0.001	m

1	2	3	4	5	6	7	8	9	10	11	12
Date	Discharge (m^3/s)	Stage (m)	Hydraulic Radius	Mean velocity (m/s)	Chezy's coefficient related to grain, C'	Bed shear velocity related to grains, u*'	Critical Shear velocity	Transport Stage Parameter, T	Reference level, a	Reference Concentration, Ca	Particle size of Suspended sediment, Ds
01.01.2009	26.483	2.323	2.082	1.977	70.568	0.088	0.053	1.708	0.023	0.001	0.00123
02.01.2009	26.483	2.323	2.082	1.977	70.568	0.088	0.053	1.708	0.023	0.001	0.00123
03.01.2009	26.222	2.319	2.078	1.974	70.554	0.088	0.053	1.703	0.023	0.001	0.00123
04.01.2009	25.788	2.311	2.071	1.970	70.530	0.087	0.053	1.694	0.023	0.001	0.00123
05.01.2009	25.788	2.311	2.071	1.970	70.530	0.087	0.053	1.694	0.023	0.001	0.00123
06.01.2009	25.631	2.308	2.069	1.969	70.521	0.087	0.053	1.691	0.023	0.001	0.00123
07.01.2009	25.474	2.305	2.067	1.967	70.512	0.087	0.053	1.688	0.023	0.001	0.00123

08.01.2009	25.317	2.302	2.064	1.966	70.503	0.087	0.053	1.685	0.023	0.001	0.00123
09.01.2009	25.159	2.299	2.062	1.964	70.494	0.087	0.053	1.681	0.023	0.001	0.00123
10.01.2009	25.002	2.296	2.060	1.963	70.485	0.087	0.053	1.678	0.023	0.001	0.00123
11.01.2009	24.845	2.293	2.057	1.961	70.476	0.087	0.053	1.675	0.023	0.001	0.00123
12.01.2009	24.688	2.290	2.055	1.960	70.467	0.087	0.053	1.672	0.023	0.001	0.00123
13.01.2009	24.531	2.287	2.052	1.958	70.457	0.087	0.053	1.668	0.023	0.001	0.00123
14.01.2009	24.374	2.284	2.050	1.956	70.448	0.087	0.053	1.665	0.023	0.001	0.00123
15.01.2009	24.217	2.281	2.047	1.955	70.439	0.087	0.053	1.662	0.023	0.001	0.00123
16.01.2009	24.06	2.278	2.045	1.953	70.429	0.087	0.053	1.659	0.023	0.001	0.00123
17.01.2009	23.903	2.275	2.042	1.952	70.420	0.087	0.053	1.655	0.023	0.001	0.00123
18.01.2009	23.746	2.272	2.040	1.950	70.410	0.087	0.053	1.652	0.023	0.001	0.00123
19.01.2009	23.589	2.268	2.037	1.949	70.400	0.087	0.053	1.649	0.023	0.001	0.00123
20.01.2009	23.432	2.265	2.035	1.947	70.391	0.087	0.053	1.645	0.023	0.001	0.00123
21.01.2009	23.275	2.262	2.032	1.945	70.381	0.087	0.053	1.642	0.023	0.001	0.00123
22.01.2009	23.118	2.259	2.030	1.944	70.371	0.087	0.053	1.638	0.023	0.001	0.00123
23.01.2009	22.961	2.256	2.027	1.942	70.361	0.086	0.053	1.635	0.023	0.001	0.00123
24.01.2009	22.804	2.253	2.025	1.940	70.351	0.086	0.053	1.632	0.023	0.001	0.00123
25.01.2009	22.646	2.249	2.022	1.939	70.341	0.086	0.053	1.628	0.022	0.001	0.00123
26.01.2009	22.489	2.246	2.019	1.937	70.331	0.086	0.053	1.625	0.022	0.001	0.00123
27.01.2009	22.489	2.246	2.019	1.937	70.331	0.086	0.053	1.625	0.022	0.001	0.00123
28.01.2009	22.489	2.246	2.019	1.937	70.331	0.086	0.053	1.625	0.022	0.001	0.00123
29.01.2009	22.489	2.246	2.019	1.937	70.331	0.086	0.053	1.625	0.022	0.001	0.00123
30.01.2009	22.489	2.246	2.019	1.937	70.331	0.086	0.053	1.625	0.022	0.001	0.00123
31.01.2009	22.489	2.246	2.019	1.937	70.331	0.086	0.053	1.625	0.022	0.001	0.00123
01.02.2009	22.489	2.246	2.019	1.937	70.331	0.086	0.053	1.625	0.022	0.001	0.00123
02.02.2009	22.489	2.246	2.019	1.937	70.331	0.086	0.053	1.625	0.022	0.001	0.00123
03.02.2009	22.489	2.246	2.019	1.937	70.331	0.086	0.053	1.625	0.022	0.001	0.00123
04.02.2009	22.489	2.246	2.019	1.937	70.331	0.086	0.053	1.625	0.022	0.001	0.00123
05.02.2009	21.942	2.235	2.010	1.931	70.295	0.086	0.053	1.612	0.022	0.001	0.00123
06.02.2009	21.864	2.233	2.009	1.930	70.290	0.086	0.053	1.611	0.022	0.001	0.00123

07.02.2009	21.864	2.233	2.009	1.930	70.290	0.086	0.053	1.611	0.022	0.001	0.00123
08.02.2009	21.634	2.228	2.005	1.928	70.275	0.086	0.053	1.605	0.022	0.001	0.00123
09.02.2009	21.25	2.220	1.998	1.923	70.249	0.086	0.053	1.596	0.022	0.001	0.00123
10.02.2009	21.25	2.220	1.998	1.923	70.249	0.086	0.053	1.596	0.022	0.001	0.00123
11.02.2009	21.25	2.220	1.998	1.923	70.249	0.086	0.053	1.596	0.022	0.001	0.00123
12.02.2009	20.723	2.208	1.989	1.917	70.212	0.086	0.053	1.584	0.022	0.001	0.00123
13.02.2009	20.648	2.207	1.988	1.917	70.207	0.086	0.053	1.582	0.022	0.001	0.00123
14.02.2009	20.648	2.207	1.988	1.917	70.207	0.086	0.053	1.582	0.022	0.001	0.00123
15.02.2009	20.648	2.207	1.988	1.917	70.207	0.086	0.053	1.582	0.022	0.001	0.00123
16.02.2009	20.13	2.195	1.978	1.911	70.170	0.085	0.053	1.570	0.022	0.001	0.00123
17.02.2009	20.056	2.194	1.977	1.910	70.164	0.085	0.053	1.568	0.022	0.001	0.00123
18.02.2009	20.056	2.194	1.977	1.910	70.164	0.085	0.053	1.568	0.022	0.001	0.00123
19.02.2009	20.056	2.194	1.977	1.910	70.164	0.085	0.053	1.568	0.022	0.001	0.00123
20.02.2009	20.056	2.194	1.977	1.910	70.164	0.085	0.053	1.568	0.022	0.001	0.00123
21.02.2009	20.056	2.194	1.977	1.910	70.164	0.085	0.053	1.568	0.022	0.001	0.00123
22.02.2009	19.548	2.182	1.967	1.904	70.127	0.085	0.053	1.555	0.022	0.001	0.00123
23.02.2009	19.475	2.180	1.966	1.903	70.121	0.085	0.053	1.553	0.022	0.001	0.00123
24.02.2009	19.475	2.180	1.966	1.903	70.121	0.085	0.053	1.553	0.022	0.001	0.00123
25.02.2009	19.475	2.180	1.966	1.903	70.121	0.085	0.053	1.553	0.022	0.001	0.00123
26.02.2009	19.475	2.180	1.966	1.903	70.121	0.085	0.053	1.553	0.022	0.001	0.00123
27.02.2009	19.262	2.175	1.962	1.900	70.105	0.085	0.053	1.548	0.022	0.001	0.00123
28.02.2009	18.906	2.167	1.955	1.896	70.078	0.085	0.053	1.539	0.022	0.001	0.00123
31.12.2015	15.223	2.072	1.877	1.845	69.761	0.083	0.053	1.435	0.021	0.001	0.001

13	14	15	16	17	18	19	20	21
Settling velocity, W_s	Shear Velocity, U*	B-factor	φ-factor	Suspension number, Z	Modified suspension number, Z'	F-factor	Suspended sediment load transport (q_{ss}), $m^3/sec/m$	Total Suspended Load (ton/day)
0.133	0.157	2.450	0.157	0.869	1.026	0.028	0.000	1060.618
0.133	0.157	2.450	0.157	0.869	1.026	0.028	0.000	1060.618
0.133	0.156	2.452	0.157	0.869	1.026	0.028	0.000	1055.082
0.133	0.156	2.457	0.157	0.868	1.025	0.028	0.000	1045.810
0.133	0.156	2.457	0.157	0.868	1.025	0.028	0.000	1045.810
0.133	0.156	2.458	0.157	0.868	1.025	0.028	0.000	1042.434
0.133	0.156	2.460	0.157	0.868	1.025	0.028	0.000	1039.048
0.133	0.156	2.461	0.157	0.868	1.025	0.028	0.000	1035.649
0.133	0.156	2.463	0.157	0.868	1.025	0.028	0.000	1032.218
0.133	0.156	2.464	0.157	0.868	1.025	0.028	0.000	1028.796
0.133	0.156	2.466	0.157	0.868	1.025	0.028	0.000	1025.363
0.133	0.156	2.467	0.157	0.868	1.025	0.028	0.000	1021.918
0.133	0.155	2.469	0.157	0.868	1.025	0.029	0.000	1018.460
0.133	0.155	2.471	0.157	0.868	1.024	0.029	0.000	1014.991
0.133	0.155	2.472	0.157	0.868	1.024	0.029	0.000	1011.509
0.133	0.155	2.474	0.157	0.868	1.024	0.029	0.000	1008.015
0.133	0.155	2.475	0.157	0.867	1.024	0.029	0.000	1004.508
0.133	0.155	2.477	0.157	0.867	1.024	0.029	0.000	1000.989
0.133	0.155	2.479	0.157	0.867	1.024	0.029	0.000	997.456

0.133	0.155	2.480	0.157	0.867	1.024	0.029	0.000	993.911
0.133	0.155	2.482	0.156	0.867	1.024	0.029	0.000	990.353
0.133	0.155	2.484	0.156	0.867	1.023	0.029	0.000	986.782
0.133	0.154	2.486	0.156	0.867	1.023	0.029	0.000	983.198
0.133	0.154	2.487	0.156	0.867	1.023	0.029	0.000	979.600
0.133	0.154	2.489	0.156	0.867	1.023	0.029	0.000	975.965
0.133	0.154	2.491	0.156	0.867	1.023	0.029	0.000	972.339
0.133	0.154	2.491	0.156	0.867	1.023	0.029	0.000	972.339
0.133	0.154	2.491	0.156	0.867	1.023	0.029	0.000	972.339
0.133	0.154	2.491	0.156	0.867	1.023	0.029	0.000	972.339
0.133	0.154	2.491	0.156	0.867	1.023	0.029	0.000	972.339
0.133	0.154	2.491	0.156	0.867	1.023	0.029	0.000	972.339
0.133	0.154	2.491	0.156	0.867	1.023	0.029	0.000	972.339
0.133	0.154	2.491	0.156	0.867	1.023	0.029	0.000	972.339
0.133	0.154	2.491	0.156	0.867	1.023	0.029	0.000	972.339
0.133	0.154	2.491	0.156	0.867	1.023	0.029	0.000	972.339
0.133	0.154	2.497	0.156	0.866	1.022	0.029	0.000	959.599
0.133	0.154	2.498	0.156	0.866	1.022	0.029	0.000	957.768
0.133	0.154	2.498	0.156	0.866	1.022	0.029	0.000	957.768
0.133	0.154	2.501	0.156	0.866	1.022	0.029	0.000	952.348
0.133	0.153	2.505	0.156	0.866	1.022	0.029	0.000	943.229
0.133	0.153	2.505	0.156	0.866	1.022	0.029	0.000	943.229
0.133	0.153	2.505	0.156	0.866	1.022	0.029	0.000	943.229
0.133	0.153	2.512	0.156	0.865	1.021	0.029	0.000	930.566
0.133	0.153	2.513	0.156	0.865	1.021	0.029	0.000	928.750
0.133	0.153	2.513	0.156	0.865	1.021	0.029	0.000	928.750
0.133	0.153	2.513	0.156	0.865	1.021	0.029	0.000	928.750
0.133	0.153	2.519	0.156	0.865	1.021	0.029	0.000	916.105
0.133	0.153	2.520	0.156	0.865	1.021	0.029	0.000	914.285
0.133	0.153	2.520	0.156	0.865	1.021	0.029	0.000	914.285
0.133	0.153	2.520	0.156	0.865	1.021	0.029	0.000	914.285

0.133	0.153	2.520	0.156	0.865	1.021	0.029	0.000	914.285
0.133	0.153	2.520	0.156	0.865	1.021	0.029	0.000	914.285
0.133	0.149	2.594	0.154	0.860	1.014	0.029	0.000	786.279

Appendix D. Calculation for Prediction of sediment deposits in the reservoir.

Table D1: Type curves and their values for computation of NZE

P	Type I	Type II	Type III	Type IV
0				
0.01	996.7	5.568	12.03	0.2023
0.02	277.5	3.758	5.544	0.233
0.05	51.49	2.233	2.057	0.2716
0.1	14.53	1.495	1.013	0.2911
0.15	6.971	1.169	0.6821	0.2932
0.2	4.145	0.9706	0.518	0.2878
0.25	2.766	0.8299	0.4176	0.2781
0.3	1.98	0.7212	0.3486	0.2656
0.35	1.485	0.6323	0.2986	0.2513
0.4	1.149	0.5565	0.2555	0.2355
0.45	0.9076	0.49	0.2212	0.2187
0.5	0.7267	0.4303	0.1917	0.201
0.55	0.586	0.3758	0.1657	0.1826
0.6	0.4732	0.3253	0.1422	0.1637
0.65	0.3805	0.278	0.1207	0.1443
0.7	0.3026	0.2333	0.1008	0.1243
0.75	0.2359	0.1907	0.08204	0.1044
0.8	0.1777	0.15	0.06428	0.08397
0.85	0.1262	0.1107	0.04731	0.0633
0.9	0.08011	0.07276	0.03101	0.04239
0.95	0.0383	0.0359	0.01527	0.02128
0.98	0.01494	0.01425	0.006057	0.008534
0.99	0.007411	0.007109	0.00302	0.00247
1	0	0	0	0

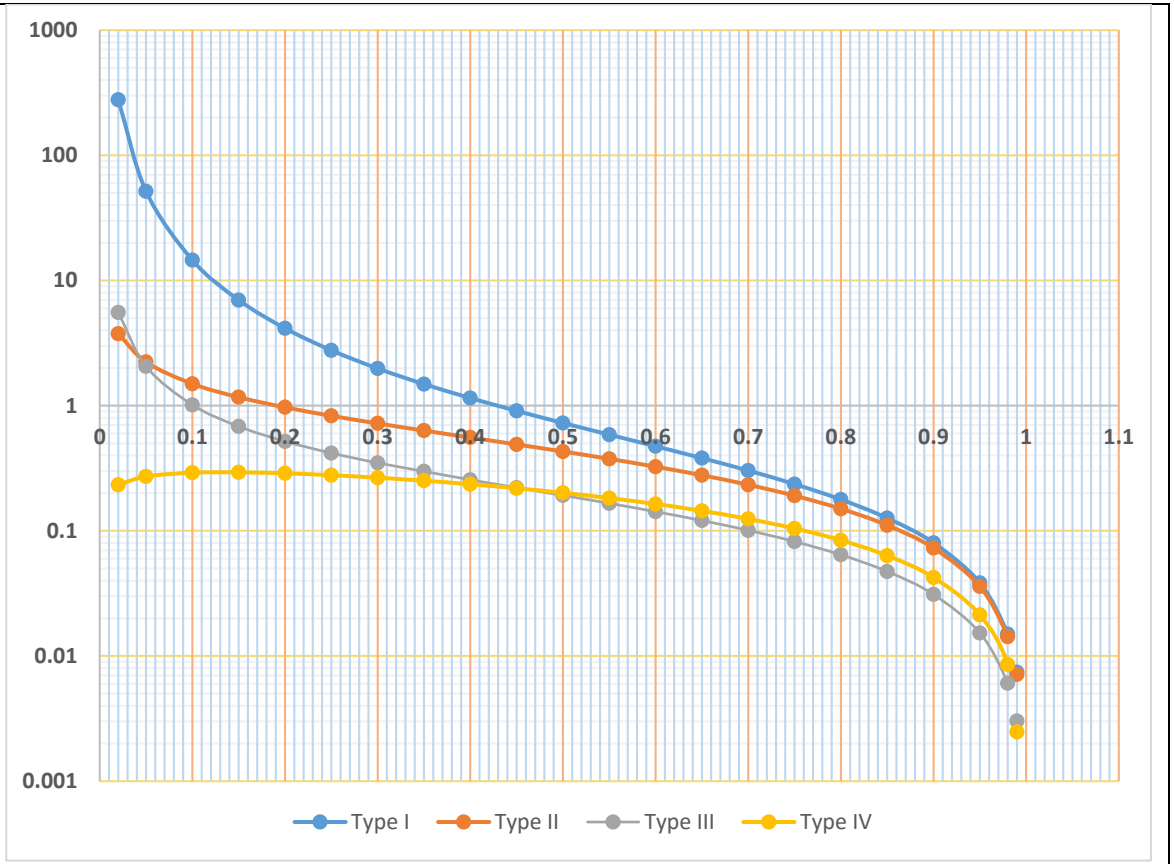

Sediment deposit estimation after various time horizons

Catchment Area (A)=	3558	[km2]
Bed level at Dam site=	1850	[m]
F.R.L elevation =	2006	[m]
Average annual sediment volume (A*r)=	1.779	[MCM]

Year	Capacity (MCM)	Capacity inflow Ratio (C/I)	Trap. Efficiency as per IS 12182	Sediment inflow in 10 years (MCM)	Sediment trapped in 10 years	Revised capacity after 10 years	Accumuated Sediment volume (MCM)
1 to 10	329.1582	0.126	88%	17.79	15.66	313.50	15.66
10 to 20	313.50	0.120	87%	17.79	15.48	298.03	31.13
20 to 30	**298.03**	**0.114**	**86%**	**17.79**	**15.30**	**282.73**	**46.43**
30 to 40	282.73	0.108	85%	17.79	15.12	267.60	61.55
40 to 50	**267.60**	**0.102**	**85%**	**17.79**	**15.12**	**252.48**	**76.67**
50 to 60	252.48	0.096	84%	17.79	14.94	237.54	91.62
60 to 70	**237.54**	**0.091**	**84%**	**17.79**	**14.94**	**222.60**	106.56

30 years expected sediment volume=	46.43	MCM
50 years expected sediment volume=	61.55	MCM
70 years expected sediment volume=	76.67	MCM

Computations for NZE corresponding to 30 years expected Sediment volume

Reservoir Area =	6.8192	[km2]
Flood River Level (FRL) =	2006	[m]
Stream bed level =	1850	[m]
Depth till bed from FRL , H =	156	[m]
Catchment Area (A) =	3558	]mil.m3]
Sedimentation rate (r) =	0.5	[mm/year]
Average Annual Sediment volume =	1.779	[MCM]
Sediment accumulation in 30 years =	46.43	[MCM]
P0 =	0.37	
The new zero-capacity elevation (h0) =	1908	[m]
Area Correction Factor =	37.58	

Elevation	Area (ha)	Elevation	Area (ha)
1910.0	75.1	1910.0	18.1
1907.0	69.5	1907.0	16.2
1900.0	56.5	1900.0	11.6

Original Data					Relative		Computed sediment Distribution			Revised	
Elevation (m)	**Area, A (ha)**	**Area, A (m2)**	**Capacity, Vh (mil. m3)**	**F value**	**Relative depth (p)**	**For Type III: Ap**	**Area, ha**	**Volume Increment (mil.m3)**	**Cumulative volume (mil.m3)**	**Area, ha**	**Capacity (mil.m3)**
2006	681.920	6819200.000	329.158		1.000	0.000	0.000	0.010	46.132	681.920	283.026
2000	627.980	6279800.000	289.872		0.962	0.008	0.318	0.159	46.123	627.662	243.749
1990	542.000	5420000.000	231.426		0.897	0.076	2.858	0.548	45.964	539.142	185.462
1980	453.970	4539700.000	181.693		0.833	0.215	8.094	1.190	45.417	445.876	136.276
1970	376.580	3765800.000	140.225		0.769	0.418	15.706	2.040	44.227	360.874	95.999
1960	308.020	3080200.000	106.053		0.705	0.668	25.096	3.030	42.186	282.924	63.866
1950	243.470	2434700.000	78.541		0.641	0.945	35.497	4.077	39.157	207.973	39.384
1940	185.700	1857000.000	57.148		0.577	1.225	46.038	5.091	35.080	139.662	22.068
1930	143.540	1435400.000	40.731	0.025	0.513	1.484	55.775	5.975	29.989	87.765	10.742
1920	117.720	1177200.000	27.689	0.102	0.449	1.696	63.723	6.631	24.014	53.997	3.675
1910	75.120	751200.000	18.127	0.242	0.385	1.833	68.888	1.384	17.384	6.232	0.743
1908	69.500	695000.000	16.000	0.281	0.372	1.849	69.500	16.000	16.000	0.000	0.000

1900	56.470	564700.000	11.569	0.396	0.321	1.871	56.470	11.569	11.569	0.000	0.000
1890	40.870	408700.000	6.723	0.623	0.256	1.784	40.870	6.723	6.723	0.000	0.000
1880	27.520	275200.000	3.326	1.004	0.192	1.552	27.520	3.326	3.326	0.000	0.000
1870	14.420	144200.000	1.264	2.008	0.128	1.163	14.420	1.264	1.264	0.000	0.000
1860	6.080	60800.000	0.268	4.867	0.064	0.618	6.080	0.268	0.268	0.000	0.000
1850	0.400	4000.000	0.000	74.410	0.000	0.000	0.400	0.000	0.000	0.000	0.000

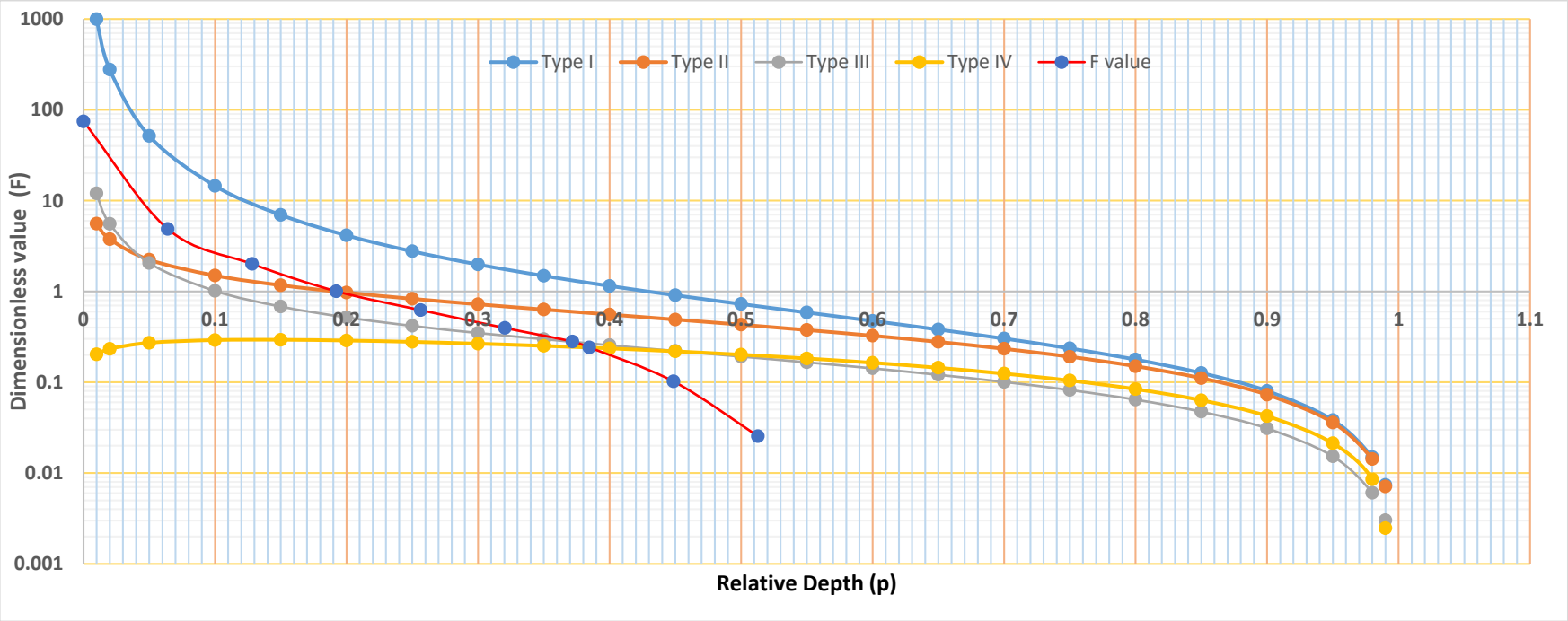

Figure D1: Plot showing F value intersecting with Type III curve at $P_0 = 0.37$

Computations for NZE corresponding to 50 years expected Sediment volume

Reservoir Area =	6.8192	[km2]
Flood River Level (FRL) =	2006	[m]
Stream bed level =	1850	[m]
Depth till bed from FRL , H =	156	[m]
Catchment Area (A) =	3558	]mil.m3]
Sedimentation rate (r) =	0.5	[mm/year]
Average Annual Sediment volume =	1.779	[MCM]
Sediment accumulation in 50 years =	76.67	[MCM]
P0 =	0.49	
The NZE (h0) =	1926	[m]
Area Correction Factor =	84.52	

Elevation	Area (ha)
1930.0	143.5
1926.0	133.2
1920.0	117.7

Elevation	Area (ha)
1930.0	40.7
1926.0	35.5
1920.0	27.7

Original Data					Relative		Computed sediment Distribution			Revised	
Elevation (m)	**Area, A (ha)**	**Area, A (m2)**	**Capacity, Vh (mil. m3)**	**F value**	**Relative depth (p)**	**For Type III: Ap**	**Area, ha**	**Volume Increment (mil.m3)**	**Cumulative volume (mil.m3)**	**Area, ha**	**Capacity (mil.m3)**
2006	681.920	6819200.000	329.158		1.000	0.000	0.000	0.021	77.025	681.920	252.133
2000	627.980	6279800.000	289.872		0.962	0.008	0.715	0.357	77.003	627.27	212.869
1990	542.000	5420000.000	231.426		0.897	0.076	6.427	1.232	76.646	535.57	154.780
1980	453.970	4539700.000	181.693		0.833	0.215	18.204	2.676	75.415	435.77	106.278
1970	376.580	3765800.000	140.225		0.769	0.418	35.325	4.588	72.738	341.26	67.487
1960	308.020	3080200.000	106.053		0.705	0.668	56.442	6.814	68.150	251.58	37.902
1950	243.470	2434700.000	78.541		0.641	0.945	79.835	9.169	61.336	163.635	17.205
1940	185.700	1857000.000	57.148	0.067	0.577	1.225	103.543	11.449	52.167	82.16	4.981

1930	143.540	1435400.000	40.731	0.161	0.513	1.484	125.441	12.158	40.718	18.10	0.013
1926	133.200	1332000.000	28.560	0.232	0.487	1.576	133.200	28.560	28.560	0.00	0.000
1920	117.720	1177200.000	27.689	0.267	0.449	1.696	117.720	27.689	27.689	0.00	0.000
1910	75.120	751200.000	18.127	0.500	0.385	1.833	75.120	18.127	18.127	0.00	0.000
1900	56.470	564700.000	11.569	0.739	0.321	1.871	56.470	11.569	11.569	0.00	0.000
1890	40.870	408700.000	6.723	1.097	0.256	1.784	40.870	6.723	6.723	0.00	0.000
1880	27.520	275200.000	3.326	1.709	0.192	1.552	27.520	3.326	3.326	0.00	0.000
1870	14.420	144200.000	1.264	3.352	0.128	1.163	14.420	1.264	1.264	0.00	0.000
1860	6.080	60800.000	0.268	8.056	0.064	0.618	6.080	0.268	0.268	0.00	0.000
1850	0.400	4000.000	0.000	122.876	0.000	0.000	0.400	0.000	0.000	0.00	0.000

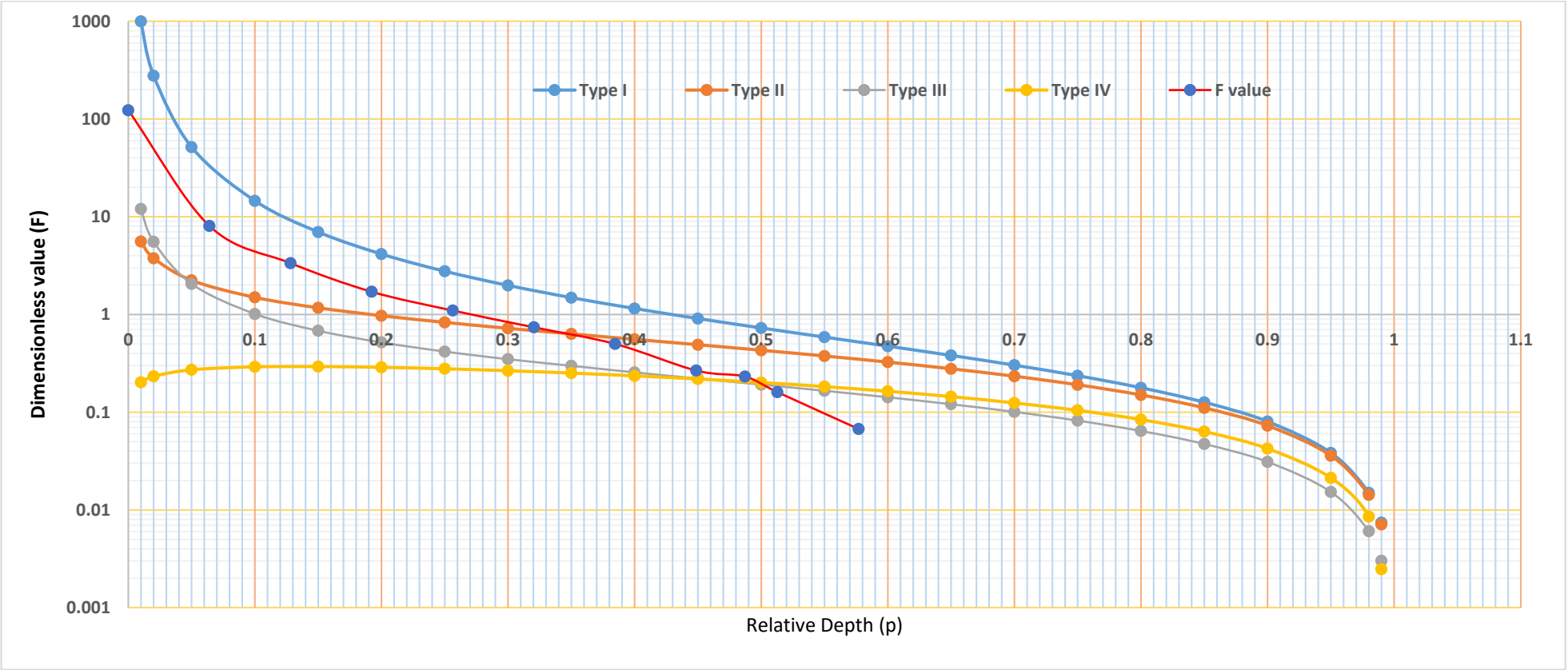

Figure D2: Plot showing dimensionless F value intersecting with selected Type III curve at p0 = 0.49

Computations for NZE corresponding to 70 years expected Sediment volume

Reservoir Area =	6.8192	[km2]
Flood River Level (FRL) =	2006	[m]
Stream bed level =	1850	[m]
Depth till bed from FRL , H =	156	[m]
Catchment Area (A) =	3558	]mil.m3]
Sedimentation rate (r) =	0.5	[mm/year]
Average Annual Sediment volume =	1.779	[MCM]
Sediment accumulation in 70 years =	106.56	[MCM]
P0 =	0.60	
The NZE (h0) =	1944	[m]
Area Correction Factor =	187.42	

Elevation	Area (ha)
1950.0	243.5
1944.0	208.8
1940.0	185.7

Elevation	Area (ha)
1950.0	78.5
1944.0	65.7
1940.0	57.1

Original Data					Relative		Computed sediment Distribution			Revised	
Elevation (m)	**Area, A (ha)**	**Area,A (m2)**	**Capacity, Vh (mil. m3)**	**F value**	**Relative depth (p)**	**For Type III: Ap**	**Area, ha**	**Volume Increment (mil.m3)**	**Cumulative volume (mil.m3)**	**Area, ha**	**Capacity (mil.m3)**
2006	681.920	6819200.000	329.158		1.000	0.000	0.000	0.048	112.929	681.920	216.230
2000	627.980	6279800.000	289.872		0.962	0.008	1.585	0.792	112.881	626.395	176.991
1990	542.000	5420000.000	231.426		0.897	0.076	14.252	2.731	112.089	527.748	119.337
1980	453.970	4539700.000	181.693		0.833	0.215	40.370	5.935	109.358	413.600	72.334
1970	376.580	3765800.000	140.225		0.769	0.418	78.337	10.175	103.423	298.243	36.802
1960	308.020	3080200.000	106.053	0.001	0.705	0.668	125.165	15.110	93.248	182.855	12.805
1950	243.470	2434700.000	78.541	0.074	0.641	0.945	177.044	18.137	78.137	66.426	0.404
1944	208.800	2088000.000	60.000	0.143	0.603	1.114	208.800	60.000	60.000	0.000	0.000
1940	185.700	1857000.000	57.148	0.171	0.577	1.225	185.700	57.148	57.148	0.000	0.000
1930	143.540	1435400.000	40.731	0.294	0.513	1.484	143.540	40.731	40.731	0.000	0.000
1920	117.720	1177200.000	27.689	0.429	0.449	1.696	117.720	27.689	27.689	0.000	0.000

1910	75.120	751200.000	18.127	0.755	0.385	1.833	75.120	18.127	18.127	0.000	0.000
1900	56.470	564700.000	11.569	1.078	0.321	1.871	56.470	11.569	11.569	0.000	0.000
1890	40.870	408700.000	6.723	1.566	0.256	1.784	40.870	6.723	6.723	0.000	0.000
1880	27.520	275200.000	3.326	2.405	0.192	1.552	27.520	3.326	3.326	0.000	0.000
1870	14.420	144200.000	1.264	4.681	0.128	1.163	14.420	1.264	1.264	0.000	0.000
1860	6.080	60800.000	0.268	11.207	0.064	0.618	6.080	0.268	0.268	0.000	0.000
1850	0.400	4000.000	0.000	170.773	0.000	0.000	0.400	0.000	0.000	0.000	0.000

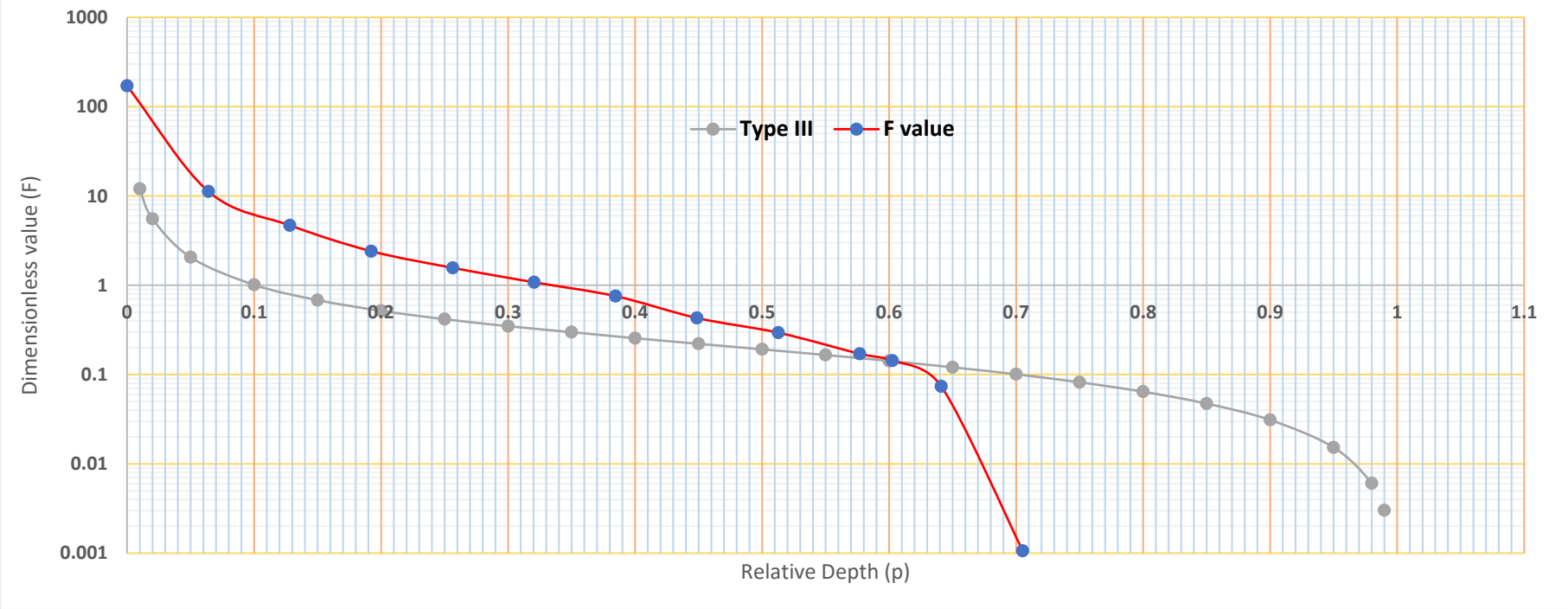

Figure D3: Plot showing dimensionless F value intersecting with selected Type III curve at p0 = 0.60

Note: **The revised reservoir capacity and area curve after predicting the sediment distribution for different time horizons are included in the main document.**